ABSTRACT

The kinetics of the catalytic hydrogenation of propylene have been studied in a static system on 20-40 mesh pumice-supported transition metals of Group VIII in the periodic table between 40 and 200° C. at 20-240 mm. Hg of hydrogen pressure and 15-200 mm. Hg of propylene pressure.

The orders of the reaction with respect to the initial pressures of the reactants, activation energies and frequency factors for various catalysts have been determined. The reaction is mostly zero order with respect to the initial propylene pressure, although a slightly negative order of -0.05 was observed for rhodium, ruthenium and iridium. The reaction order with respect to the initial hydrogen pressure ranges from 0.6 to 1.0 for all metals except osmium. The unusually high order of 1.6 with respect to hydrogen for the osmium-pumice catalyst is attributed to the strong adsorption of propylene on the surface.

The apparent activation energies for pumice-supported nickel, iron, cobalt, platinum, palladium, rhodium, iridium, ruthenium, and osmium catalysts are 13, 10, 8.1, 16, 11, 13, 15, 6.5, and 7.4 kcal/mole, respectively. The order of catalytic activities of the series of metals is

$$Rh > Ir > Ru > Pt > Pd > Ni > Fe > Co > Os$$

The activity of the palladium-pumice catalyst was found to decrease gradually. This is probably due to the poisoning by mercury vapor.

Attempts have been made to correlate the catalytic activity and activation energy with the electronic and geometric structures of the metals. The present work shows that the geometric structure of the metals would affect the activation energy. However, the catalytic activity is probably determined by the electronic rather than the geometric factor.

The compensation effect was used to correlate the kinetic parameters of the catalysts, but the most active catalysts deviated considerably from the overall correlation.

ACKNOWLEDGEMENTS

The financial support from the Imperial Oil Company Ltd., Ontario, Canada, is gratefully acknowledged.

The author wishes to express his sincere thanks to Dr. R.S. Mann for his guidance in carrying out this work and his help in the preparation of this thesis; to Dr. B. C. -Y. Lu and his staff for providing the facility in which the work was conducted, and to Dr. K.J. Laidler for his valuable discussions.

To Mr. M.C. Lin for his help in the sample analysis; to Mr. C.J. Pan, Mr. K.C. Yao, and Mr. C. C. Hong for their help in the preparation of the thesis; to Mr. W.R. Smith for his proofreading the manuscript, and to Mrs. C. Hundrieser for her skillful typing, the author wishes to remember.

Finally, the author would like to note, with affection, the unreserved help given by his fiancee, and the encouragement of his parents who live far away in the homeland.

TABLE OF CONTENTS

LIST OF FIGURES

LIST OF TABLES

I. INTRODUCTION

The catalytic hydrogenation of light olefins has been widely studied in the past since the time of Sabatier. In spite of all the work carried out in this field, the nature of catalytic reaction on the surface of metals and particularly the mechanism of the reaction are not very clear and need further elucidation.

Though a considerable amount of work has been done in the past on the catalytic hydrogenation of ethylene, the hydrogenation of propylene, the second one in the series, has been much neglected.

The catalytic hydrogenation of propylene has been studied in a constant volume system over all the transition metals of Group VIII, supported on pumice, for a wide range of temperature and reactants' pressures.

The object of the detailed kinetic study of the catalytic hydrogenation of propylene was:

1. to study the behaviour shown by all the metals of the series and to determine their activation energies, frequency factors and relative catalytic activities.
2. to find if the geometric or electronic structures of the metals are related in any way to the catalytic activity.
3. to correlate the kinetic parameters of the catalysts to the properties of the metals, and finally,
4. to find out as to how the kinetics of the propylene hydrogenation differ from ethylene hydrogenation over the same type of catalysts.

II. LITERATURE SURVEY

The literature on catalytic hydrogenation of light olefins, especially of ethylene, is voluminous. This chapter is divided into four sections. The first part is a general review of the experimental work done on the hydrogenation of light olefins, particularly of ethylene. Studies made by Beeck and his co-workers[4,5,6,7], and Schuit and van Reijen[41] are described in detail in the second part. A brief survey of the postulated mechanisms for the hydrogenation reaction is given in the third section. In the last section, the compensation effect is discussed.

Results of studies on the hydrogenation of light olefins have been reviewed by Eley[16, 17, 19], Bond[8, 10], Hoelscher et al.[26], Laidler[29], and Taylor[47]. However, the most recent review on this topic was made by Bond and Wells[11].

A. The Kinetics of Catalytic Hydrogenation of Light Olefins

1. Olefin Hydrogenation over Nickel

The hydrogenation of ethylene with nickel as catalyst has been widely studied. Substantially agreeable results have been recorded by Rideal and co-workers[27, 39, 51], Schuster[42], Twigg[52, 53], Beeck and co-workers[4, 5, 6, 7], Schuit and van Reijen[41], and Paul, Comings and Smith[34]. All these hydrogenation studies, with the exception of that by Paul et al., were made at pressures lower than atmospheric in static systems. Paul et al., however, used a differential reactor and studied the hydrogenation reaction over a pressure range of 1 to 5 atmospheres.

The results of the above investigators showed that at temperatures below 100°C., the rate is given approximately by

$$r = k (P_H)^m (P_U)^n \qquad \text{(II-1)}$$

where k is the rate constant, P_H and P_U are the pressures of hydrogen and olefin, respectively. The order of reaction of hydrogen, m, is generally found to be unity or less, and the order of ethylene, n, is zero. However, fractional orders of m and n have been reported [27, 41]. A zero order reaction, although infrequent, was observed by some investigators [25, 51]. The ethane formed has no effect on the rate of reaction other than that of dilution. At room temperatures, values of apparent activation energy have been determined to be 3.2[39], 3.6[42], 4.6[40], 8.2[52], 10.7[4], 11.6 Kcal/mole[34]. The last three values seem more acceptable.

As the reaction temperature is increased, the Arrhenius plot (log r vs. 1/T) begins to fall off, and usually peaks at 130° to 200° C., depending on gas pressure and composition[27, 53, 56]. But the peak at 60° C. has been reported at low pressure by Zur Strassen[56] who found that the temperature optimum decreased as the partial pressure of ethylene was lowered. Jenkin[27] found 160° - 165° C. as a temperature optimum when the partial pressure of ethylene was 20 mm. Hg.

Analysis of the kinetic data is made very difficult due to the coverage of a large part of the catalyst surface with an acetylenic complex which does not itself enter into the hydrogenation reaction. Beeck[5], Jenkins and Rideal[27] reported that upon addition of ethylene to a clean nickel surface, ethane appeared in the gas phase. This "self-hydrogenation" was explained by the postulation that the ethylene molecule underwent dissociative chemisorption to form two chemisorbed hydrogen atoms and the "acetylenic complex" $\begin{matrix} CH = CH \\ | \quad\quad | \\ Ni - Ni \end{matrix}$. Ethylene from the gas phase then reacted with the adsorbed hydrogen atoms to give un-adsorbed ethane. Jenkins and Rideal[27] found that the final structure of the nickel film on admission of the two gases was of some 80% coverage by

acetylenic complexes, 10% by hydrogen on double sites, and 10% on single sites. This chemisorbed hydrogen on the 10% of double sites on the covered surface readily reacted with gaseous ethylene to form ethane. This poisoning by ethylene, however, has been observed by most of investigators.

Schuster[42] reported that the hydrogenation of ethylene and propylene over 1% nickel-charcoal was first order with respect to hydrogen. He also found that the activation energy increased with increasing molecular weight of olefin.

Both ethylene and propylene hydrogenations have been investigated over nickel filaments over a wide range of temperature by Toyama[48, 49, 50]. He concluded that in the low temperature range of -78° to 0°C. the rate equation

$$r = A \frac{P_H P_U}{(1 + BP_H + CP_U)^2} \qquad \text{(II-2)}$$

based on Langmuir's isotherm explained the experimental results quite satisfactorily. This implied that surface reaction between the two adsorbed reactants was the rate-controlling step. But in the temperature range of 99° to 165° C., he found that the approximated form of the equation $r = AP_H P_U / (1 + BP_U)$ was acceptable. This approximated form was also used to correlate his experimental results on propylene hydrogenation in the temperature range of 25-178°C. The activation energies for ethylene and propylene hydrogenations were 6 kcal/mole and 2 kcal/mole, respectively. The lower values of the activation energies may be due to the poisoning of catalyst, which was clearly observed during these investigations.

The hydrogenation of propylene over nickel film produced by the thermal decomposition of nickel carbonyl was studied by Baker and Bernstein[1]. For equimolar mixtures of hydrogen and propylene at 37° and 80°C., the rate was expressed satisfactorily by the

equation $r = AP^2/(1 + BP^2)$, where P is the partial pressure of either reactant. The theory of competitive adsorption was also postulated.

Fair[23] studied the hydrogenation of propylene and isobutylene over a nickel-kieselguhr catalyst between 100° and 200° F., at pressures of 1 to 4 atmospheres, for feed compositions of 20-33% olefins. He found that the rate-determining step of the reaction was a surface reaction taking place between adsorbed hydrogen atoms and olefin molecules.

2. Olefin Hydrogenation over other Metals

Farkas and Farkas[24] used a platinized platinum foil to hydrogenate ethylene in a static system. The pressure-time curve was represented approximately by the equation:

$$P = P_0 \exp(-kt) \qquad \text{(II-3)}$$

where P_0 and P are the pressures of the reactant (not in excess) at the start of the reaction and at any time t respectively. It was found that the initial rate increased as initial hydrogen pressure increased, but increased with decreased ethylene pressures, thus supporting the notion of competitive adsorption. For 40 mm. Hg of hydrogen and 20 mm. Hg of ethylene, a maximum rate occurred at about 160° C. Below 160° C. an activation energy of 10 kcal/mol was estimated. Postovskaya[38] found that the rate expression, $r = k(P_H)^1 (P_U)^0$, could explain the hydrogenation of ethylene over platinized silica gel. He obtained an overall activation energy of 4.3 kcal/mole in the temperature range of 44° to 138° C., which is considerably smaller than the usually reported values.

The hydrogenation of propylene over platinum-aluminum catalyst was studied by Rogers[40] in a flow system. The study was restricted to a narrow temperature range of 1.4° to 34.3° C., for a pressure range of 0.25 to 4 atmospheres, and feed compositions

of propylene from 5 to 45 mole %. The reaction rate was found to increase with the decreased partial pressures of propylene, although the reaction was practically of zero order with respect to propylene at low temperatures. The activation energy was found to be 15 kcal/mole. It was suggested that the rate-controlling step was the surface reaction between molecularly adsorbed hydrogen and the adsorbed propylene, both competing for the same site.

Kayser and Hoelscher[28] investigated the hydrogenation of propylene over alumina-supported palladium in a differential packed-bed reactor. They reported that the rate-controlling step in the reaction was the mass transfer of the reactants from the ambient gas stream to the catalyst surface. The activation energy was found to be 11.7 kcal/mole in the temperature range of 55° to 75° C.

The hydrogenation of ethylene, propylene, and 2-butene over iron catalyst was reported by Emmett and Gray[21]. At -20°C. the relative reaction rates for ethylene, propylene and 2-butene were 1:0.47:0.16. The apparent activation energies for the same series were 4.2 (-20° to -50° C.), 3.2 (-5° to -60° C.) and 2.8 kcal/mole (-29° to 20°C.). The order of the reaction was approximately 0.6 with respect to hydrogen pressure for the three olefins studied. The reaction order was slightly positive with respect to ethylene, negative with respect to propylene, and zero order with respect to 2-butene.

Several hydrogenation studies have been made by using copper catalysts. Pease[35, 36] found that the order of hydrogenation reaction of ethylene changed with temperature. The rate could be approximately expressed as $r = kP_H^1P_U^{0.5}$ at 0°C., $r = k'P_H^1P_U^0$ at 100° C., and $r = k''P_H^1P_U^1$ at 200° C., with apparent activation energies falling from 13.2 kcal (0-100° C.) to 10.8 kcal (150°-200° C.), and to 7.0 kcal (200°-250°C.).

Constable[14] found that the maximum rate of ethylene hydrogenation at 0° C. occurred at 18% ethylene, but as the temperature was raised to 100° C. and 200° C., the optimum values increased to 42% and 50%, respectively.

Wynkoop and Wilhelm[55] investigated the hydrogenation of ethylene over a 50-50 mole % copper-magnesia catalyst in a fixed-bed flow-type reactor. The reaction was first order with respect to hydrogen, with an apparent activation energy of 13.3 kcal/mole. Sussmann and Potter[45] used the same catalyst to hydrogenate propylene. They used the Hougen-Watson method to correlate their own data and those obtained by Wynkoop and Wilhelm. For constant propylene pressure, the reaction rate changed linearly with hydrogen concentration, and for constant hydrogen pressure, it increased at low propylene concentrations, but decreased at moderate and high concentrations. Propane reduced the reaction rate. The activation energy in the temperature range 48°-76° C. at 1 atmosphere was found to be 10.46 kcal/mole. It was found that most likely the rate-determining step was the surface reaction between the adsorbed olefin and atomically adsorbed hydrogen.

B. The Work of Beeck[5] and of Schuit and van Reijen[41].

Beeck contributed a major study on the adsorptive and catalytic properties of evaporated metal films. He studied ethylene hydrogenation over a series of metal films in a non-flow system with a magnetically driven glass turbine to circulate the gas inside the reaction vessel. He found that in all cases the reaction rate could be expressed by $r = k (P_H)^1 (P_U)^0$. The remarkable difference in reaction rates was attributed to the temperature-independent constants, since the activation energies are 10.7 kcal/mole for all catalysts, (though 2.4 kcal/mole for tungsten). The effect of pretreatment of fresh nickel film with ethylene was studied, and Beeck gave the following figures for the rates

of hydrogenation at 0° C. after the pretreatment, as a percentage of the rate over fresh catalyst: Ta 10%, W 20%, Ni 40%, Pt and Rh 95%.

In order to investigate the influence of the electronic structure of the different metals, Beeck measured the differential heat of adsorption as a function of coverage of the catalyst surface for hydrogen and ethylene. The results for hydrogen at 23° C. are given in Figure 1. It shows that metals with the largest initial heats of adsorption deviate most from Langmuir behaviour. Adsorption curves for ethylene show similar trends, except that the heats of adsorption are much higher.

Beeck found that the rate of the hydrogenation of ethylene over evaporated films of transition elements depended strongly upon the heat of adsorption of either ethylene or hydrogen. Figure 2 shows the initial heats of adsorption of hydrogen over sparsely covered surfaces, plotted against the logarithm of the rate constants. A parallel curve was obtained for ethylene also.

An attempt to relate the phenomenon of heterogeneous catalysis to the nature of the chemical bond was also made by correlating the heat of adsorption and the rate constant with percentage d-character of the cohesive metallic bond.

The transition metals are characterized by a partially filled electronic d-shell. Pauling[33] developed his theory to interpret the cohesive bonding strength shown by the various metals by assuming that some of the d-orbitals are not available for bond formation. Starting from this hypothesis, he calculated the percentage d-characters of various metals. In simple terms, the percentage d-character is an indication of the degree of participation of the d-electrons in that bond. The percentage d-characters of some metals are listed in Table 1.

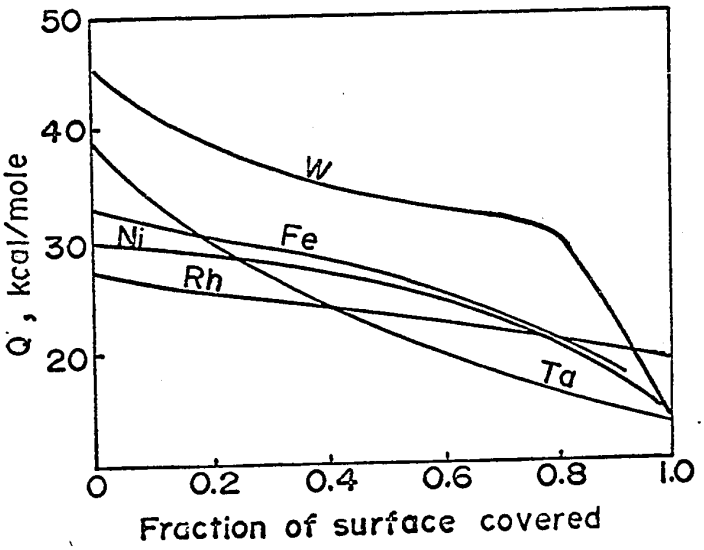

Figure 1. Heats of adsorption of hydrogen. (From Reference 5).

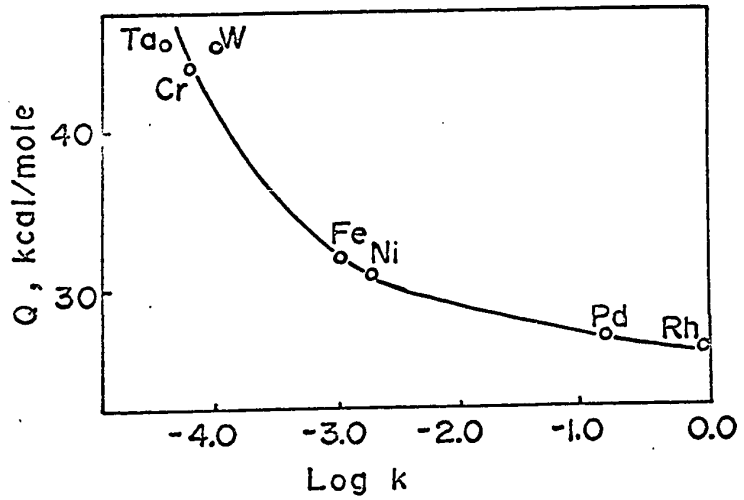

Figure 2. Correlation of heat of adsorption of hydrogen with logarithm rate constant. (From Reference 5).

If a metal has a high d-character, then there will be a low d-electron availability for covalent bonding with a molecule being adsorbed. Thus, the greater the percentage d-character, the lower are the heats of adsorption, and the higher are the rates of reaction. This could be seen from Beeck's correlations given in Figures 3 and 4. It is interesting to note that the large increase in the rate of reaction observed from iron to rhodium for a relatively small decrease in heat of adsorption (Figure 2) can be shown more clearly when plotted against percentage d-character (Figure 4). A review of the electronic consideration in heterogeneous catalysis was made by Baker and Jenkins[2].

Table 1. Percentage d-characters of some Transition Metals

Mn	Fe	Co	Ni	Cu
40.1	39.5	39.7	40	36
Tc	Ru	Rh	Pd	Ag
46	50	50	46	36
Re	Os	Ir	Pt	Au
46	49	49	44	-

Another important study was made by Schuit and van Reijen[41], who followed Beeck's work, except that they used metal-on-silica catalysts instead of evaporated films. Their study showed the similarity between the two systems, one using commercial supported metal catalyst and the other, special evaporated metal film.

Extensive investigations of the physical and chemical adsorptions, and catalytic properties of supported nickel catalyst were carried out. They found that the trend of the heat of adsorption for hydrogen was similar to the one found by Beeck.

Power Rate Law, due to Schuit and van Reijen, was used to correlate the data of hydrogenation of ethylene over supported catalysts.

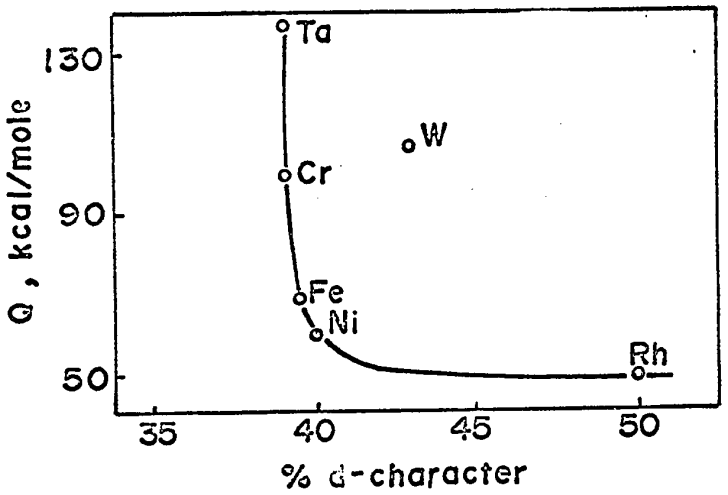

Figure 3. Correlation of heat of adsorption of ethylene with % d-character of metals. (from Reference 5)

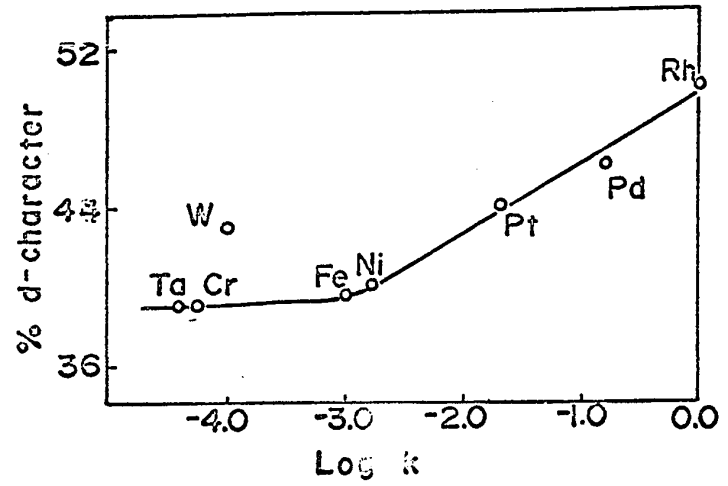

Figure 4. Correlation of rate constant for ethylene hydrogenation with % d-character of metals (from Reference 5).

The Power Rate Law assumes that the rate of an arbitrary reaction $aA + bB \rightleftarrows (A_a B_b)^{*} \longrightarrow$ Product(s) may be simply expressed as:

$$r = kP_A^{m} P_B^{n} \qquad \text{(II-4)}$$

where k is the rate constant and m, n are the experimentally determined orders of reaction of reactants A and B, respectively, generally not equal to the number of molecules of A and B participating in the stoichiometric equation. Strictly speaking, the Power Rate Law treats the kinetics of a heterogeneous reaction as a homogeneous reaction.

The kinetic results of their work are shown in Table 2, in which the catalytic activity relative to rhodium (the relative reaction rates at a standard set of conditions) is also given. For comparison, the results of Beeck are also included.

It can be seen that the kinetics of the reaction differs considerably between the two systems. Schuit and van Reijen found that in all cases, the hydrogen exponent, m, was less than one, and a negative ethylene order, n, was obtained for all active catalysts except platinum. Beeck found that the reaction was always zero order with respect to ethylene and first order with respect to hydrogen. Over the temperature range of 195° to 273° K., Schuit and van Reijen obtained an activation energy of 8.4 ± 0.4 kcal/mole for all catalysts. However, 10.7 kcal/mole was noted for metal films by Beeck.

Table 2. Kinetics of Ethylene Hydrogenation and Relative Activities of Various Metals. (From Reference 41)

Metal	Temperature °K.	m	n	log (activity relative to rhodium)	
				Supported Catalyst[41]	Evaporated Film[5]
Rh	197	0.85±0.11	-0.74±0.18	0	0
Ru	203	0.95± 0.05	-0.59± 0.08	-0.3	
Pd	243	0.66± 0.05	-0.03± 0.07	-0.9	-0.6
Pt	233	0.77± 0.07	0.25± 0.07	-1.5	-1.6
Ni	233	0.67± 0.10	-0.08± 0.12	-1.5	-2.8
Ir				-2.0	
Co	213	0.55± 0.06	-0.19± 0.10	-2.1	
Fe	303	0.91± 0.11	-0.04± 0.13	-3.4	-3.0
Cu	353	0.69± 0.09	0.06± 0.12	-4.1	

C. The Mechanism of Catalytic Hydrogenation of Light Olefins

Though many studies have been made on the kinetics of the catalytic hydrogenation of light olefins, no satisfactory mechanism has been proposed yet. Theories advanced so far are not in agreement; sometimes they are even contradicting.

A knowledge of the species that are formed when olefins become chemisorbed, is of great importance. Eley[18] supported the "associative" mechanism based on the agreement between experimental and calculated values of heats of adsorption. Beeck et al.[4, 5], Jenkins and Rideal[27] favoured the "dissociative" mechanism, in view of the evidence of the self-hydrogenation of ethylene. The new technique has enabled many workers[20, 31, 43] to investigate the form of olefins over the supported metals. The results showed that both "associative" and "dissociative" forms could exist, depending on the nature of surface, temperature, partial pressures of hydrogen, and the presence or absence of a layer of preadsorbed hydrogen. Unfortunately, reliable information on the adsorbed state of an olefin during hydrogenation is not available.

The establishment of a mechanism through which olefins are hydrogenated on a metal surface is hampered by the complexity of the reaction. Two types of mechanism have been postulated in the past. The first type is the Langmuir-Hinshelwood mechanism which states that the reaction proceeds through the adsorption of the two species on adjacent sites, followed by their interaction and the desorption of product(s). To elucidate this mechanism, Laidler[30] presented a theoretical approach based on Absolute Rate Theory. The experimental results obtained in static systems[24, 48] and in flow systems[1, 40, 45, 46, 55] support this mechanism.

The second type, Rideal-Eley mechanism, assumes that the reaction involves interaction between a surface-adsorbed atom or molecule and a gaseous molecule. Two distinctive mechanisms are possible in this case. Rideal and his co-workers[27, 51], Paul et al.[34] and Beeck[4] suggested that hydrogen is adsorbed on the small fraction of the surface not occupied by acetylenic complex and the reaction takes place between the adsorbed hydrogen and ethylene in the gas phase. An alternative possibility is that the adsorbed ethylene molecules react with gaseous hydrogen molecules in the van der Waals layer above and between chemisorbed molecules of ethylene. This mechanism has been supported by Eyring[22], and Twigg[52, 53].

The complexity of heterogeneous reactions makes it impossible to make a distinction between the various postulated mechanisms on the basis of kinetic measurement alone. Moreover, most studies on the hydrogenation of ethylene were made over a nickel catalyst. The information on the use of other catalysts is rarely available. Therefore, extensive research is required for a satisfactory explanation of the mechanism of olefin hydrogenation.

D. Catalytic Activity and the Compensation Effect

A survey of heterogeneous catalysis reveals that two different approaches have been used to correlate the catalytic activity. In the first approach, a given reaction is studied over a series of catalysts, and some kinetic parameters are correlated to the properties of the solid catalyst or of a complex between the catalyst and reactants. In the second approach, a series of related reactions are investigated on a certain catalyst and some kinetic parameters are used for correlating the properties of the reacting molecules.

The activity can be defined as the rate constant k, or as the rate itself under the same conditions. Since it is generally true that the empirical rate constant k obeys the Arrhenius equation, $k = A \exp(-E/RT)$, activity variations are the result of variations in the activation energy E or in the frequency factor A, or in both simultaneously.

A frequently observed linear relation between log A and E

$$\log A = mE + C \qquad \text{(II-5)}$$

is of great interest. This is usually referred to as the compensation effect or the Theta Rule in literature.

The former name is meaningful, since an increase in log A at constant E implies a higher rate, while an increase in E at constant log A implies a lower rate, and a simultaneous increase or decrease in E and log A therefore tend to compensate the rate constant, and hence reaction rate, as could be seen from the Arrhenius equation. Furthermore, when a compensation effect exists, it is possible to observe marked variations in E and log A for a relatively small change in activity; alternatively when the effect does not exist (i.e., when either E or log A alone changes), marked variation in activity results.

Few attempts have been made to interpret the nature of the compensation effect, but none can be considered as satisfactory. These interpretations were reviewed by Cremer[15] and Bond[10].

III. EXPERIMENTAL

A. Apparatus

The apparatus consisted essentially of four sections:

(1) a section for the purification and storage of hydrogen

(2) a section for the purification and storage of propylene

(3) a reaction section, and

(4) a standard high vacuum system.

A schematic diagram of the apparatus is presented in Figure 5.

The first two will be described under the title, purification of reactants. The reaction section mainly consisted of a pyrex reaction vessel, R, attached to a manometer M_1 which was in turn fixed on a mirror scale G. The capacity of the reaction vessel R was about 130 cc., including 15 cc. for glass tube lines. A furnace with a heating element was used to maintain the reaction vessel at the desired temperature, by either a Fisher model 44 temperature controller below 160° C., or Honeywell's Pyr-O-Vane Temperature Controller above 160° C. The sensing elements W_1 of the temperature controllers were inserted into the furnace near the heating element. The temperature of the vessel could be controlled to within $\pm$ 0.1° C. by the Fisher model 44, but within $\pm 1^{\circ}$ C. by the Honeywell temperature controller.

The catalyst was placed at the bottom of the vessel, and its temperature was measured by the thermocouple W_2 attached to the bottom and connected to a Honeywell potentiometer. The thermocouple and the potentiometer were calibrated at 0° and 100° C.

The other three sections were all connected to the standard high vacuum system through a manifold. The high vacuum was obtained by a mercury diffusion pump D, backed by

Figure 5. Schematic diagram of the apparatus

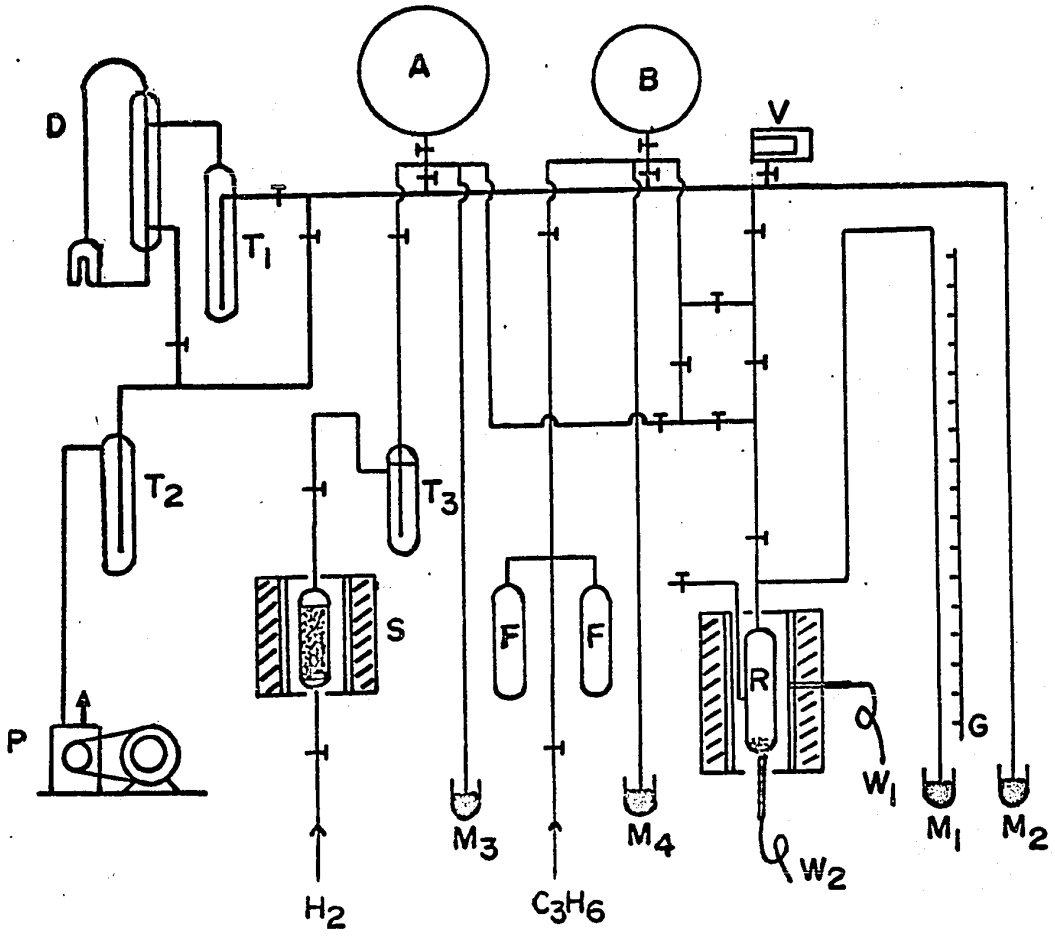

A = hydrogen reservoir
B = propylene reservoir
D = mercury diffusion pump
F = fractional bulbs
G = mirror scale
M_1, M_2, M_3, and M_4 = mercury manometers
P = oil vacuum pump
R = reaction vessel
S = palladium-asbestos vessel
T_1, T_2, and T_3 = liquid nitrogen traps
V = vacustat
W_1 = thermistor or thermocouple wires connected to temperature controllers
W_2 = thermocouple wire connected to potentiometer
⊣ = stopcock

a rotary oil pump P. Two liquid nitrogen traps T_1 and T_2 were used for condensing organic compounds and thus accelerating the pumping speed. The vacuum attained by the system was measured by Vacustat V, manufactured by Edwards Co. Vacustat V was connected at the other end of the manifold. A vacuum of 0.001 mm. Hg could be obtained in the apparatus in 5-10 minutes.

B. Purification of Reactants

1. Hydrogen:

Hydrogen in cylinders supplied by Linde Co. was purified before use. It was first passed over a palladium-asbestos catalyst in the vessel S at a temperature of about 200°C. The purpose of this was to convert residual oxygen left in the previously evacuated connection hose, and oxygen impurity(less than 0.005% as noted)in the cylinder hydrogen into water vapour. Water thus formed was condensed in the liquid nitrogen trap T_3. To prevent continuous infiltration of atmospheric air into the hydrogen stream through the connections, the upper part of the vessel was kept at 3 psig. The purified hydrogen was first pumped out for fifteen minutes, and then was stored in the bulb A or used as such for reduction of the catalysts. It usually took about 3 hours to fill the 5-litre bulb A with purified hydrogen at 1 atmosphere pressure.

2. Propylene:

A C.P. grade propylene cylinder from Matheson Co. was used. Propylene from the cylinder was introduced to the fractional distillation system and condensed in one of the two fractionating bulbs F (Figure 5) by liquid nitrogen. The gas was released on gentle warming. The head and tail fractions were rejected and the middle fraction condensed in the second liquid nitrogen trap. The second trap was warmed and the middle fraction containing pure dry propylene was collected and stored in the 3-litre reservoir B.

C. Preparation of Catalysts

Catalysts of group VIII metals were all supported on pumice, which is an inert porous carrier with a low surface area, less than 1 m^2 gm. $^{-1}$ [10]. In order to investigate the kinetics of catalytic hydrogenation of propylene over a series of catalysts, and to compare their activities thereafter, it was essential to prepare all the catalysts in the same manner as far as possible.

Since all the catalysts, except osmium (due to its peculiar physical properties), were prepared in the same way, only the procedure for the preparation of the nickel and osmium catalysts is described in detail here. The catalysts studied in the present work are given in Appendix A. General information about the preparation of the catalysts has been given by Ciapetta and Plank[13].

1. Preparation of Nickel Catalyst

The pumice-supported nickel catalyst (10% by weight of nickel) was prepared by impregnating 20-40 mesh crushed pumice stone, supplied by Fisher Scientific Co., with nickel nitrate solution. The pumice stones were cleaned by boiling with concentrated hydrochloric acid for half an hour, and washed with warm distilled water until the addition of a silver nitrate solution did not give any precipitate. The pumice granules were dried in an oven at 105° C. for about 10 hours. Nickel nitrate solution containing 4.9532 grams of $Ni(NO_3)_2 . 6H_2O$, or equivalent to 1 gram of nickel, was mixed with 9 grams of pumice granules in a crucible. The mixture was vigorously stirred for one hour and slowly evaporated to dryness in an oven at 105° C. for at least 10 hours at 400° C. in a muffle furnace.

2. Preparation of Osmium Catalyst

It is known[32, 44] that osmium has a remarkable tendency to combine with oxygen to form the volatile tetroxide even at room temperature. Therefore, the method described above for the preparation of nickel catalyst could not be used to prepare the osmium catalyst. Osmium catalysts were generally prepared by reducing an aqueous solution of osmium salts, or of osmium tetroxide by an alkali formate[32]. In this work ammonium chlorosmate $(NH_4)_2OsCl_6$, which does not decompose below 170° C., was used. It could be reduced to osmium sponge when heated in hydrogen. Furthermore, it is sparingly soluble in water[32, 44].

Pumice-supported osmium catalyst was prepared as follows: a weighed 20-40 mesh pumice stone was impregnated with an aqueous solution of a known amount of ammonium chlorosmate in a flask. The mixture was placed in a water bath, and dried in a stream of nitrogen. The dried pumice-supported salt was then stored in a bottle for future use.

D. Reduction and Aging of Catalysts

A weighed amount of the catalyst was placed on the bottom of reaction vessel and the vessel sealed. After the reactor had been evacuated to below 0.001 mm. Hg. at 400°C., purified hydrogen was admitted into the reaction vessel. The catalyst thus underwent reduction in a stream of hydrogen (approximately at the rate of 6 liters per hour) at 400°C. for 10 hours. Water vapour or HCl vapour formed was expelled by the hydrogen stream. After 10 hours, the flow of hydrogen was stopped and the vessel allowed to cool to 30°C.

Each fresh catalyst sample was extremely active, but its activity decreased exponentially run after run before a stable value was reached. This time lapse before the catalyst gets stabilized is generally known as the aging period. The time required for the aging of the catalyst generally depends on the method of treatment and the nature of the

catalyst itself. In the present study, the aging or stabilization of the catalyst was attained by hydrogenating the olefin over the catalyst for a sufficient period at 30° C., so that no further drop in activity was observed. The initial pressures of hydrogen and propylene used for such stabilization were always 120 and 30 mm. Hg., respectively.

For platinum, it required only 15 runs before the catalyst became stabilized, whereas for most of the catalysts studied, more than 30 runs were necessary. In some cases when the reaction was either too fast or too slow to be measured over the temperature range (30° - 160° C.), a new estimated amount of catalyst was used. This new catalyst was reduced and aged similarly.

The aging curve of the platinum catalyst is given in Figure 6. It is readily seen that the activity of the catalyst after aging was much less than that at the beginning. The reason for this has been discussed by Beeck, Rideal, et al. (see Chapter II-A).

E. Experimental Procedure

The required weight of the catalyst was placed in the reaction vessel, and was reduced in the way described previously. At the start of the run, the hydrogen in the reaction vessel was pumped off and a high vacuum (less than 0.001 mm. Hg.) was obtained. The reactants were admitted in succession. After one of the reactants was admitted to the reaction vessel, the connecting lines between the reaction vessel and storage vessels were evacuated for 2 minutes. The second reactant was then admitted. In most of the runs, hydrogen was admitted first.

Hydrogen was introduced into the reaction vessel prior to propylene so as to avoid undesired access of olefin to catalyst. The 15-minute evacuation time of the reaction

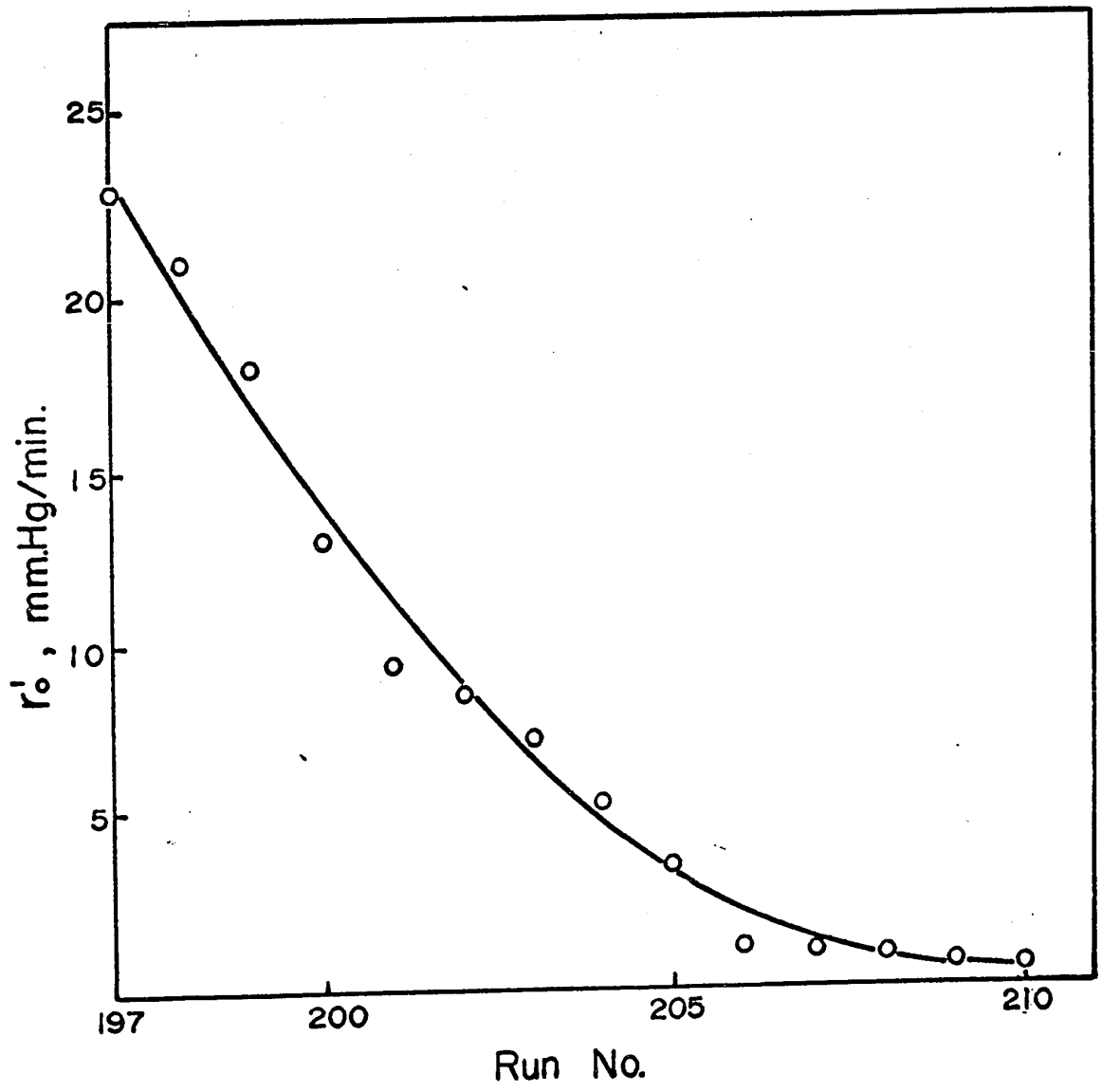

Figure 6. Aging curve of platinum-pumice catalyst for propylene hydrogenation

Temperature = 30° C., P_{H_2} = 120 ± 1 mm. Hg, $P_{C_3H_6}$ = 30 ± 1 mm. Hg
(Run number 197 is the first run over the catalyst. See Table 9.)

vessel was arbitrarily set. It was observed that a vacuum in the reaction vessel of the order of 0.001 mm. Hg. could be obtained in less than 10 minutes.

The following procedure was adopted for studying the kinetics of the catalyst:

1. The dependence of reaction rates on the initial hydrogen pressure P_{H_2} was investigated at several temperatures by taking a series of runs at constant initial pressure of propylene (at 30 mm. Hg.) while the hydrogen pressure was varied.

2. The dependence of reaction rates on the initial propylene pressure $P_{C_3H_6}$ was investigated at several temperatures by taking a series of runs at constant P_{H_2} while $P_{C_3H_6}$ was varied.

At a particular temperature, a series of runs were made at random, in order to reduce experimental error to a minimum in the evaluation of the reaction order due to the change of the catalytic activity. In the present study, reactions between 120 mm. Hg. of hydrogen and 30 mm. Hg. of propylene were considered as standard runs. The activity of the catalyst was checked periodically by the rates of these standard runs.

It was found that once a catalyst had been aged to stable activity, it remained fairly stable for several days. It was considered desirable to finish the runs in as short a time as possible. Usually, the necessary runs at two or three different temperatures were made in a day. In between a series of runs, the catalyst was left in hydrogen at a pressure of 100 mm. Hg.

The catalytic hydrogenation of propylene was studied over various catalysts between 40° and 200° C. for 20-240 mm. Hg. of hydrogen and 15-200 mm. Hg. of propylene.

F. Chromatographic Analysis

Previous workers[1, 23, 28, 40, 45] reported that at moderate temperature neither any side reaction nor pyrolysis was observed in the hydrogenation of propylene. In the hydrogenation reactions over palladium, iron, cobalt and osmium in the present study, some qualitative sample analyses have been done by means of a Perkin Elmer Vapour Fractometer. The results obtained in these analyses agreed very well with those reported by the previous workers.

A typical analysis chart for run number 263 is shown in Figure 8, in which the specifications of the analyzer and operating conditions are also listed. The presence of an excess amount of hydrogen in the sample resulted in the formation of a peak, though the conductivity of hydrogen is very close to that of helium.

Since two moles of reactants produce one mole of product, the rate of reaction can be simply expressed as:

$$r = \frac{dP_{C_3H_8}}{dt} = -\frac{dP}{dt} \qquad \text{(III -1)}$$

where $P_{C_3H_8}$ is the pressure of propane formed, and P, total pressure in the reactor.

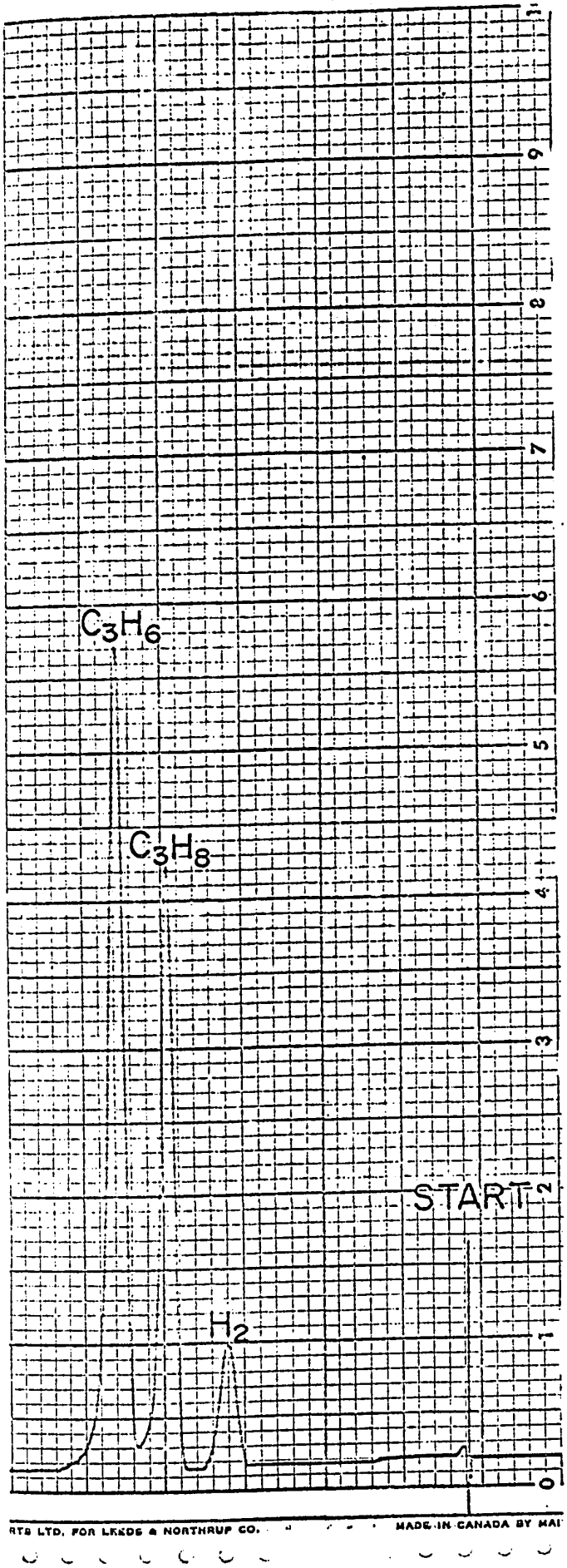

Figure 7. Typical Analysis of Chromatographic Analysis

Instrument: Perkin-Elmer Vapor Fractometer Model 154
Column length: 12 ft.
Column material: 2, 5-hexane-dione on 60/80 mesh fire brick
Column temp.: 0° C.
Carrier gas: Helium
Flow meter: 5.5 cm
Detector Temp.: 30° C.
Detector voltage: 8 V.
Recorder: 10 uV.
Chart speed: 0.5 in./min.

Sample: Run number 263 (Table 10)
Initial hydrogen pressure: 240.0 mm. Hg
Initial propylene pressure: 30.0 mm. Hg
Catalyst: 0.5% palladium-pumice
Time elapsed after the start of the experiment when sample was taken: 2 min.

IV. RESULTS

A. Interpretation of Experimental Data

The Power Rate Law (see Chapter II-B) was used to correlate the experimental results. It was found to be satisfactory for calculating the kinetic parameters in the experimental ranges studied, except at very low pressures of propylene.

According to the Power Rate Law, the initial rate of the reaction, r_0, can be expressed as:

$$r_0 = kP_{H_2}{}^m P_{C_3H_6}{}^n \qquad \text{(IV-1)}$$

$$= A \exp(-E/RT) \qquad \text{(IV-2)}$$

E is the activation energy, k is the rate constant, and A is the frequency factor. P_{H_2} and $P_{C_3H_6}$ represent the initial pressures of hydrogen and propylene, respectively. The exponents m and n are the orders of the reaction with respect to hydrogen and propylene, respectively. The units of r_0 and A are mm. Hg/(min. -gm. metal).

Since it was impossible to obtain a measurable reaction rate (less than 15 mm. Hg/min.) at moderate temperature by using 1 gm. of metal in this system, the initial rates r_0' obtained by the experiments are based on the particular weight of the metal used. Therefore, r_0 can be estimated by the following relationship:

$$r_0 = r_0' / (\text{weight of metal}) \qquad \text{(IV-3)}$$

The initial rate r_0' of the reaction over a catalyst is the slope of the curve of total pressure drop versus reaction time. The kinetic parameters m, n, E and A can be estimated if the values of the initial rates at various conditions, i.e., reaction temperature, reactant pressure, are available. At a particular reaction temperature, the pressure exponents m and n are determined by the slopes of Log r_0' vs. Log P_{H_2} at constant $P_{C_3H_6}$

and of Log r_0' vs. Log $P_{C_3H_6}$ at constant P_{H_2} as shown in the following equations:

$$m = \left(\frac{d \text{ Log } r_0'}{d \text{ Log } P_{H_2}} \right)_{T,\ P_{C_3H_6}} \qquad \text{(IV-4)}$$

and

$$n = \left(\frac{d \text{ Log } r_0'}{d \text{ Log } P_{C_3H_6}} \right)_{T,\ P_{H_2}} \qquad \text{(IV-5)}$$

The activation energy E is calculated from the slope of the Arrhenius plot of Log r_0 against 1/T as expressed by the following equation:

$$E = -2.303\ R \left(\frac{d \text{ Log } r_0}{d(1/T)} \right)_{P_{H_2},\ P_{C_3H_6}} \qquad \text{(IV-6)}$$

In the present study, the logarithmic values of the initial rates of standard runs r_{0S}, i.e., the initial rates measured at 120 mm. Hg of hydrogen and 30 mm. Hg of propylene, were chosen for this plot. The frequency factor A can then be estimated from equation (IV-2).

The experimental data in the present work are shown in Appendix B. Sample calculations of the kinetic parameters of the hydrogenation of propylene over the platinum-pumice catalyst are given in Appendix C.

In the experimental data reported in Appendix B, the pressures could be measured with an accuracy of ± 0.3 mm. Hg. At moderate rates of 10 mm. Hg/min., the error in the observed reaction rate would be of the order of ± 3%. The error of the pressure dependency orders is within ± 0.05 for all catalysts, except for osmium. Due to the scattering of the data, the error of the pressure dependency orders amounts to ± 0.2 for osmium.

In all cases, the method of least squares was employed for estimating the activation energy and the frequency factor. The probable errors of activation energy and frequency factor thus calculated depend on the experimental data for each catalyst. In general, the results show that the probable error in the activation energy E is within $\pm$ 10% and that of Log A within $\pm$ 5 %.

B. Reaction over Nickel

The experimental data obtained for the hydrogenation of propylene over 0.460 gm. of 10% nickel-pumice catalyst are given in Table 6.

The reaction had a measurable rate at 60° C. in the pressure ranges of the reactants studied. When the catalyst attained a constant activity, the data were taken. The pressure-fall against time curves observed at 80° C. for the various ratios $\bar{R}$ of initial hydrogen pressure to initial propylene pressure, are shown in Figure 8. It can be seen that the pressure decreases linearly with reaction time at the initial stage. The initial rates can thus be obtained from the slopes of these lines.

The dependence of the initial rate on the initial hydrogen and propylene pressures at various temperatures is shown in Figures 9 and 10. The reaction order with respect to hydrogen is one (Figure 9) and with respect to propylene, zero (Figure 10). These results are consistent with the findings of most of the investigators for the hydrogenation of ethylene on the nickel catalysts. The reaction rate, therefore, can be expressed as:

$$r = k (P_{H_2})^{1.0} (P_{C_3H_6})^{0.0} \qquad \text{(IV-7)}$$

The Arrhenius plot of log r_{os} against 1/T for the reaction between the temperature range of 50° to 100° C. (Figure 11) gives an activation energy of 13 kcal/mole, and a frequency

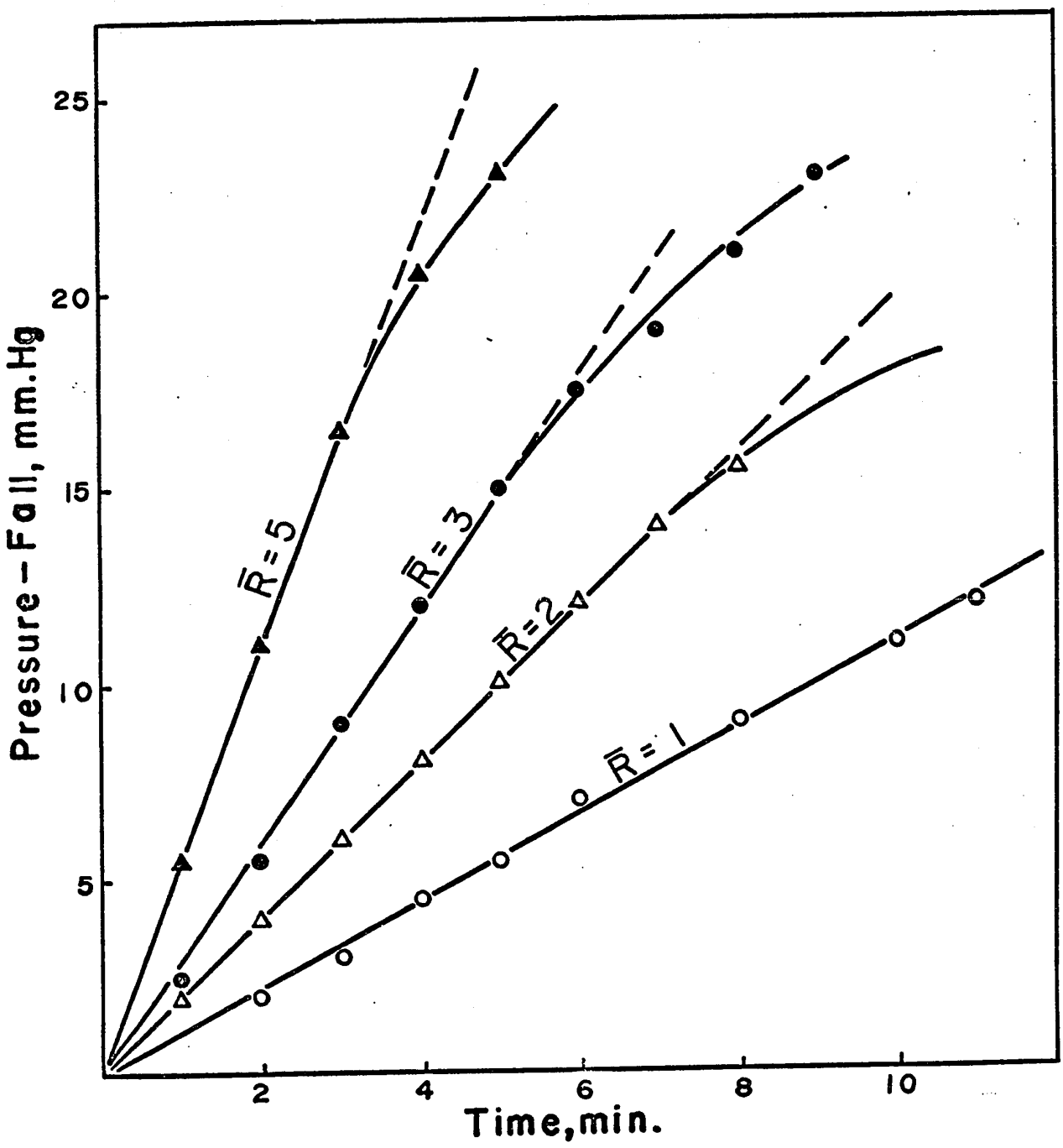

Figure 8. Pressure-fall against time curves for propylene hydrogenation over nickel-pumice catalyst at 80° C.

○ Run number 10 △ Run number 8
◉ Run number 9 ▲ Run number 13
$\bar{R} = P_{H_2} / P_{C_3H_6}$
Weight of nickel used = 4.48×10^{-2} gm.

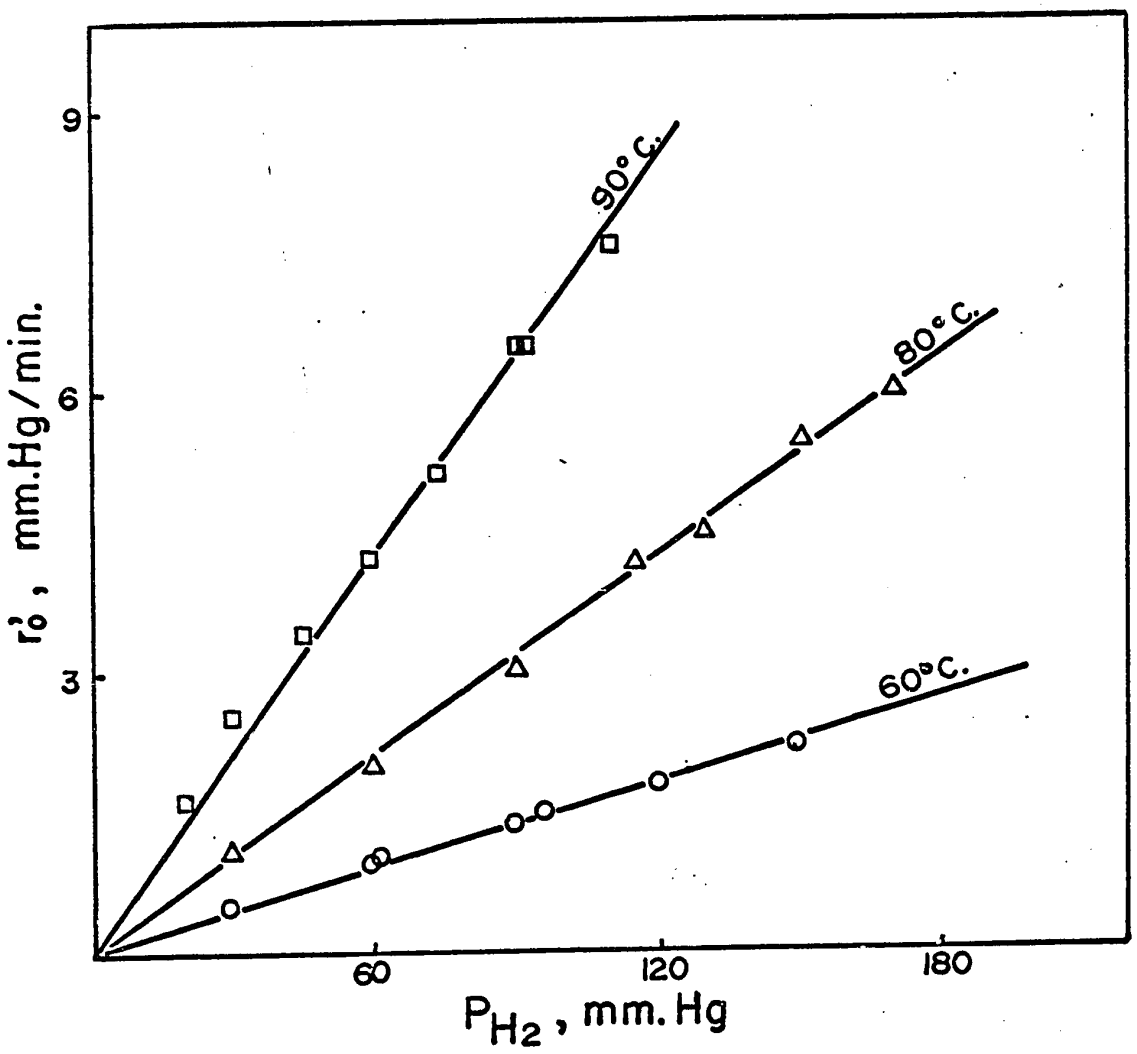

Figure 9. The dependence of initial rate on initial hydrogen pressure over nickel-pumice catalyst

$P_{C_3H_6}$ = 30 ± 1 mm. Hg
Weight of nickel used = 4. 48 x 10^{-2} gm.

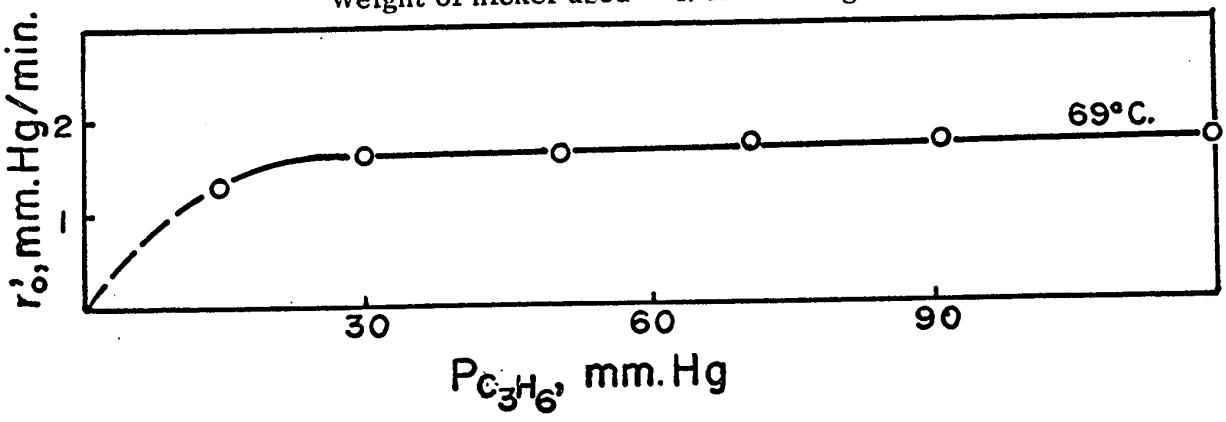

Figure 10. The dependence of initial rate on initial propylene pressure over nickel-pumice catalyst

P_{H_2} = 60 ± 1 mm. Hg
Weight of nickel used = 4. 48 x 10^{-2} gm.

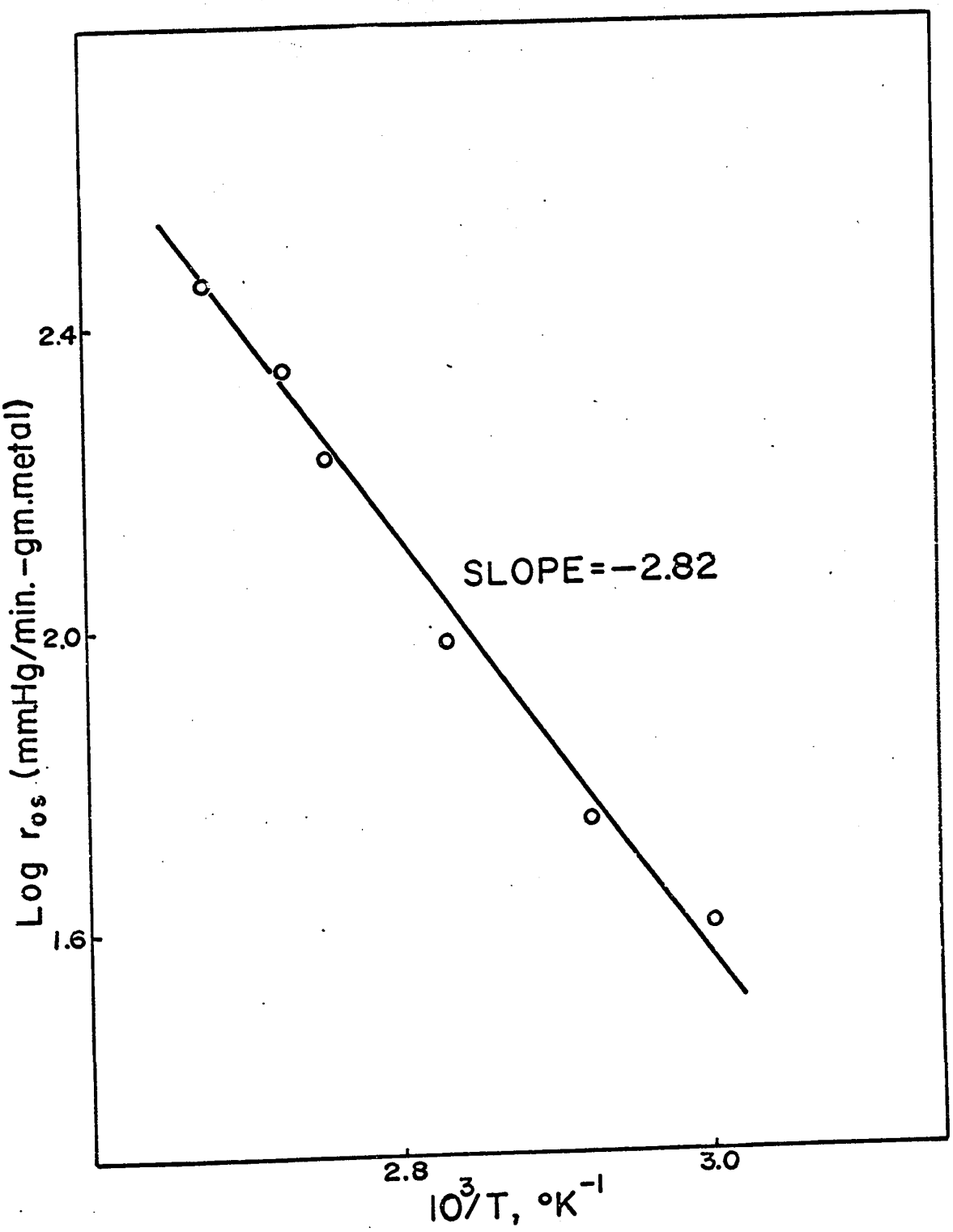

Figure 11. Arrhenius plot for propylene hydrogenation over nickel-pumice catalyst

factor of 1.0×10^{10} mm. Hg/(min. -gm. metal).

C. Reaction over Iron

The experimental data obtained for the hydrogenation of propylene over 0.785 gm. of 20% iron-pumice catalyst are listed in Table 7. The reaction had a measurable rate at 50° C. When the catalyst attained a constant activity, the data were taken. The pressure-time curves were of the same shape as obtained with the nickel-pumice catalyst.

The dependence of the initial rate on the initial hydrogen pressure at various temperatures is shown in Figure 12. Over the iron-pumice catalyst, the reaction order with respect to hydrogen is 0.65. An interesting result, however, was observed while studying the dependence of the initial rate on the initial propylene pressure $P_{C_3H_6}$. When the initial hydrogen pressure P_{H_2} is kept constant (Figure 13), the initial rate r_0 increases exponentially with increased $P_{C_3H_6}$ in the low pressure range, and then attains a constant value at a certain $P_{C_3H_6}$. This pressure depends on the reaction temperature and P_{H_2}. The higher the temperature, the greater is the value of $P_{C_3H_6}$ required for r_0' to reach to the constant rate. This can be seen by comparing the r_0' vs. $P_{C_3H_6}$ curves at various temperatures, when P_{H_2} is kept constant at 60 mm. Hg. (Figure 13). Similarly when P_{H_2} increases, the required $P_{C_3H_6}$ increases proportionally. As shown in Figure 13, r_0' reaches a constant value around $P_{C_3H_6}$ of 60 mm. Hg. and P_{H_2} of 60 mm. Hg. at 19°C. However, r_0' reaches a constant value around $P_{C_3H_6}$ of 120 mm. Hg. at the same temperature, when P_{H_2} is raised to 120 mm. Hg. Constable[14] reported a similar phenomenon, while studying the hydrogenation of ethylene over a copper catalyst.

It was noted that when propylene was first admitted into the reaction vessel, the rate was somewhat smaller than when hydrogen was admitted first. In some cases,

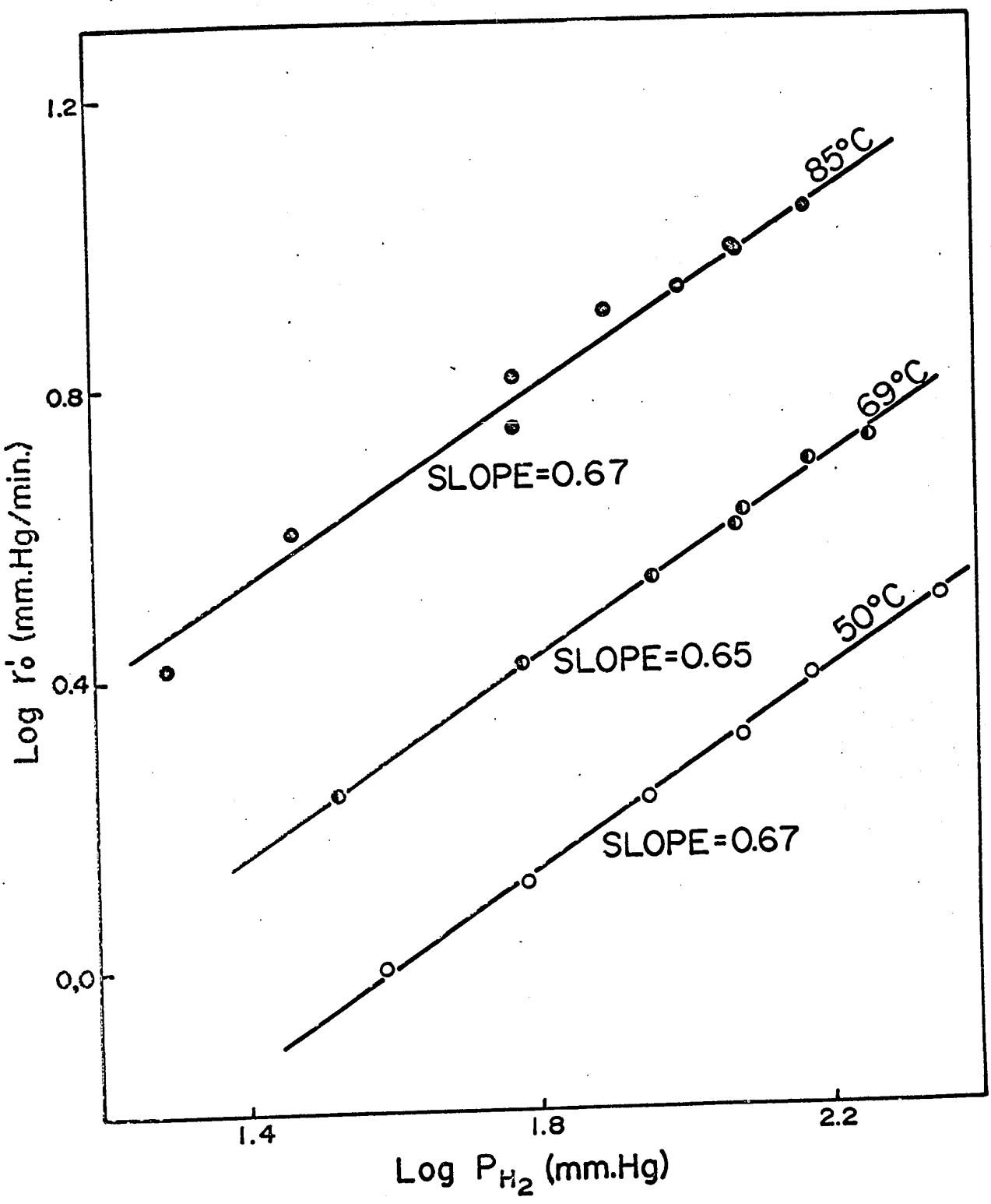

Figure 12. The dependence of initial rate on initial hydrogen pressure over iron-pumice catalyst

$P_{C_3H_6}$ = 30 ± 1 mm. Hg
Weight of iron used = 14.52 x 10^{-2} gm.

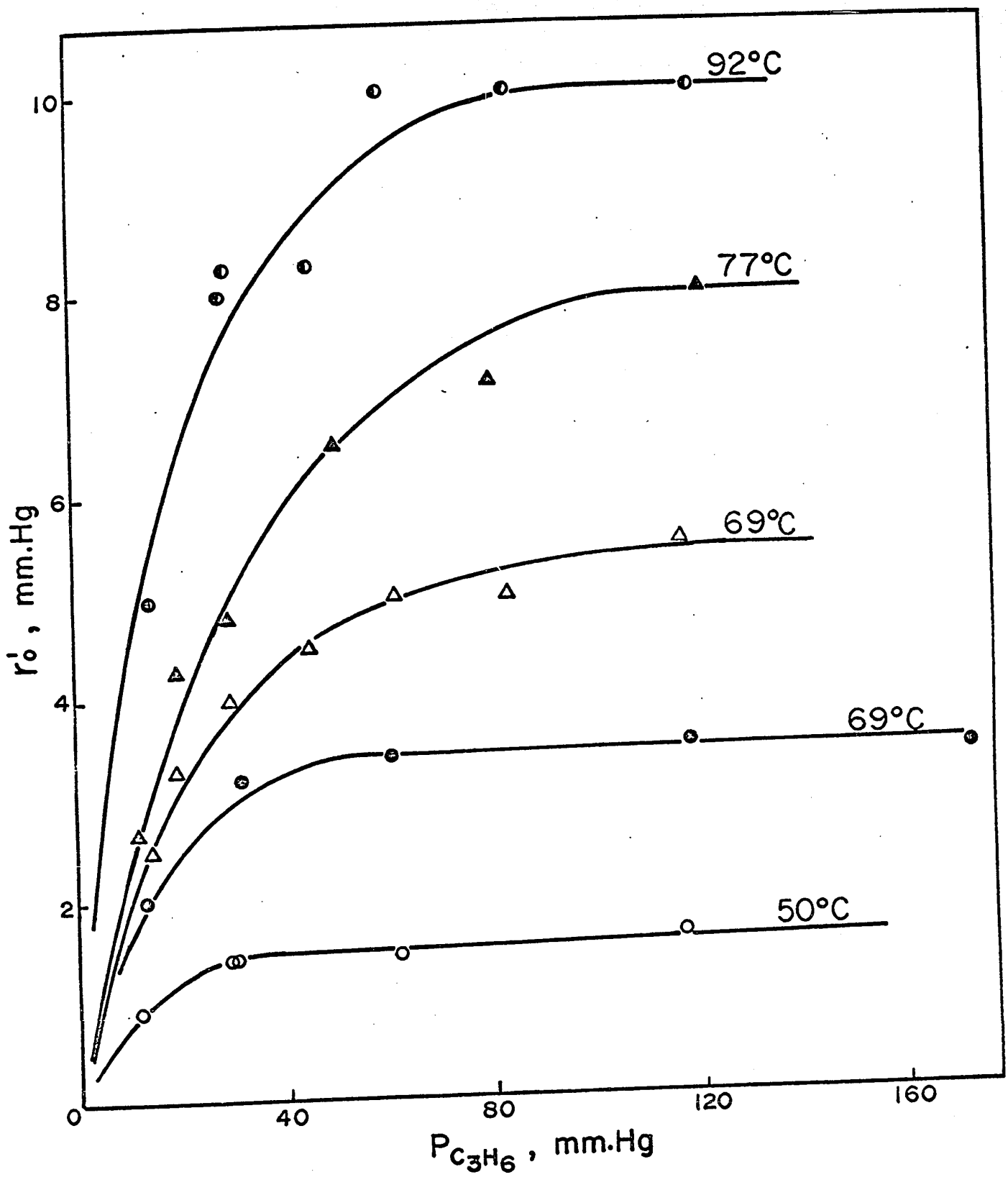

Figure 13. The dependence of initial rate on initial propylene pressure over iron-pumice catalyst

○, ◎, ◉ P_{H_2} = 60 ± 1 mm. Hg
△, ▲ P_{H_2} = 120 ± 1 mm. Hg
Weight of iron used = 14. 52 x 10^{-2} gm.

complete inhibition also resulted[39, 46]. In the present study, a 10% decrease in the reaction rate resulting from admitting propylene first was observed (run numbers 129 to 133, Table 7).

The Arrhenius plot of log r_{os} against 1/T for the reaction between 50° and 92° C. (Figure 14) gives an activation energy of 10 kcal/mole. The corresponding value of the frequency factor is 7.7×10^7 mm. Hg/(min.-gm. metal). Over the iron-pumice catalyst, the reaction rate can be expressed as:

$$r = k (P_{H_2})^{0.65} (P_{C_3H_6})^{0.0} \qquad \text{(IV-8)}.$$

D. Reaction over Cobalt

Over 0.900 gm. of 10% cobalt-pumice catalyst, the reaction had a measurable rate at 52° C. When the catalyst attained a constant activity, the series of runs were carried out. The experimental data are given in Table 8. The shapes of the pressure-time curves with the cobalt-pumice catalyst are similar to those obtained with the nickel-pumice catalyst.

The dependence of initial rate on the initial hydrogen and propylene pressures for various temperatures is shown in Figure 15. The orders of the reaction with respect to hydrogen and propylene are 0.95 and zero, respectively. Therefore, the reaction rate is expressed by the equation:

$$r_0 = k (P_{H_2})^{0.95} (P_{C_3H_6})^{0.0} \qquad \text{(IV-9)}$$

Interestingly enough, the initial rates of the standard runs at 125° C. (run numbers 183, 184, Table 8) were found to be similar to those at 109°C. (run numbers 178, 182, Table 8). As a result of this, in the Arrhenius plot (Figure 16), the linear relationship between log r_{os} and 1/T does not hold beyond 100° C. It appeared that beyond 100° C., the catalyst started getting deactivated. As mentioned previously, this phenomenon was reported

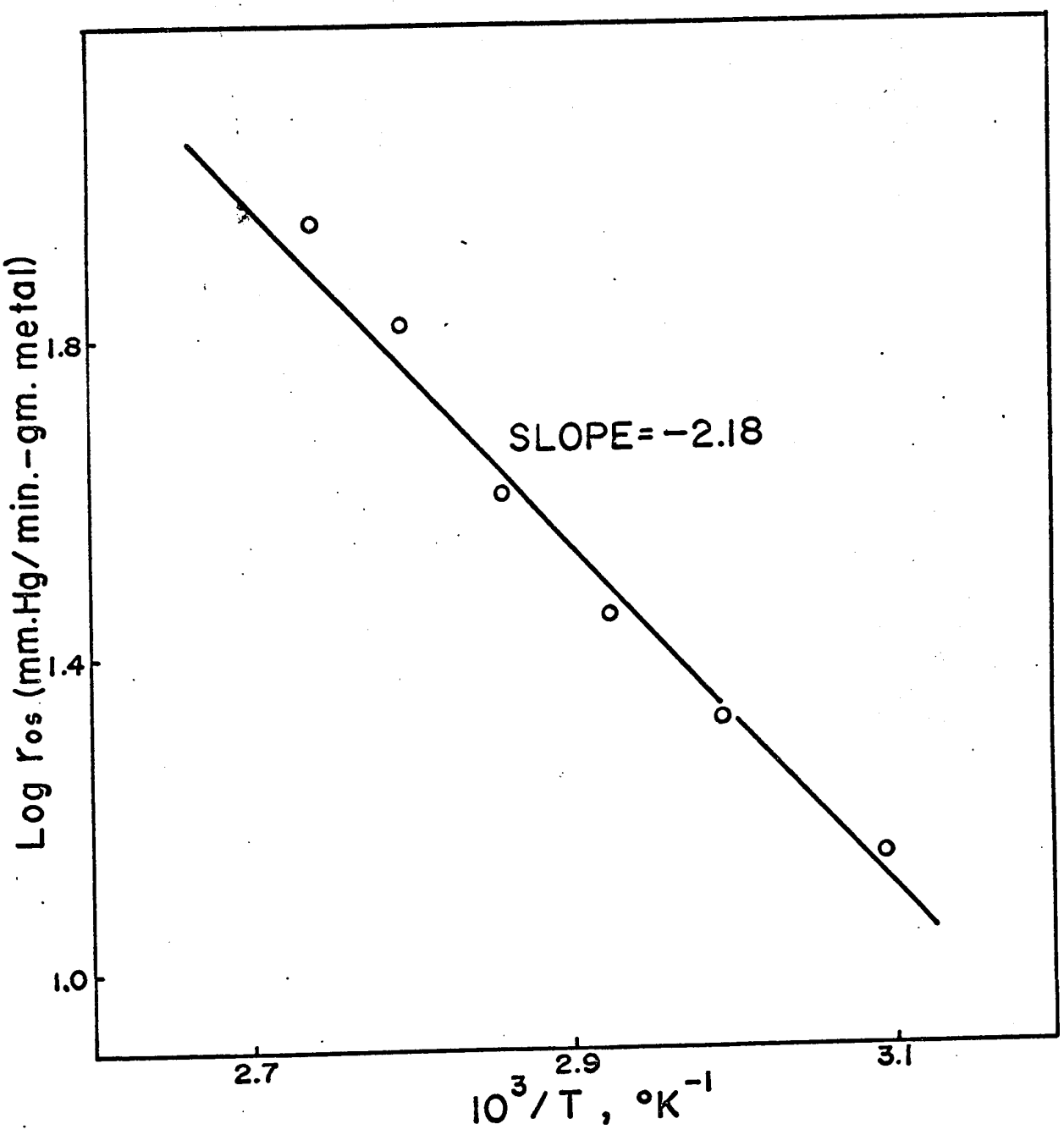

Figure 14. Arrhenius plot for propylene hydrogenation over iron-pumice catalyst

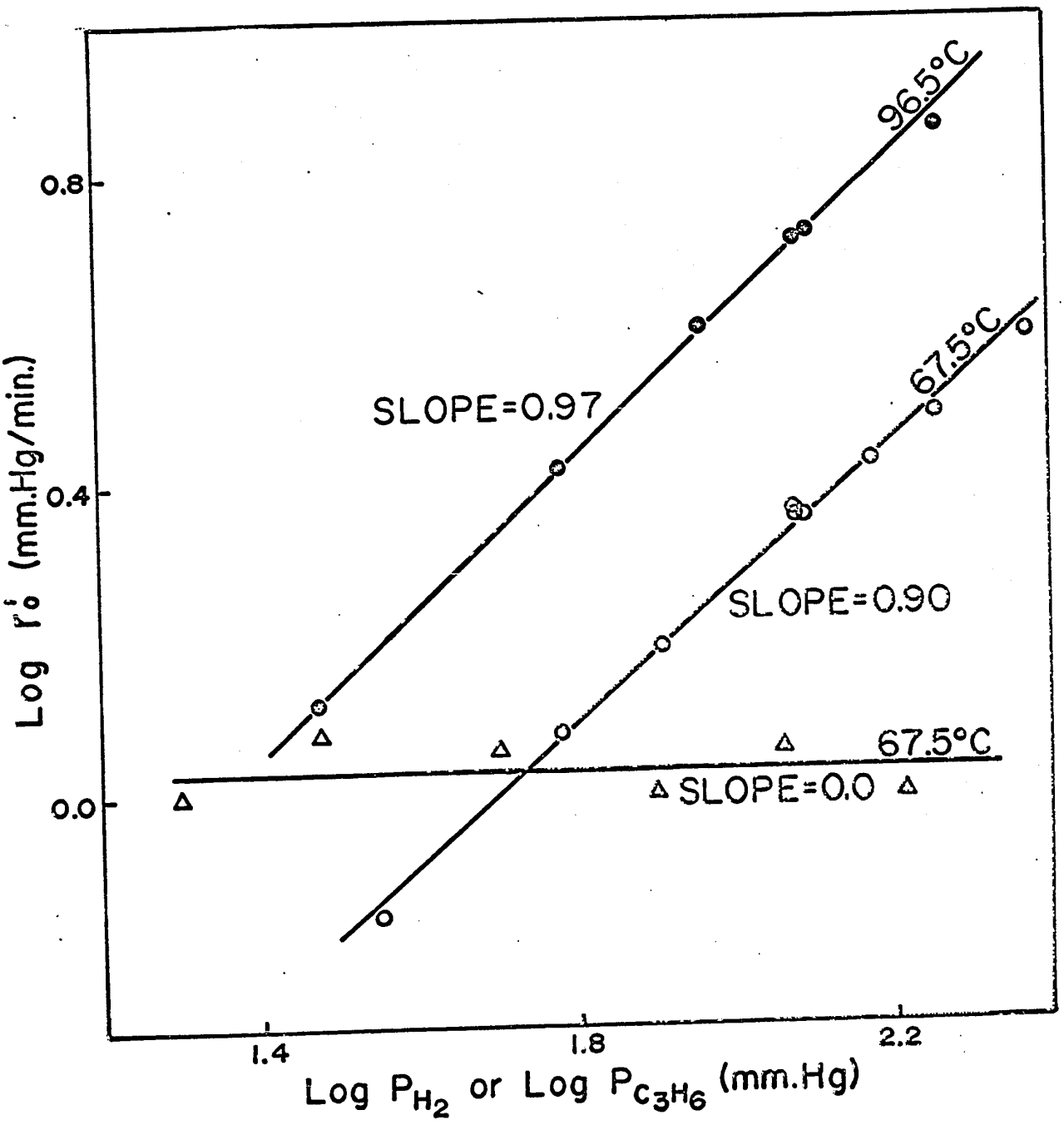

Figure 15. The dependence of initial rate on initial hydrogen and propylene pressures over cobalt-pumice catalyst

○,● Log r_0' vs. Log P_{H_2}, $P_{C_3H_6}$ = 30 ± 1 mm. Hg
△ Log r_0' vs. Log $P_{C_3H_6}$, P_{H_2} = 120 ± 1 mm. Hg
Weight of cobalt used = 8.76 x 10^{-2} gm.

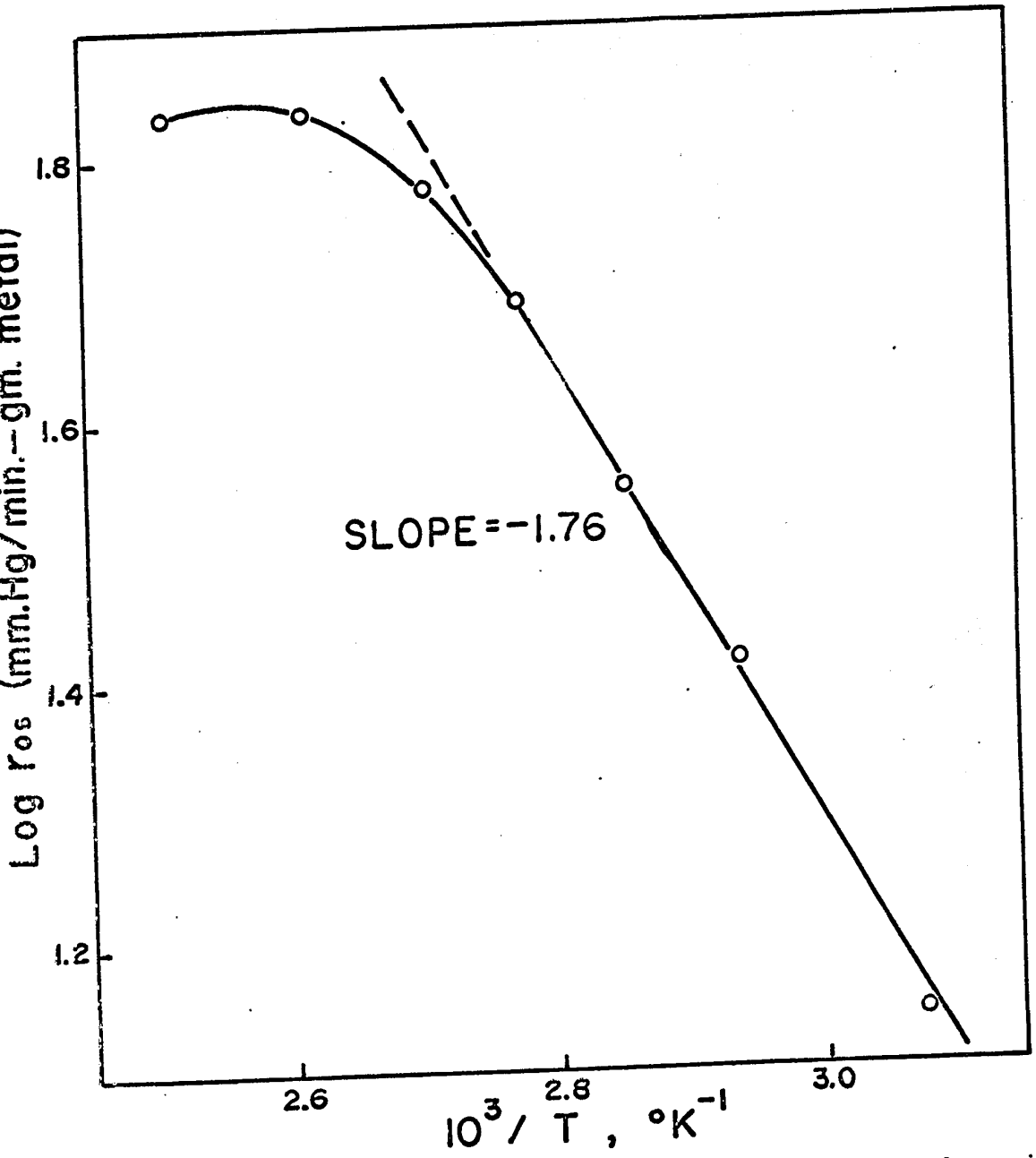

Figure 16. Arrhenius plot for propylene hydrogenation over cobalt-pumice catalyst

for the hydrogenation of ethylene by several workers[27, 53, 56]. The falling-off of the catalytic activity at higher temperatures was attributed to the desorption of reactants.

Below 100°C., the Arrhenius plot (Figure 16) gives an activation energy of 8.1 kcal/mole, and a frequency factor of 3.6×10^6 mm. Hg/(min.-gm. metal).

E. Reaction over Platinum

0.40 grams of 0.5% platinum-pumice catalyst (equivalent to 0.0020 grams of platinum) gave a measurable rate for the hydrogenation of propylene at 89° C. The catalyst attained a constant activity after 14 successive runs. Experimental data obtained are given in Table 9, and the aging curve is shown in Figure 6. Sample calculations of the kinetic parameters for the reaction over the platinum-pumice catalyst are given in Appendix C. The shapes of the pressure-time curves are similar to those obtained for the nickel-pumice catalyst.

The dependence of the initial rate on the initial hydrogen and propylene pressures for various temperatures is shown in Figure 17. The orders of the reaction with respect to hydrogen and propylene are 0.80 and zero, respectively. The reaction rate can be expressed as:

$$r = k (P_{H_2})^{0.80} (P_{C_3H_6})^{0.0} \qquad \text{(IV-10)}$$

The activity of the catalyst was very stable throughout the investigation. No change in the catalytic activity was observed when the catalyst was left overnight in propylene at a pressure of 100 mm. Hg., instead of hydrogen.

The reaction is very sensitive to temperature, as indicated by the apparent activation energy of 16 kcal/mole, obtained from the slope of Arrhenius plot (Figure 18).

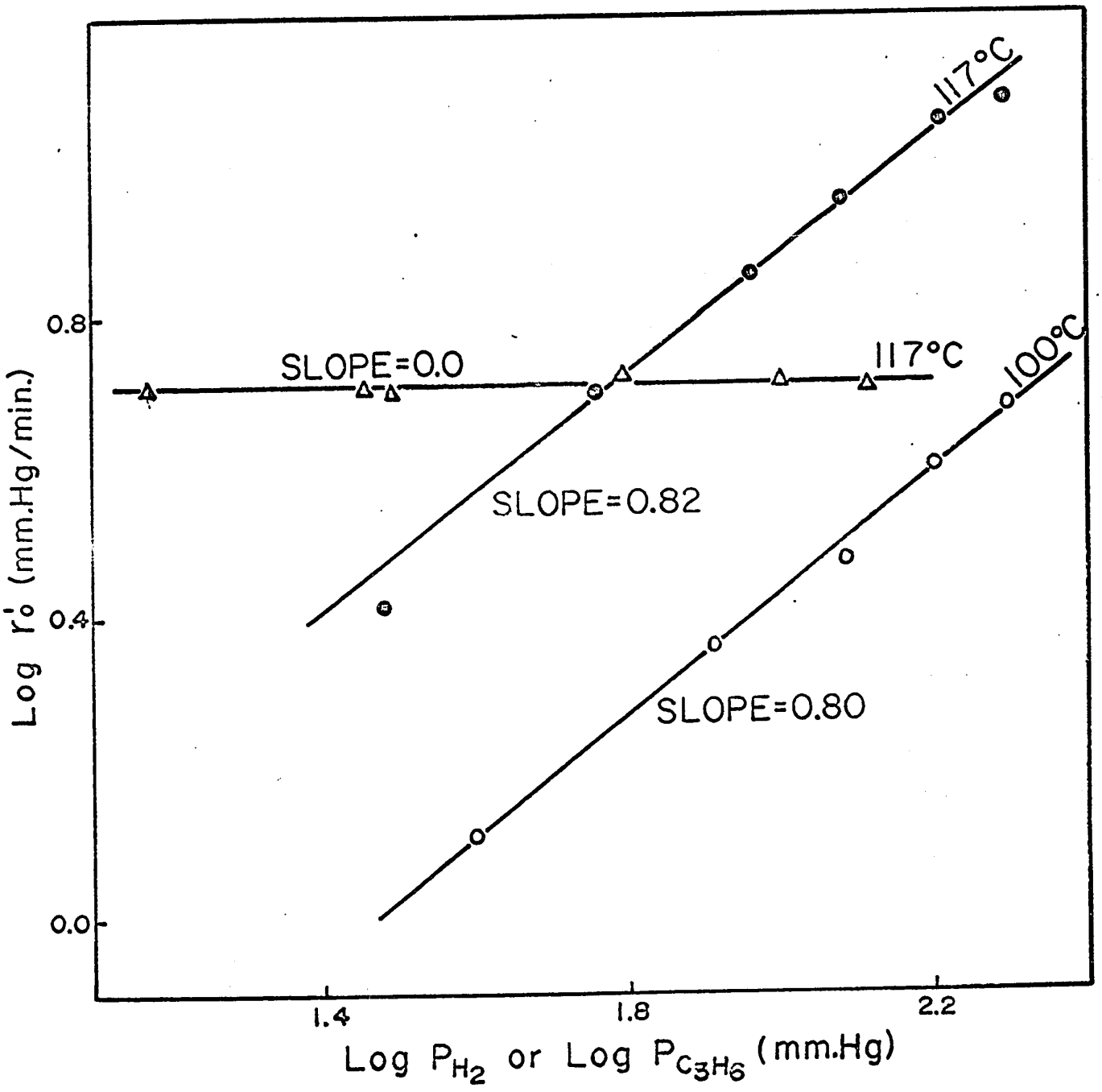

Figure 17. The dependence of initial rate on initial hydrogen and propylene pressures over platinum-pumice catalyst

○, ● Log r_0' vs. Log P_{H_2}, $P_{C_3H_6}$ = 30 ± 1 mm.Hg
△ Log r_0' vs. Log $P_{C_3H_6}$, P_{H_2} = 60 ± 1 mm.Hg
Weight of platinum used = 0.20×10^{-2} gm.

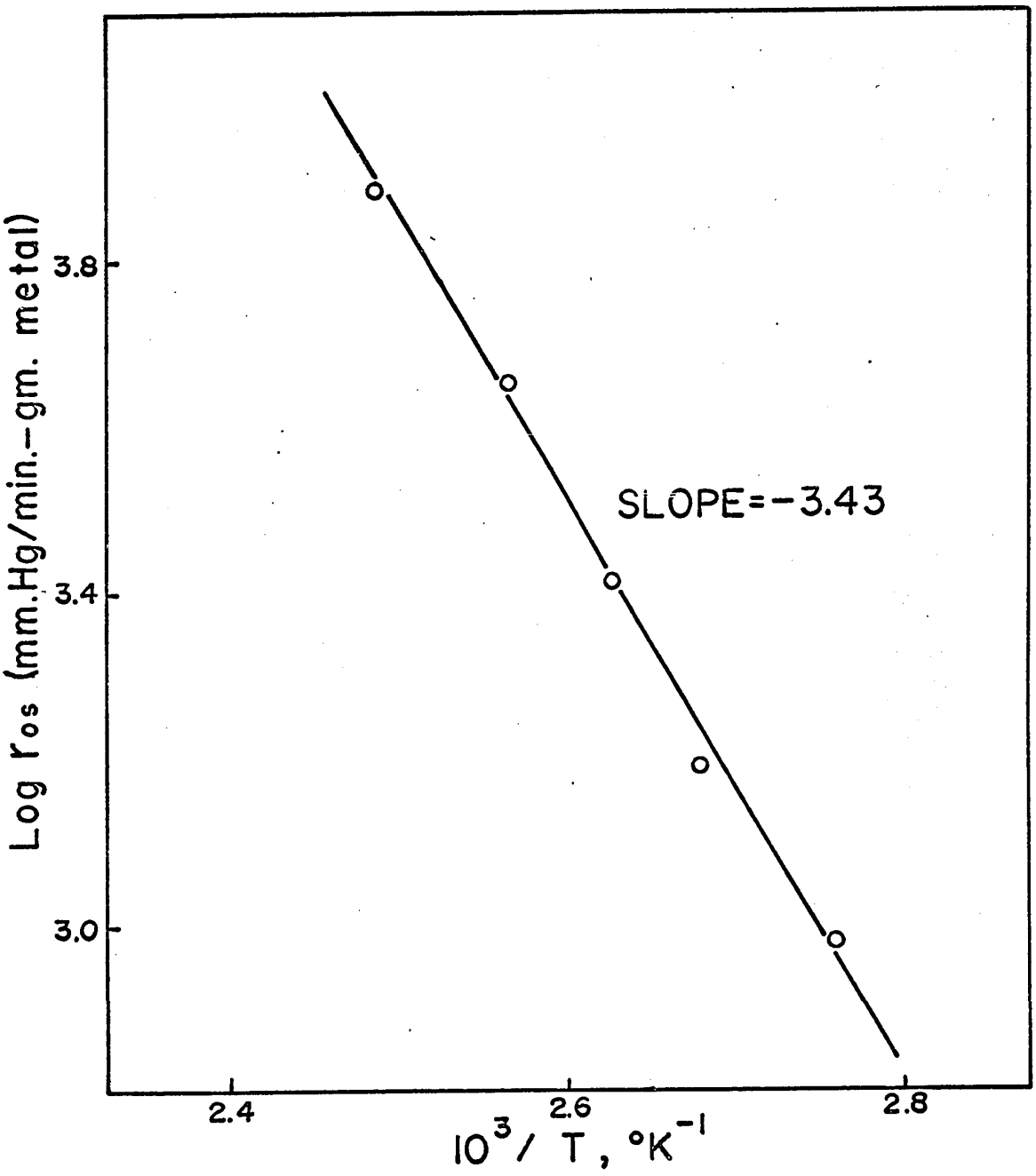

Figure 18. Arrhenius plot for propylene hydrogenation over platinum-pumice catalyst

The value of frequency factor is 2.5×10^{12} mm. Hg/(min. -gm. metal).

F. Reaction over Palladium

It was observed that the palladium-pumice catalyst gradually lost its ability to catalyse the hydrogenation of propylene. The unstable nature of the catalytic activity made the study of the reaction almost impossible. After careful investigation, it was found that the deactivation of the catalyst was probably due to the poisoning of the catalyst by mercury vapor.

Mercury could cover the surface of the catalyst and thus prevent surface reaction[10]. In the apparatus (Figure 5) used for the present study, mercury vapor was evidently present although the amount was small. The reactants were unavoidably contaminated with 0.01 mm. mercury vapor (vapor pressure of mercury at room temperature) from manometers M_3 and M_4. Furthermore, mercury from the manometers M_1 and M_2 was being continuously evaporated and condensed in the trap T_1 during the evacuation. This minute amount of mercury vapor (less than 0.01 mm. Hg.) might poison the palladium catalyst resting on the bottom of the reaction vessel during evacuation period, if the palladium catalyst has an affinity for mercury.

The poisoning of palladium catalyst by mercury vapor was recently studied by Bond and Wells[9]. The deactivation by mercury vapor was detected by measuring the hydrogenation rates of both acetylene and ethylene. Interestingly enough, they used the same apparatus as used in the present study, except that they put two taps between the reaction vessel and the manometer which were used to follow the reaction and to contribute mercury vapor as the poisoning substance. The intentional poisoning periods were the times allowed for the access of mercury vapor to the reaction vessel by opening the taps. They found that

mercury vapor affected the activity of palladium catalyst more severely for ethylene hydrogenation than for acetylene hydrogenation.

In order to determine whether mercury poisoning was the cause for deactivation of the palladium-pumice catalyst in the present work, a series of investigations were carried out. Each new sample of the catalyst was reduced and studied as usual. A linear relationship, similar to the result obtained by Bond and Wells[10], was found to exist when $\log \frac{(r_0)n}{(r_0)1}$, the logarithmic value of the initial rate ratio of the run number n and the first run, is plotted against the total time of evacuation. The results are shown in Figure 19.

Catalysts A and B were studied under similar conditions, except that in the case of A, the stopcock before the mercury vacuum gauge V (Figure 5), was opended to the system in order to contribute more mercury vapor to the system. The result showed that catalyst A became poisoned much faster than catalyst B. Catalyst C was studied at 118°C., and the result with this catalyst indicated that the higher the temperature, the faster the poisoning, confirming the result of Bond and Wells[10], which is shown in Figure 20 for comparison. If the poisoning was due to the adsorbed propylene then the deactivation of the catalyst should not be faster at higher temperatures, since the adsorption rates of the olefin are slower at higher temperatures as compared to lower temperatures.

From the foregoing investigations one might suspect that the mercury vapor might also affect the activities of other metals for hydrogenation. Bond and Wells[10] found that the platinum catalyst did not become deactivated by the mercury vapor. This finding was also confirmed by the present investigations of propylene hydrogenation over the pumice-supported

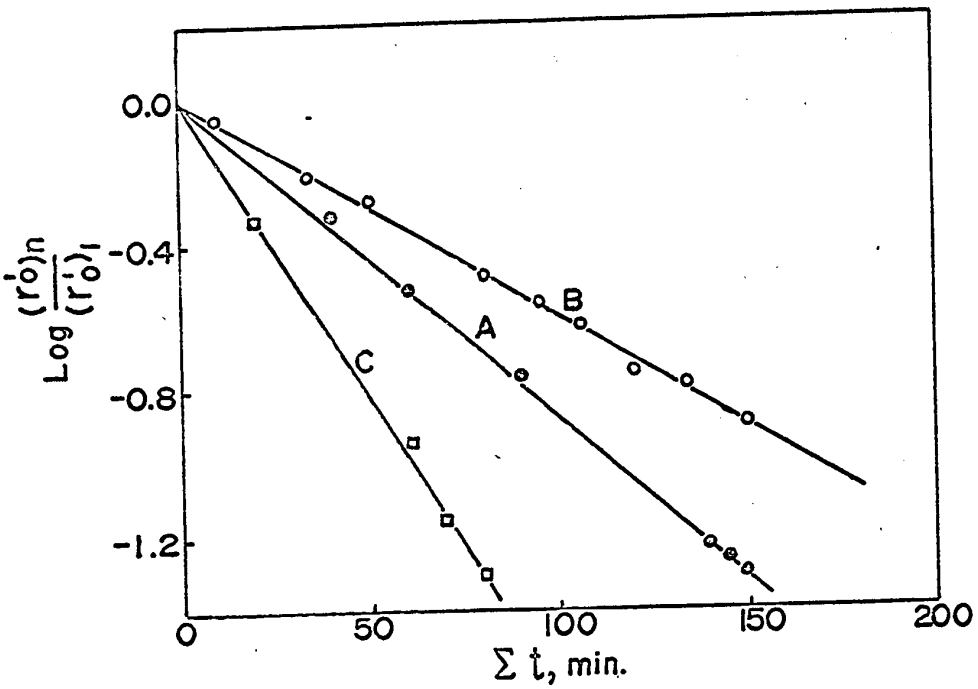

Figure 19. Poisoning curves for palladium-pumice catalyst

A. 0.2004 gm. of 0.5%Pd-pumice, at 30°C. Mercury vapor from the vacuum gauge gained access to the catalyst.

B. 0.2002 gm. of 0.5%Pd-pumice, at 30° C.

C. 0.2003 gm. of 0.5%Pd-pumice, at 118° C.

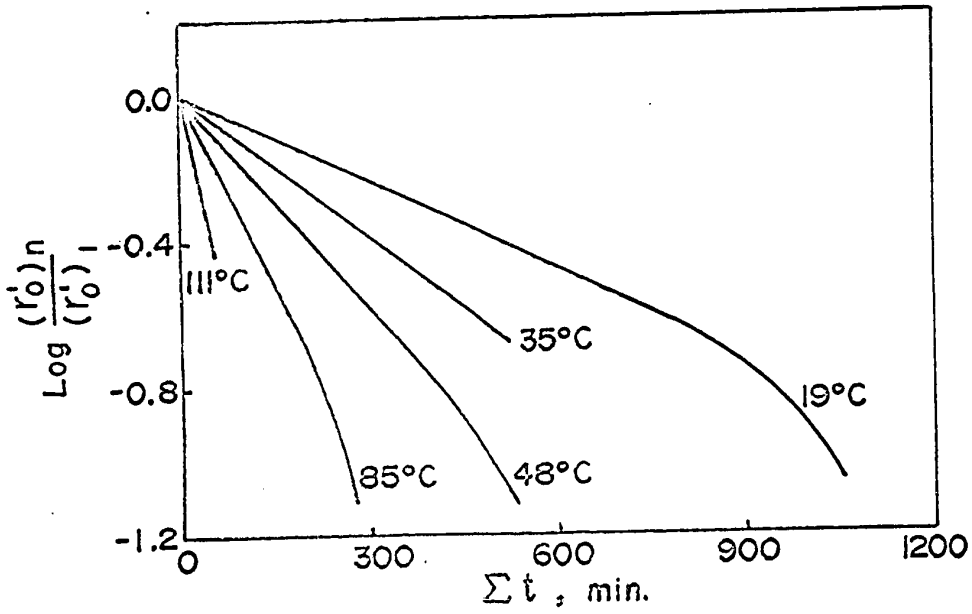

Figure 20. The dependence of the poisoning curve on reaction temperature. (From Reference 9)

platinum catalyst. The catalytic activity of platinum for propylene hydrogenation remained constant and did not drop even after the reaction vessel had been evacuated for more than 4 hours at one time (run number 259, Table 9). The selective catalyst poisoning for the hydrogenations of cyclopropane and propylene was investigated by Campbell and Thomson[12]. They reported that cyclopropane hydrogenation over the nickel film was seriously inhibited in the presence of mercury vapor evaporating from manometer used for measurement, while propylene hydrogenation over the same catalyst was slightly affected only. From the results of the present work, palladium shows much more susceptibility to poisoning by mercury vapor than any other metal of the Group VIII.

Further study of the 0.5% palladium-pumice catalyst was made by using three different weights (0.402, 0.500, and 1.00 grams) of the catalyst for the hydrogenation of propylene. Similar to the finding of Bond and Wells[10] for hydrogenation of ethylene, it was found that above 120° C. there was a residual activity of the catalyst which was poisoned very slowly.

In order to make use of this finding, a kinetic study of the hydrogenation of propylene over 0.500 grams of 0.5% palladium-pumice was made. The evacuation time between two successive runs was reduced to 8-10 minutes. The reaction had a measurable rate at 120° C. in the pressure ranges of the reactants studied. The experimental data obtained are listed in Table 10. It was observed that the activity of the catalyst decreased slightly with the progress of the experiment. The shapes of pressure-time curves are similar to those obtained for the nickel-pumice catalyst.

The reaction orders with respect to hydrogen and propylene are 0.80 and zero respectively (Figure 21). The Arrhenius plot (Figure 22) gives an activation energy of

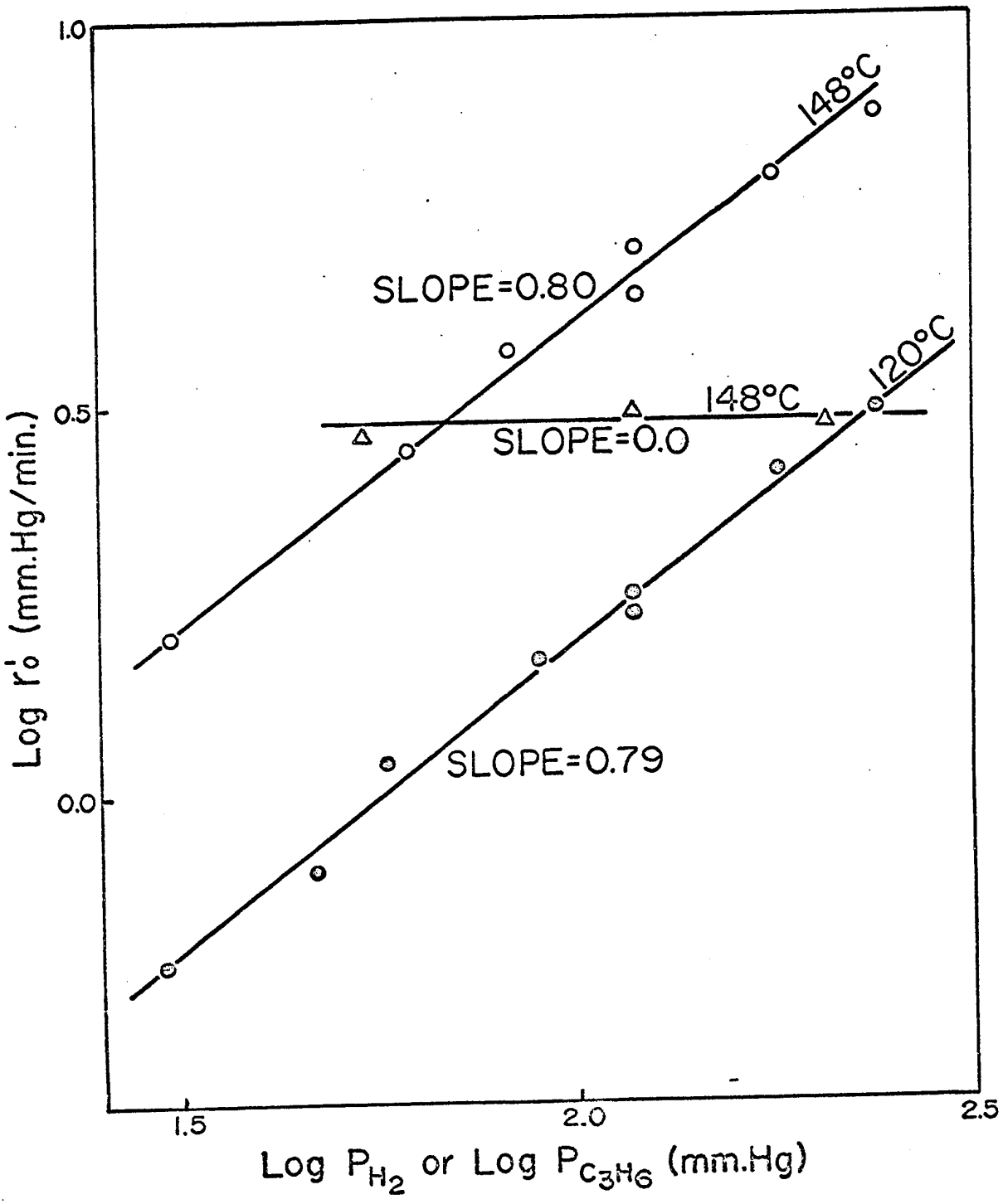

Figure 21. The dependence of initial rate on initial hydrogen and propylene pressures over palladium-pumice catalyst

○, ⊙ Log r_0' vs. Log P_{H_2}, $P_{C_3H_6}$ = 30 ± 1 mm. Hg

△ Log r_0' vs. Log $P_{C_3H_6}$, P_{H_2} = 60 ± 1 mm. Hg

Weight of palladium used = 0.25×10^{-2} gm.

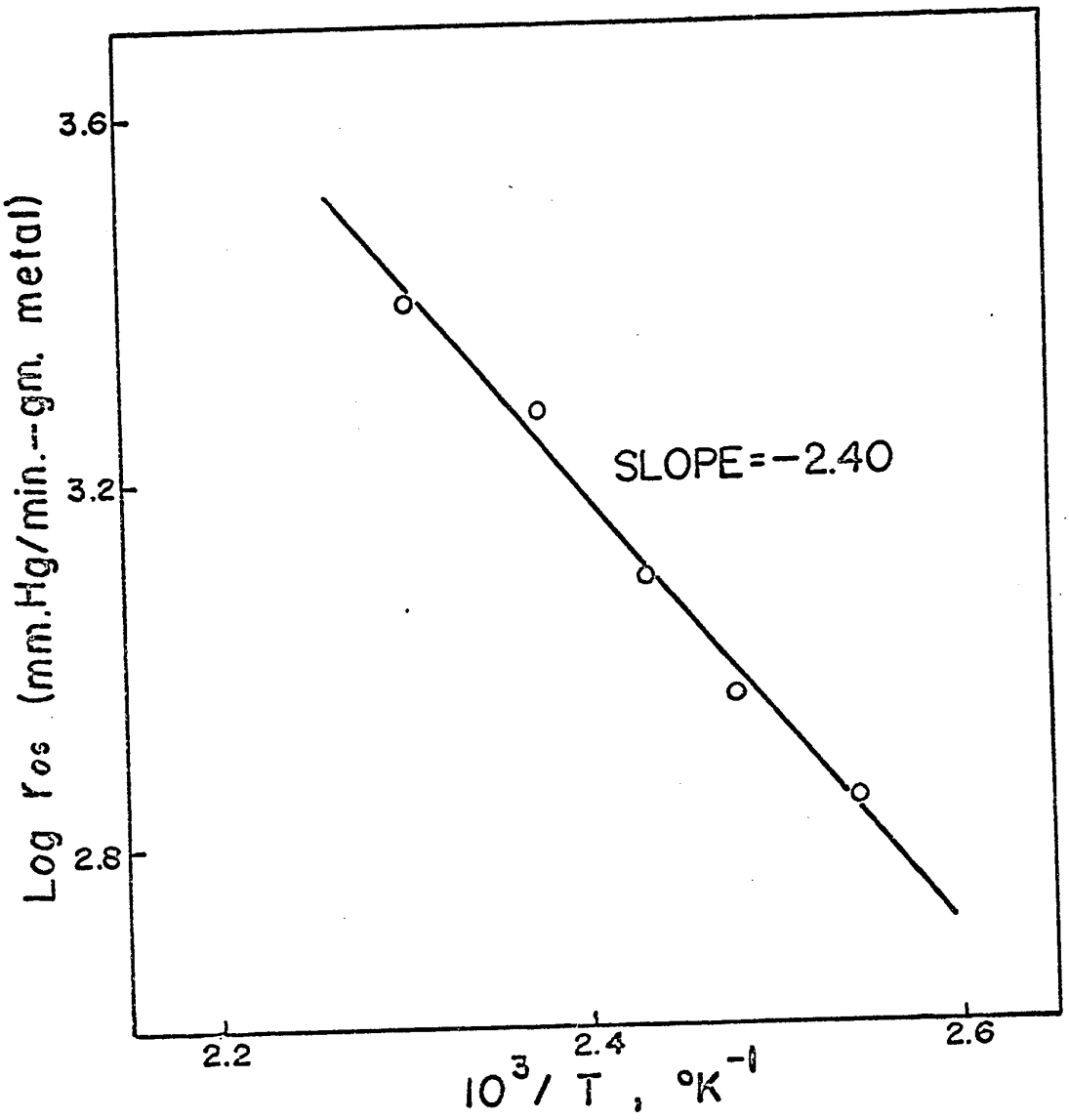

Figure 22. Arrhenius plot for propylene hydrogenation over palladium-pumice catalyst

11 kcal/mole and a frequency factor of 8.7×10^8 mm. Hg/(min. -gm. metal). The reaction rate can be expressed by the following equation:

$$r = k (P_{H_2})^{0.80} (P_{C_3H_6})^{0.0} \qquad \text{(IV-11)}$$

G. Reaction over Rhodium

The hydrogenation of propylene over 0.400 gm. of 0.5% rhodium-pumice catalyst had a measurable rate at 40° C. When the catalyst attained a constant activity the data were taken. The experimental data are tabulated in Table 11. They show that rhodium is the most active metal for propylene hydrogenation in the present study.

The reaction orders are 1.0 and - 0.05 with respect to hydrogen and propylene, respectively (Figure 23). The reaction rate, therefore, can be expressed as:

$$r = k (P_{H_2})^{1.0} (P_{C_3H_6})^{-0.05} \qquad \text{(IV-12)}$$

The effect of the order of admission of the reactants to the reaction vessel was also investigated. No appreciable change in the reaction rate was observed when propylene was first admitted instead of hydrogen.

An activation energy of 13 kcal/mole and a frequency factor of 1.0×10^{12} mm. Hg/(min. -gm. metal) were estimated from the slope of the Arrhenius plot (Figure 24) in the temperature range of 40° to 91° C.

H. Reaction over Iridium

The experimental data obtained for the hydrogenation of propylene over 0.500 gm. of 0.5% iridium-pumice catalyst are given in Table 12.

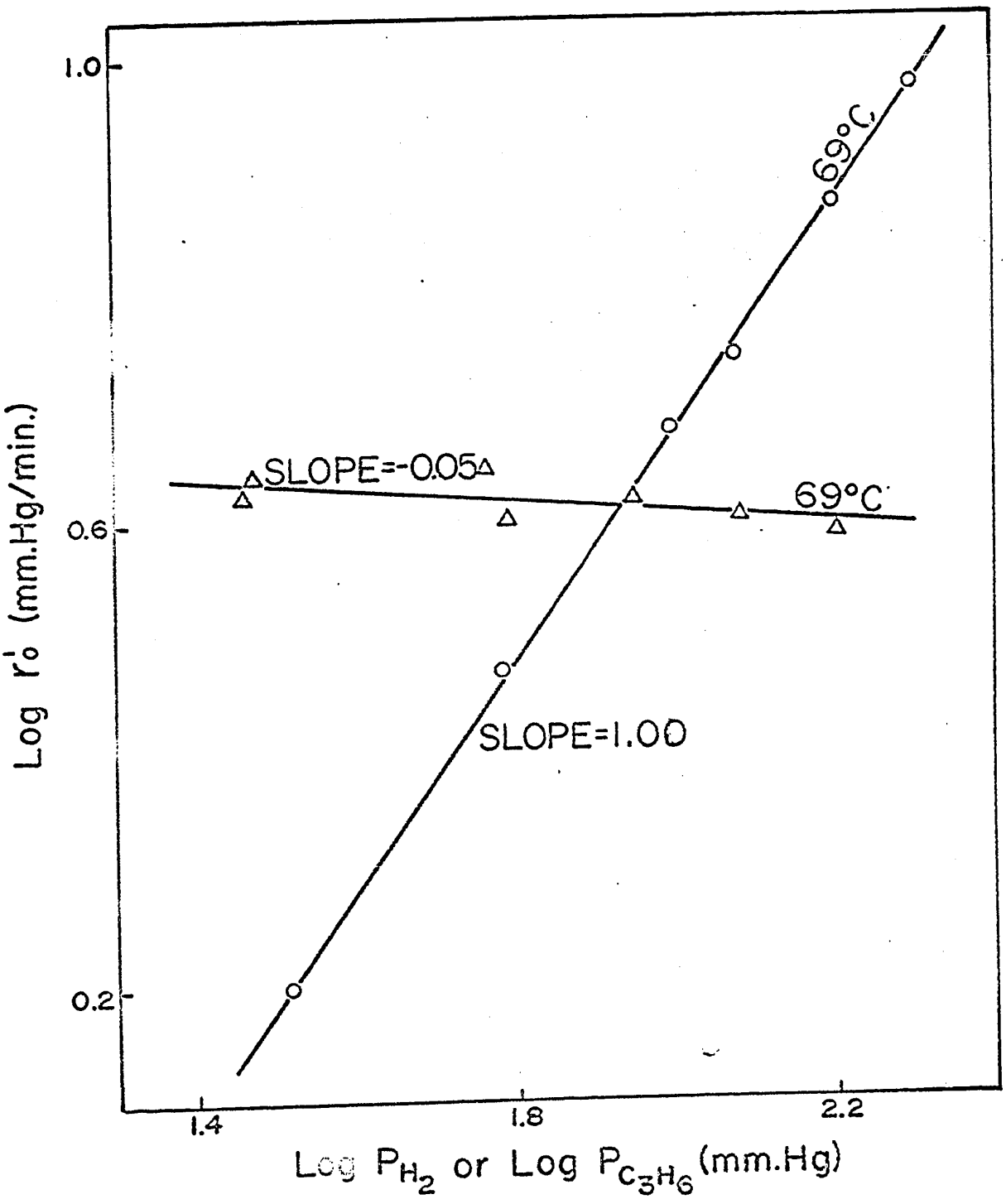

Figure 23. The dependence of initial rate on initial hydrogen and propylene pressures over rhodium-pumice catalyst

○ Log r_0' vs. Log P_{H_2}, $P_{C_3H_6}$ = 30 ± 1 mm. Hg.

△ Log r_0' vs. Log $P_{C_3H_6}$, P_{H_2} = 80 ± 1 mm. Hg.

Weight of rhodium used = 0.20×10^{-2} gm.

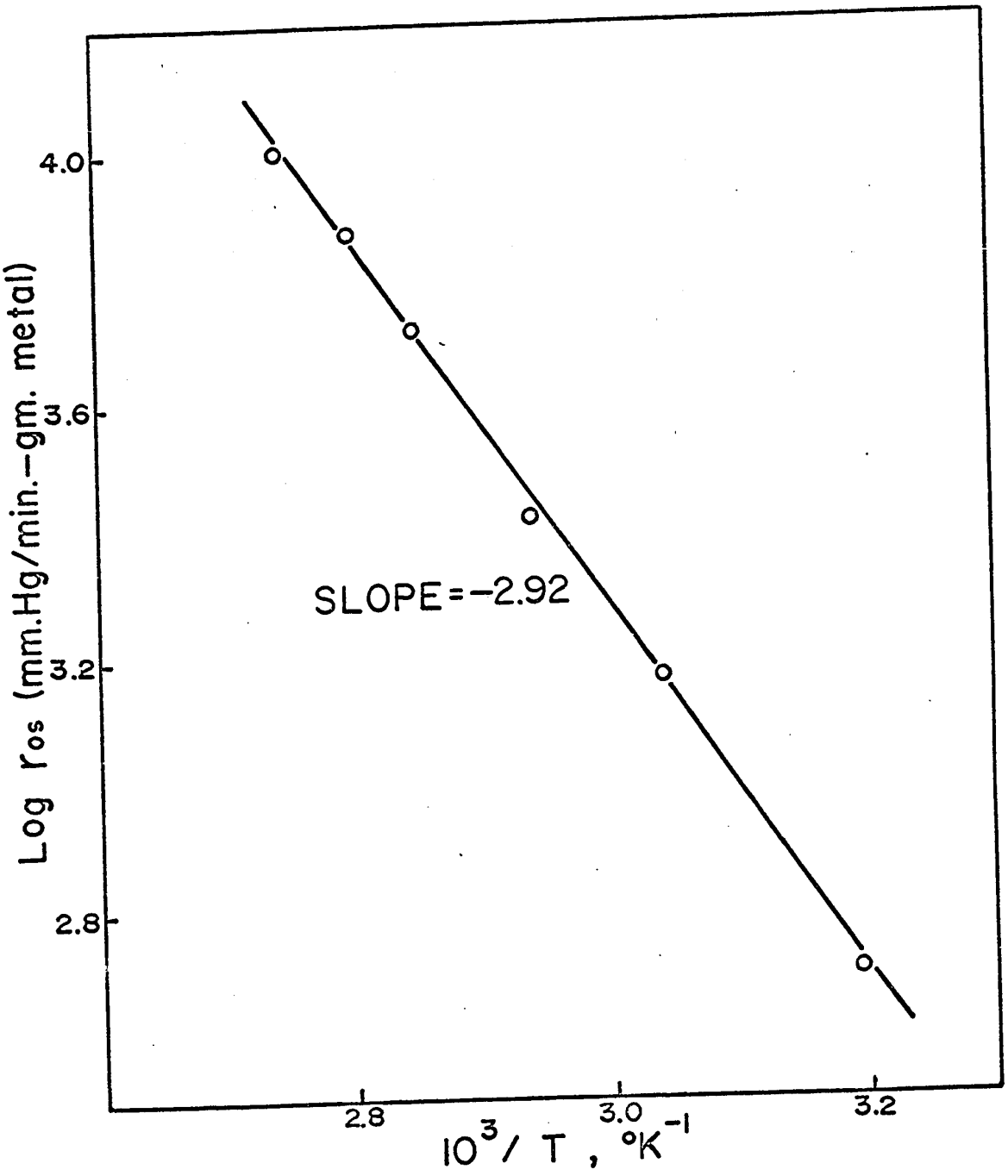

Figure 24. Arrhenius plot for propylene hydrogenation over rhodium-pumice catalyst

The reaction had a measurable rate at 70° C. When the catalyst attained a constant activity, the data were taken. The shapes of the pressure-time curves are similar to those obtained with the nickel-pumice catalyst.

The orders of the reaction with respect to hydrogen and propylene are 1.0 and nearly zero (-0.05) respectively (Figure 25). The kinetics of the reaction over iridium are similar to that over rhodium.

The reaction rate can be expressed by the equation:

$$r_0 = k\,(P_{H_2})^{1.0}\,(P_{C_3H_6})^{-0.05} \qquad \text{(IV-13)}$$

The slope of the Arrhenius plot (Figure 26) starts to fall off around 100° C. This phenomenon was also found in the study of the cobalt-pumice catalyst, as mentioned earlier. Between the temperature range of 70° to 100° C., the activation energy of the reaction is 15 kcal/mole and the frequency factor 2.5×10^{12} mm. Hg/(min. -gm. metal).

I. Reaction over Ruthenium

The kinetics of the hydrogenation of propylene over 0.4 gm. of 0.5% ruthenium-pumice catalyst was studied between 60.5° and 124° C. After the catalyst attained a constant activity, the data were taken. The experimental data are listed in Table 13.

The dependence of initial rate on the initial hydrogen and propylene pressures at various temperatures is shown in Figure 27. The reaction orders with respect to hydrogen and propylene are 0.75 and - 0.05, respectively. The reaction rate is expressed as:

$$r = k\,(P_{H_2})^{0.75}\,(P_{C_3H_6})^{-0.05} \qquad \text{(IV-14)}$$

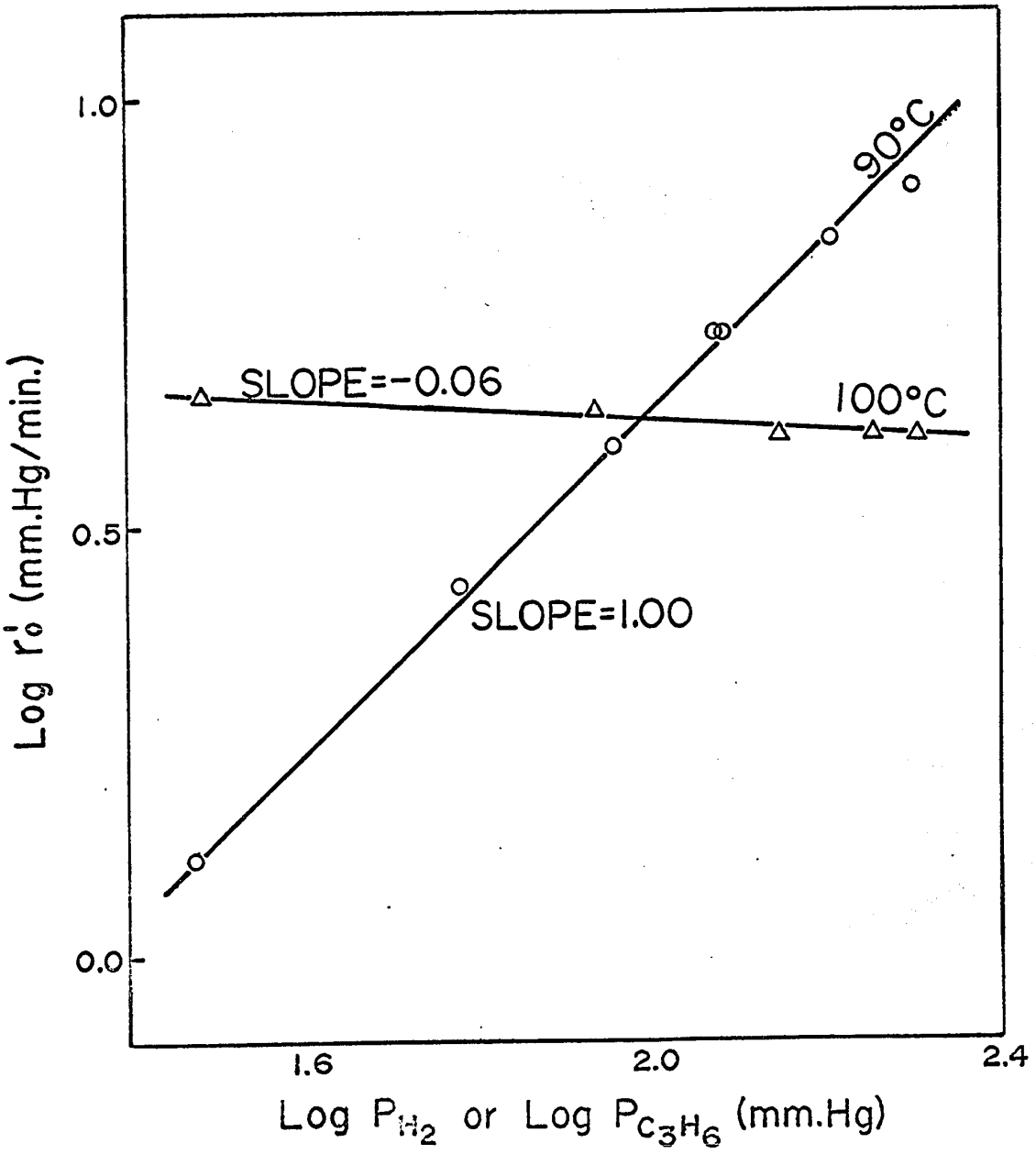

Figure 25. The dependence of initial rate on initial hydrogen and propylene pressures over iridium-pumice catalyst

○ Log r_0' vs. Log P_{H_2}, $P_{C_3H_6}$ = 30 ± 1 mm. Hg

△ Log r_0' vs. Log $P_{C_3H_6}$, P_{H_2} = 60 ± 1 mm. Hg

Weight of iridium used = 0.25×10^{-2} gm.

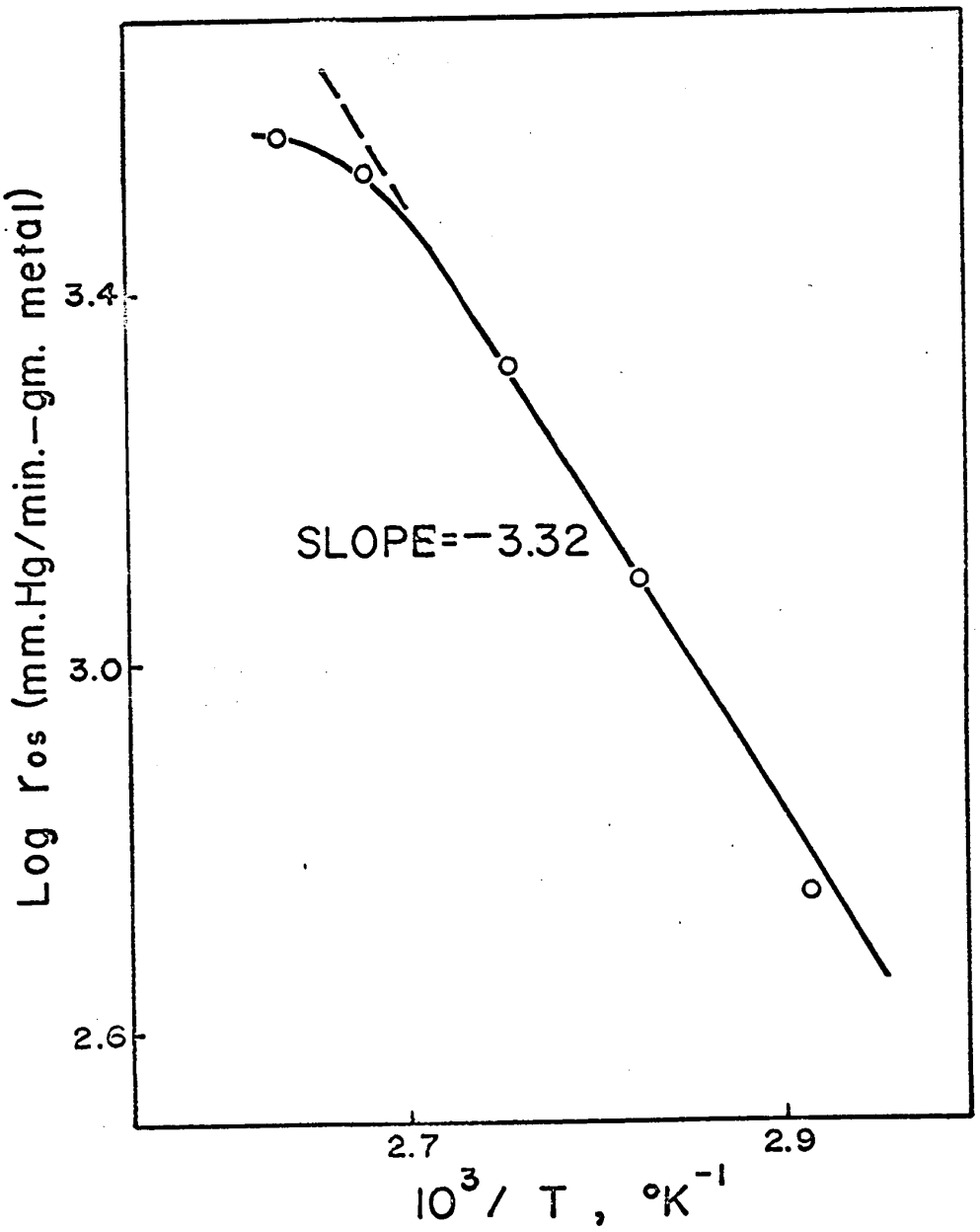

Figure 26. Arrhenius plot for propylene hydrogenation over iridium-pumice catalyst

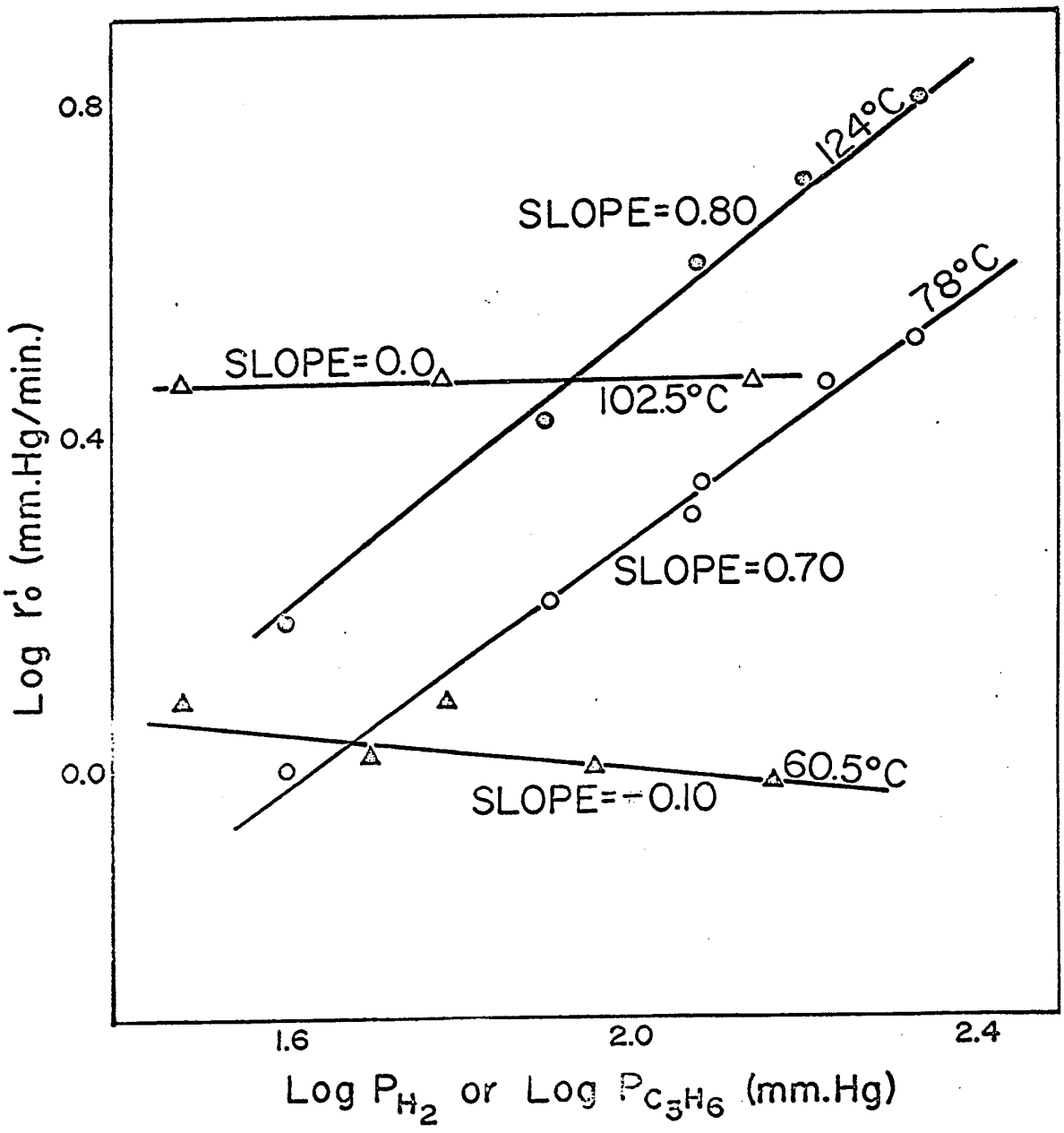

Figure 27. The dependence of initial rate on initial hydrogen and propylene pressures over ruthenium-pumice catalyst

O,O Log r_0' vs. Log P_{H_2}, $P_{C_3H_6}$ = 30 ± 1 mm. Hg

Δ,Δ Log r_0' vs. Log $P_{C_3H_6}$, P_{H_2} = 120 ± 1 mm. Hg

Weight of ruthenium used = 0.20×10^{-2} gm.

The reaction rates over the ruthenium-pumice catalyst are much less sensitive to temperature than the other catalysts studied, as indicated by the apparent activation energy of 6.5 kcal/mole (Figure 28). The frequency factor is 1.2×10^7 mm. Hg/(min.-gm. metal).

J. Reaction over Osmium

The kinetics of the hydrogenation of propylene over 2.00 gm. of 0.5% osmium-pumice catalyst was studied in the temperature range of 143° to 188° C. Below 143° C., the reaction rate was too slow to be measured. The experimental data obtained are given in Table 14.

The kinetics of the reaction over the osmium-pumice catalyst was found to be highly unusual. The results show that the order of reaction with respect to initial hydrogen pressure is as high as 1.6 over the temperature range studied, while the order with respect to propylene is nearly zero (Figure 29).

The aging curve of the osmium-pumice catalyst is the most severe one in the series of catalysts studied. It was found that the reaction rate was reduced substantially when the catalyst was exposed to propylene. The shapes of the pressure-time curves are similar to those obtained for the nickel-pumice catalyst, except that the linear pattern of the curves is shorter. A measurable reaction rate was observed at a temperature which was as low as 30° C., after the catalyst was cooled down from 143° C. However, almost no reaction was observed in the succeeding runs under similar conditions. The reason for this was probably that the sites on the catalyst surface available as a result of desorption of adsorbed propylene at high temperature were rapidly covered by propylene again at low temperature.

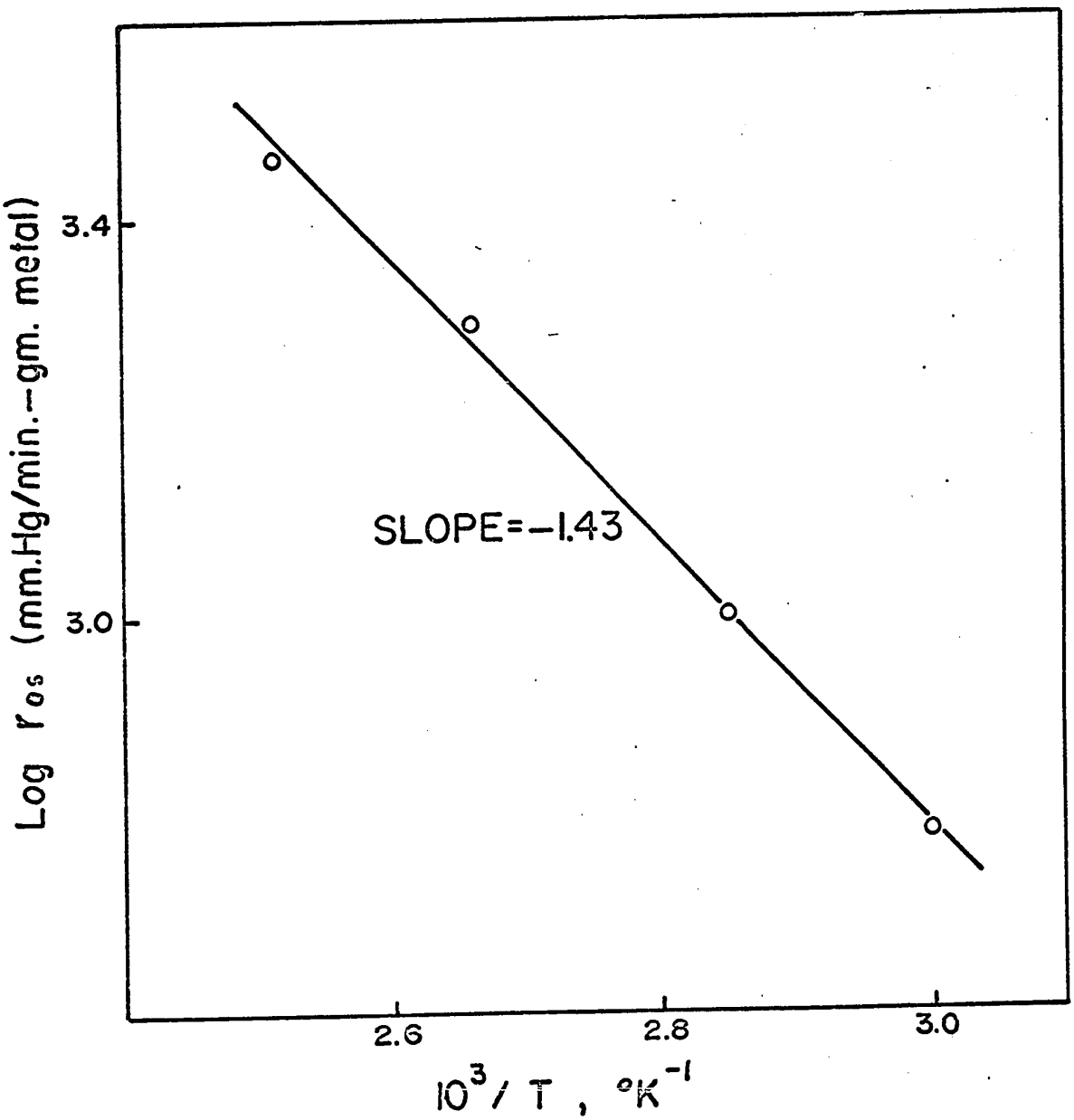

Figure 28. Arrhenius plot for propylene hydrogenation over ruthenium-pumice catalyst

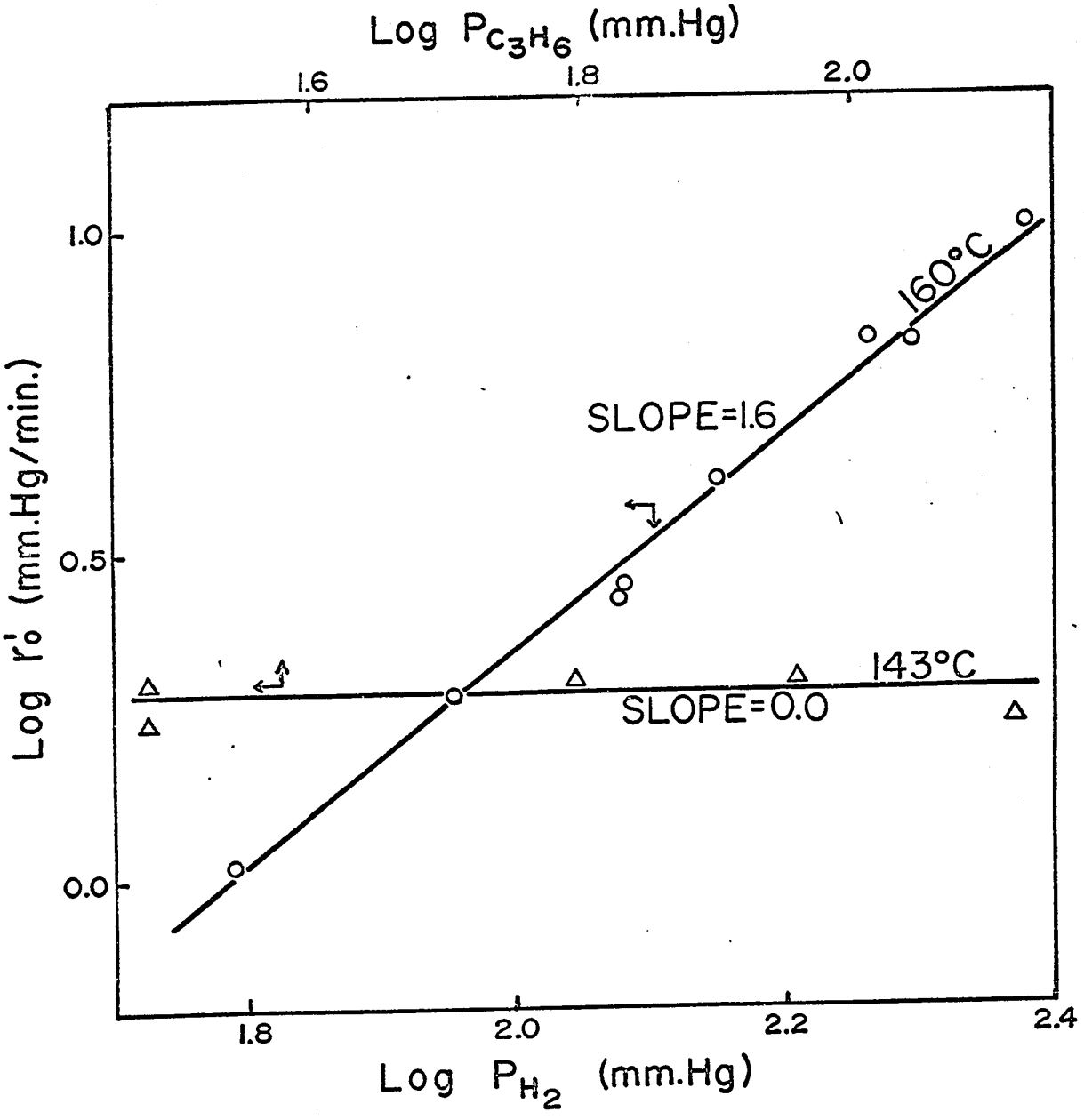

Figure 29. The dependence of initial rate on initial hydrogen and propylene pressures over osmium-pumice catalyst

○ Log r_0' vs. Log P_{H_2}, $P_{C_3H_6}$ = 30 ± 1 mm. Hg
Temperature = 160°C.

△ Log r_0' vs. Log $P_{C_3H_6}$, P_{H_2} = 120 ± 1 mm. Hg
Temperature = 143°C.

Weight of osmium used = 1.00×10^{-2} gm.

From the above findings during the experiment, the unusually high order of reaction (1.6) with respect to hydrogen for osmium catalyst is probably due to the strong adsorption of propylene. Before a run was carried out, a small fraction of the catalyst surface would be cleaned by hydrogen which was usually admitted to the reaction vessel before propylene. This fraction of the clean surface might contribute to a faster initial reaction rate. However, upon the subsequent addition of propylene, the fraction of the clean surface was covered by propylene again. This postulation may be tested, if both reactants can be introduced into the reaction vessel at the same time, which was not attempted.

Owing to the lack of information on the kinetic studies of the addition reaction, and the adsorption of reactants over osmium, any conclusion about the osmium catalyst seems to be impractical. However, the results show that osmium is the least active metal in Group VIII, for the hydrogenation of propylene.

From the experimental results obtained for propylene hydrogenation, the reaction rate can be expressed as:

$$r_0 = k (P_{H_2})^{1.6} (P_{C_3H_6})^{0.0} \qquad \text{(IV-15)}$$

An activation energy of 7.4 kcal/mole, and a frequency factor of 1.7×10^6 mm. Hg/(min.-gm. of metal) were estimated from the slope of the Arrhenius plot (Figure 30).

K. Summary of the Experimental Results

The kinetic parameters for the hydrogenation of propylene over the series of pumice-supported metals of Group VIII are listed in Table 3. The reaction order with respect to hydrogen pressure over all the catalysts except osmium is always positive and generally between 0.6 and 1.0. This result is in agreement with the finding of Schuit

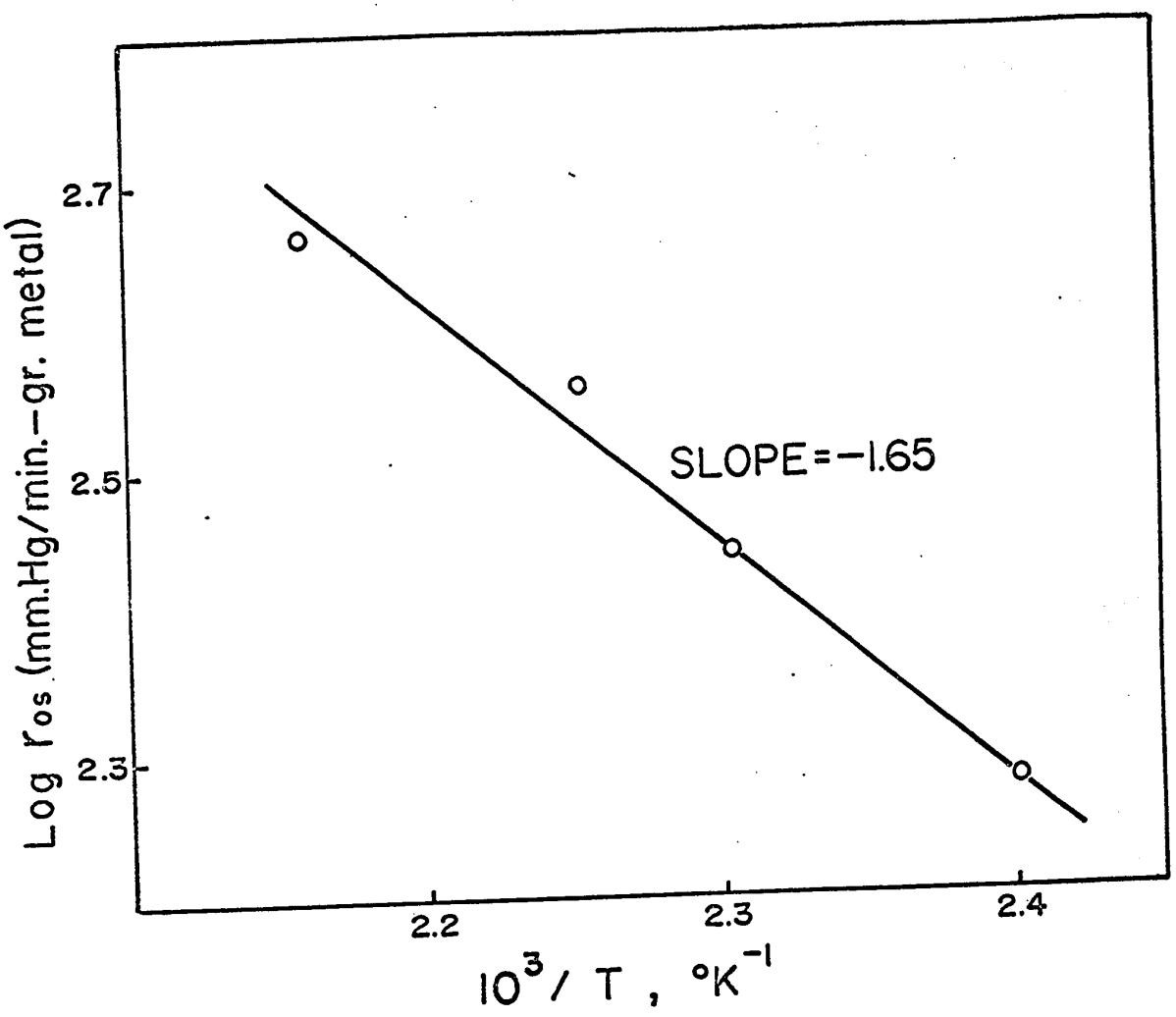

Figure 30. Arrhenius plot for propylene hydrogenation over osmium-pumice catalyst

and van Reijen[41] for the hydrogenation of ethylene over various catalysts supported on silica. The reaction rates are almost independent of propylene within the pressure range of 30-200 mm. Hg., although the reaction rates over rhodium, ruthenium and iridium slightly decrease with increased propylene pressures. It should be noted that the Power Rate Law could not satisfactorily explain the order of propylene at very low pressures.

All the catalysts listed in Table 3, were supported on pumice stone of 20-40 mesh size. These catalysts were aged to a constant activity before the experimental runs were carried out, and were not subjected to any further regeneration later. It was found that after the aging treatment, the activities of the catalysts remained fairly constant during the series of runs. An exception to this was the pumice-supported palladium catalyst. As explained previously, mercury poisoning was probably responsible for the constant fall in the activity of the palladium catalyst. The constant activities of the catalysts were probably due to the fact that a greater fraction of the surface was covered by strongly adsorbed propylene. In such cases since a large fraction of surface was already covered with propylene, further poisoning by propylene on the residual surface would be negligibly slow, unless the partial pressure of propylene was very high.

The Arrhenius plots for all the metals except for palladium and osmium are given in Figure 31. It can be seen that the slopes of the plots for ruthenium, and cobalt differ considerably from those for the other catalysts. This implies that activation energies for the series of metals are remarkably different, in contrast to the conclusion made by Beeck[5], and Schuit and van Reijen[41] for the hydrogenation of ethylene. It is interesting to note that the Arrhenius plots of both iridium and cobalt start to fall off around 100° C., and the peak in the Arrhenius plot for cobalt appears to be around 125° C. This is in line with the findings of several workers for the hydrogenation of ethylene[27, 53, 56].

The relative activities of the metals for propylene hydrogenation can be made on the basis of the reaction rates as the parameters. These rates are all chosen from the Arrhenius plots under the similar conditions, i.e., 80° C., 120 mm. Hg of initial hydrogen pressure, 30 mm. Hg of initial propylene pressure, and unit weight (1 gm.) of metal. By choosing rhodium catalyst as the standard of reference, the order of the relative catalytic activities of the various metals for propylene hydrogenation as shown in Table 3, is as follows:

$$Rh > Ir > Ru > Pt > Pd > Ni > Fe > Co > Os$$

Table 3. Kinetics of Propylene Hydrogenation over Transition Metals.

Metal[x]	Temp. Range °C.	$r = kP_{H_2}^{m}P_{C_3H_6}^{n}$ m	n	E kcal/mole	log r_{os}[xx] at 80°C.	Relative activity Log $\frac{r_{os,metal}}{r_{os,Rh}}$	Log A[xx]
Rh	40 - 91	1.0	- 0.05	13	3.77	0	12.0
Ir	70 - 107	1.0	- 0.05	15	3.06	- 0.71	12.4
Ru	60.5 - 124	0.75	- 0.05	6.5	3.03	- 0.74	7.07
Pt	89 - 129	0.80	0.0	16	2.71	- 1.06	12.4
Pd	120 - 161	0.80	0.0	11	2.07	- 1.70	8.94
Ni	60 - 100	1.0	0.0	13	2.04	- 1.73	10.0
Fe	50 - 92	0.66	0.0	10	1.72	- 2.05	7.86
Co	52 - 96.5	0.95	0.0	8.1	1.59	- 2.18	6.56
Os	143 - 188	1.6	0.0	7.4	1.50	- 2.27	6.24

x All metals are supported on pumice in 20-40 mesh, see Table 5.

xx r_{os} and A are in mm. Hg/(min. -gm. of metal)

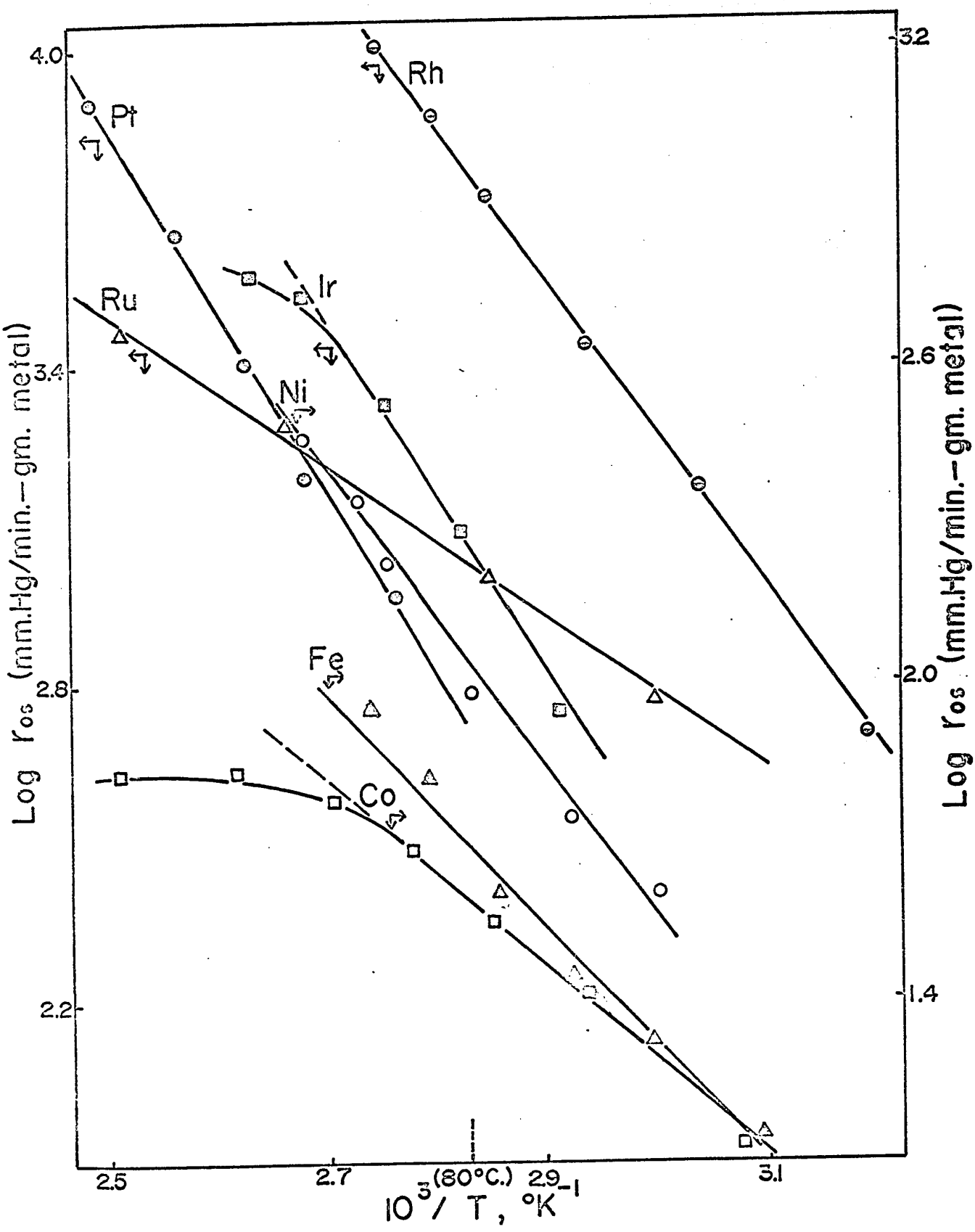

Figure 31. Arrhenius plots for propylene hydrogenation over various pumice-supported metal catalysts

V. DISCUSSION

A. The Kinetics of the Reaction

Propylene is expected to behave similarly to its homologue, ethylene. From the experimental results obtained in the present work, this appears to be true to some extent. The metal catalysts of Group VIII in the periodic table are quite as active for the hydrogenation of propylene as they are for the hydrogenation of ethylene (see Chapter II-A).

The simple form of the rate equation, $r = k P_H^1 P_U^0$, suggested by Beeck[5] for evaporated films could not interpret the hydrogenation rates over supported transition metals. Schuit and van Reijen[41], who patterned their work after Beeck, reported the fractional orders of pressure dependence in the hydrogenation of ethylene over metal-on-silica catalysts (Table 2). The range of fractional orders with respect to hydrogen pressure for the propylene hydrogenation in the present study is in good agreement with those obtained for the ethylene hydrogenation by Schuit and van Reijen[41]. In their work, a negative order with respect to ethylene pressure was obtained for most of the catalysts, especially rhodium and ruthenium. However, in the present work, the reaction order with respect to propylene pressure was found to be zero for most of the catalysts, although a slightly negative order was observed for rhodium, ruthenium, and iridium.

Schuit and van Reijen[41] regenerated the catalysts with hydrogen at 500° C. between runs. In this work, however, catalysts were not subjected to any regeneration after they had been aged to a fairly constant activity. Previous workers (see Chapter III-A) have shown that olefins greatly inhibit the activity of the catalyst for hydrogenation. The poisoning of the catalysts is proportional to the ratio of ethylene to hydrogen and is inversely proportional to the reaction temperature[41]. Therefore, in the investigation

of the reaction over fresh surface as used in the work of Schuit and van Reijen, a negative order with respect to olefin pressure may result, especially at low temperatures. In the present study, the aged catalysts were found to be quite stable. After the catalysts attained a constant activity, the poisoning by the olefin was not appreciable as explained in the previous chapter. Therefore, the pressure dependence orders of the reaction over the aged surface are probably more reliable than those over the fresh surface.

B. The Energy of Activation

Beeck[5] and Schuit and van Reijen[41] found that the activation energy for the hydrogenation of ethylene is independent of the various metals. Contrary to their results, the present work shows that the activation energy for the hydrogenation of propylene depends on the various metals, ranging from 6.5 to 16.0 kcal/mole.

It should be pointed out that the activation energies mentioned here are "apparent" and not "true". In general, a gaseous molecule must first overcome a barrier (Figure 32) to arrive at the adsorbed state, then a second barrier to give product(s) still in the adsorbed state. The height of the second barrier E_s is the energy of surface reaction. Q_{ads} and E_{app} are the heats of adsorption of reactants, and the apparent activation energy, respectively. The apparent activation energy is equal to the sum of the energy of surface reaction and the heat of adsorption of the reactants, and is expressed as

$$E_{app} = E_s + Q_{ads} \qquad (V-1)$$

Q_{ads} is positive when the adsorption is endothermic, and negative when the adsorption is exothermic. Since heat is evolved in case of most adsorptions, E_{app} is always less than E_s by Q_{ads}. Therefore, the apparent activation energies may vary due to the variations in either the heats of adsorption or energies of surface reaction. Only in the case in which

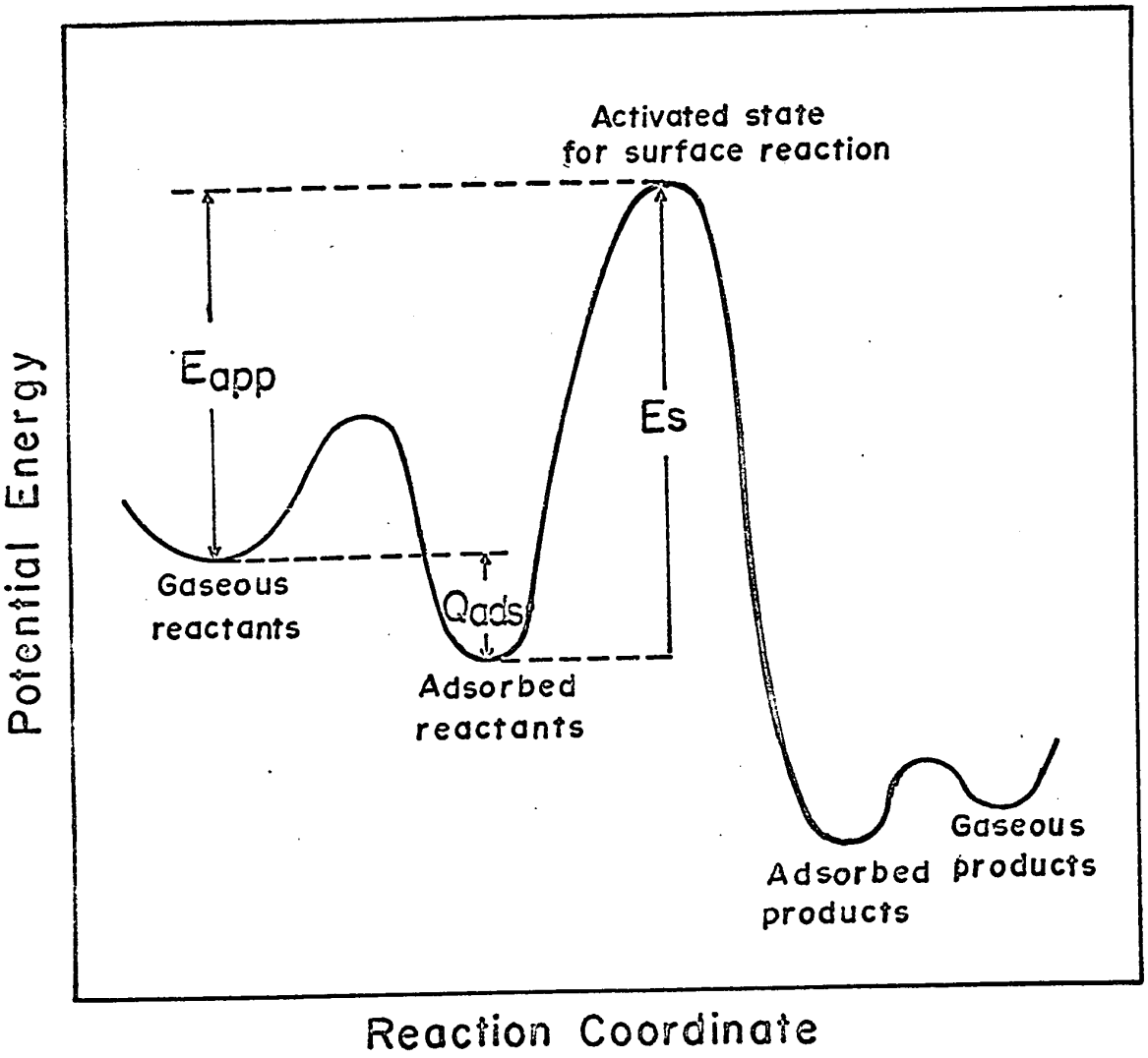

Figure 32. Potential energy diagram for the reaction path

both E_s and Q_{ads} do not change appreciably, or in the one in which the change in E_s is balanced by the change in Q_{ads}, E_{app} can remain constant for a series of catalysts. One of the two cases mentioned above might exist in Beeck's work on the hydrogenation of ethylene over rhodium, palladium, platinum and nickel metals[5]. Therefore, Beeck concluded that the apparent activation energy for these metals had a constant value of 10.7 kcal/mole. However, he noted that the activation energy over tungsten and tantalum was only 2.4 kcal/mole. In order to interpret this result, it is helpful to refer to Figure 1. It shows that the heats of adsorption of hydrogen on tungsten and tantalum are much higher than those on other metals when the fraction of surface covered by reactant is equal to zero, i.e. when the surface is clean. The adsorption of ethylene on these two metals was also found to be strongly exothermic[5]. According to equation (V-1), the apparent activation energies for these two catalysts should be much less than those for the other metals studied, if the energy of surface reaction does not change appreciably for the series of catalysts, or if the change of the heats of adsorption could not be compensated by the change in the energy of surface reaction.

Many factors, such as the nature of the chemical bond in metals, the configuration of crystal lattice, the physical forms of the metals, the methods of preparation of the metals and the fraction of surface covered by the reactants, can affect both the energy of surface reaction and the heats of adsorption of the reactants, and thus the apparent activation energy. For the hydrogenation of propylene, the values of the apparent activation energy have been determined to be 2[51], 4.8[42], and 8.6 kcal/mole[23] with the nickel catalysts, 15 kcal/mole[40] with a platinum catalyst, 11.7 kcal/mole[28] with a palladium catalyst, and 10.5 kcal/mole[45] with a copper catalyst. For the reasons mentioned above, it is not surprising that widely varying activation energies have been reported.

C. Geometric Considerations

It has been mentioned previously that the activity of the various metals for the hydrogenation of propylene in the present work is in the order of

Rh > Ir > Ru > Pt > Pd > Ni > Fe > Co > Os

The order of the relative activities of the metals is very similar to that obtained for the hydrogenation of ethylene by Beeck[5], Schuit and van Reijen[41], viz.,

Rh > Pd > Pt > Ni > Fe > W > Cr > Ta

The similar order of activity for the hydrogenation of olefins suggests that certain characteristics of the catalysts may affect the rates of the hydrogenations similarly. Early in 1929, Balandin[3] stressed the importance of the geometric factor in catalysis. In line with the geometric approach to the study of catalysis, Beeck[5], in summarizing his work, plotted the logarithm of the activity of the various metallic films for ethylene hydrogenation as a function of the lattice distance of the metals.

In consideration of the geometric effect, the activation energy E and the logarithmic value of the frequency factor A obtained in the present work are listed in Table 4, along with the lattice structure of the series of metals. It can be seen that the activation energies for the metals with a face-centred cubic structure are greater than the activation energy for iron, which has a body-centred cubic structure. The metals with a closed-packed hexagonal structure have the lowest activation energies. The same tendency is observed for log A. A clear picture of these tendencies can be observed by plotting both E and log A against the lattice distance of the unit cell (Figure 33). The scattering of the data for palladium could be due to the poisoning by mercury vapor, as explained previously. The results show that the larger the lattice distances, the greater the activation energies and log A. Never-

Table 4. Metal Lattice Structures, Activation Energies and Frequency Factors

Metal	Lattice Structure	Unit Cell Size Å a_0	Unit Cell Size Å c_0	Unit Cell molecules *	E kcal/mole	Log A mm. Hg/min. -gm. metal
Pt	f.c.c.	3.91		4	16	12.4
Pd	f.c.c.	3.85		4	11	8.9
Rh	f.c.c.	3.82		4	13	12.0
Ir	f.c.c.	3.82		4	15	12.4
Ni	f.c.c.	3.49		4	13	10.0
Fe	b.c.c.	2.85		2	10	7.9
Os	c.p.h.	2.71	4.32	2	7.4	6.4
Ru	c.p.h.	2.68	4.27	2	6.5	7.1
Co	c.p.h.	2.51	4.10	2	8.1	6.6

* From Reference 54

a_0, c_0=Edge length of unit cell along the a and c-crystallographic axes, respectively

f.c.c. = face-cubic center

b.c.c. = body-cubic center

c.p.h. = close-packed hexanol

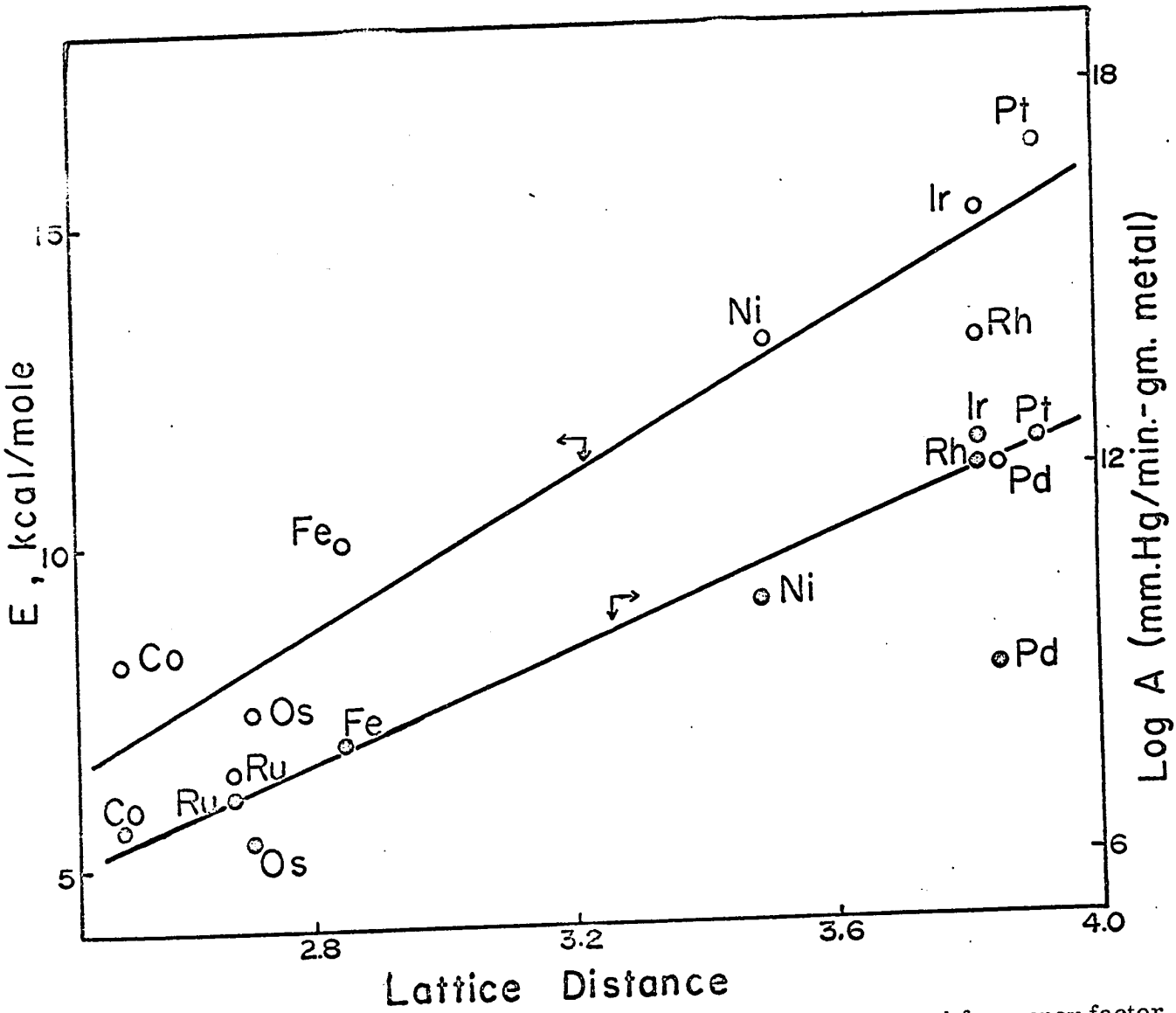

Figure 33. Correlation of lattice distance with activation energy and frequency factor

○ E vs. Lattice distance
◎ Log A vs. Lattice distance

theless, the variations in catalytic activity could not be explained in terms of lattice spacing only. The experimental results (Table 3) show that ruthenium is at least 25 times more active than cobalt, though the lattice spacings of these two metals are nearly equal (Figure 33). Furthermore, the marked difference in the catalytic activity of the face-centred cubic metals could not be interpreted by the small differences in the lattice spacings. However, it can be concluded that the lattice distance of the metals must have an influence on the activation energy, if the surface is capable of making chemical bonds with the adsorbate. It is postulated that the longer axis (denoted by c_0 in Table 4) of the metals with a close-packed hexagonal structure might not play an important role in the reaction, for it requires a higher activation energy for the adsorbate to react over such a long axis, as shown in Figure 33.

D. Electronic Considerations

A recent interesting approach in hererogeneous catalysis considers crystal spacings less important as compared to the properties which determine the bond strength in the metal. The general relationship between the rate of reaction and the heats of chemisorption (equivalent to strength of surface bonds) of the reactants has been well established, as shown in Figure 3[5]. The formation of the bonds depends particularly on the electronic properties of the metal. A correlation between Pauling's percentage d-character and catalytic activity has been made by Boudart and Beeck[5] as shown in Figure 4.

The relative activities of the series of metals studied are listed in Table 3. The correlation of the relative activity to the percentage d-character of metals is shown in Figure 34, in which the results obtained by Beeck[5], Schuit and van Reijen[41] for the hydrogenation of ethylene are also plotted for comparison. It can be seen that the results for several supported catalysts scatter considerably. Considering the fact that the supported

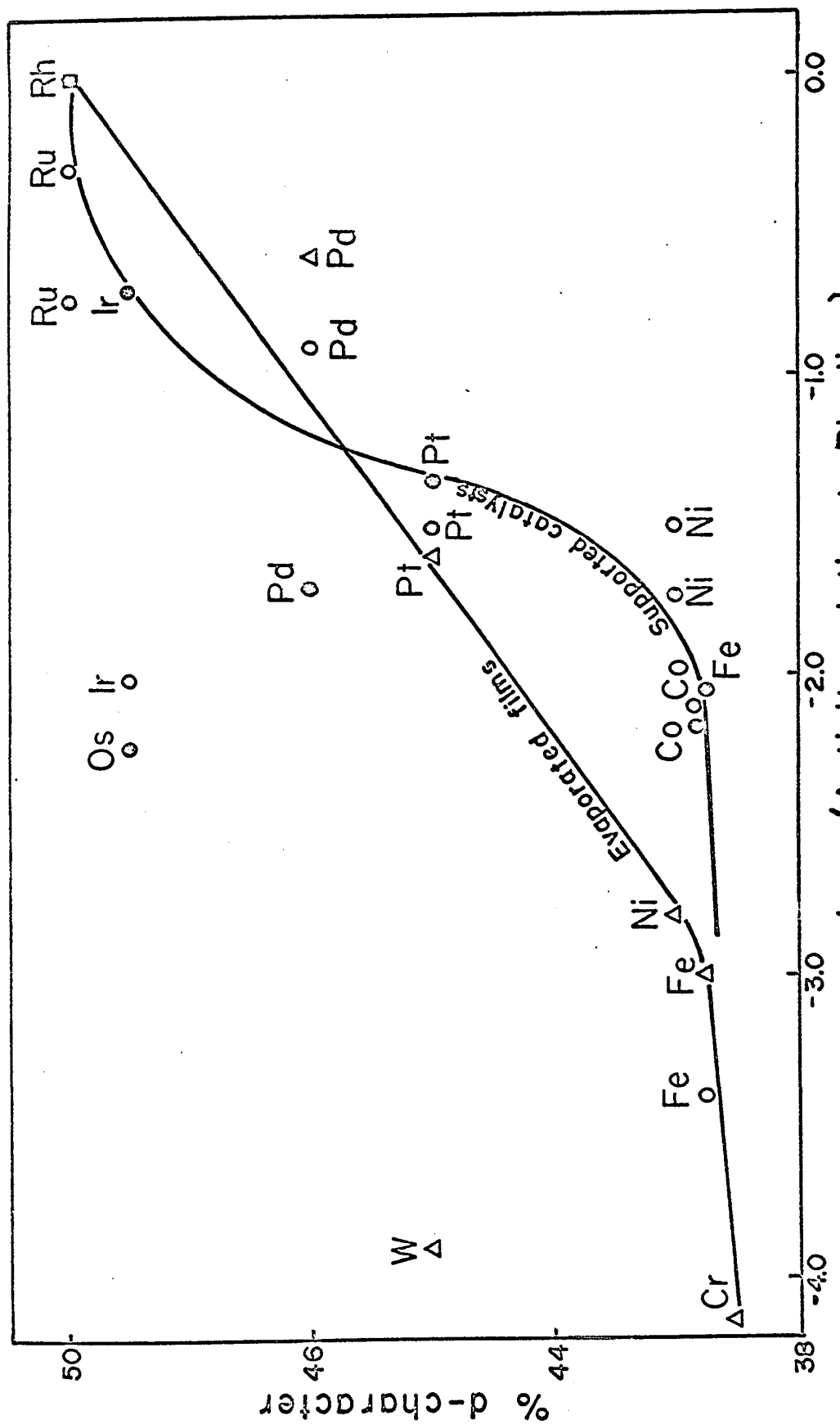

Figure 34. Correlation between catalytic activity and % d-character for the hydrogenations of ethylene and propylene

● Present Work
○ Schuit and van Reijen } supported catalysts
△ Beeck, evaporated films

catalysts as used in the present work and in the work of Schuit and van Reijen could not be as pure as the evaporated films, it seems that a good correlation holds between the percentage d-character and the catalytic activity in the present work. However, osmium as studied in this work, tungsten in Beeck's work, and iridium as investigated by Schuit and van Reijen do not fall on the smooth curves. Therefore, the electron theory of catalysis cannot be regarded as completely satisfactory.

E. Compensation Effect

According to the compensation effect (see Chapter II-D), a linear relationship sometimes exists between the activation energy E and the frequency factor A for a given reaction over a series of related catalysts. This relation is expressed by:

$$\text{Log } A = mE + C \qquad \text{(II-5)}$$

The correlation of log A to E is shown in Figure 35. The best-fitting line determined by the method of least squares is expressed by the equation:

$$\text{Log } A = 0.75\ E + 0.87 \qquad \text{(V-2)}$$

It can be seen that the above equation correlates well most of the data of the catalysts, except those of rhodium and ruthenium. The reason for the exception of these two catalysts must be due to their remarkably high activities.

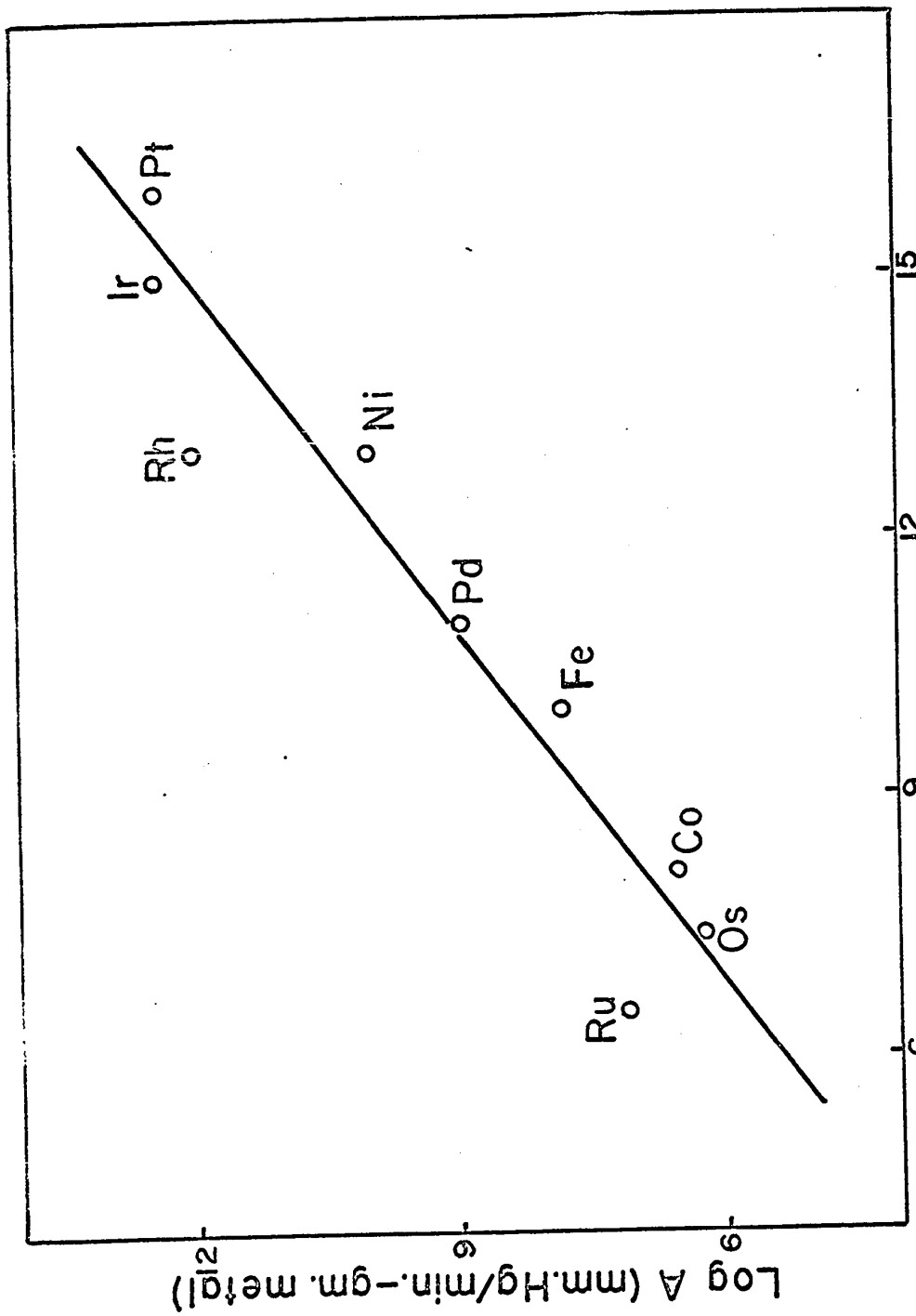

Figure 35. Compensation effect for propylene hydrogenation over pumice-supported metal catalysts

VI. CONCLUSIONS

The pumice-supported metals of Group VIII in the periodic table are quite active for the hydrogenation of propylene. The aged surface of the catalysts except that of palladium is fairly stable, and further poisoning by the adsorbed propylene is not appreciable. The gradual decrease in the activity of the palladium-pumice catalyst is probably due to the poisoning by mercury vapor from the manometers of the apparatus.

The experimental results show that propylene has the same behaviour as ethylene in the hydrogenation reaction. Over the catalysts studied, the propylene hydrogenation is mostly zero order with respect to propylene, though a slightly negative order of -0.05 was observed for rhodium, ruthenium and iridium. The reaction order with respect to hydrogen ranges from 0.6 to 1.0 for all metals except osmium. The unusually high order of 1.6 with respect to hydrogen for the osmium-pumice catalyst is attributed to the strong absorption of propylene on the metal surface. The order of catalytic activities of the series of metals is

$$Rh > Ir > Ru > Pt > Pd > Ni > Fe > Co > Os$$

The activation energy of the reaction over the catalysts ranges from 6.5 to 16 kcal/mole. The present study shows that the geometric structure of the metals is probably important, possibly affecting the adsorption of species on the surface sites. However, the catalytic activity of the metals can be better correlated with the electronic rather than the geometric structure of the metals. Nevertheless, the correlation of the catalytic activity with percentage d-character cannot be regarded as completely satisfactory, in view of the discrepancy of some data. It seems that both geometric and electronic factors must be considered in understanding the activity of the various metal catalysts.

The activation energy was correlated with the frequency factor. The compensation effect may exist in the moderately active catalysts, but not in the most active ones.

VII. RECOMMENDATIONS

To clarify the general picture of the addition reaction of double bonds, it is recommended that the hydrogenation of other light olefins be investigated by using the same series of metals.

As explained before, the usually reported activation energy is apparent. It is a function of the activation energy of the surface reaction and the heats of adsorption of reactants as shown in the equation (V-1). Therefore, it is worthy to understand the variation of the heat of adsorption with the fraction of the aged surface covered by the reactants, and changes in the extent of surface coverage with temperature.

It is suggested that propylene hydrogenation be studied in a wider range of temperature, preferably below the room temperature, for the desorption of the adsorbed reactants at high temperatures would lead to the fall-off of the Arrhenius plot.

Finally, a mercury-free system with a device to introduce the reactants into a reaction vessel simultaneously is recommended for further work.

VIII. REFERENCES

1. Baker, L. L., and Bernstein, R. B., J. Amer. Chem. Soc., 73, 4434 (1951).

2. Baker, M. McD., Jenkins, G. I., in "Advances in Catalysis" Vol. VII, Academic Press, New York (1955).

3. Balandin, A. A., in "Advances in Catalysis", Vol. X, Academic Press, New York, (1958).

4. Beeck, O., Rev. Mod. Physics, 17, 61(1945).

5. Beeck, O., Disc. Farad, Soc., 8, 118 (1950).

6. Beeck, O., and Ritchie, A. W., Disc. Farad. Soc., 8, 159 (1950).

7. Beeck, O., Smith, A. E., and Wheeler, A., Proc. Roy. Soc. (London), 177, 62 (1940).

8. Bond, G. C., Quart. Rev., 8, 279 (1954).

9. Bond, G. C., and Wells, P. B., Proc. 2nd International Congress on Catalysis (Editions Techniq, Paris, 1961), 1, 1135, 1159. And unpublished work.

10. Bond, G. C., "Catalysis by Metals", Academic Press, New York, 1962.

11. Bond, G. C., and Wells, P. B., in "Advances in Catalysis", Vol. XV, Academic Press, New York (1964).

12. Baker, M. McD., Jenkins, G. I., in "Advances in Catalysis", Vol. VII, Academic Press, New York (1955).

13. Ciapetta, F. G., and Plank, C. J., in "Catalysis", Vol. 1 (P. H. Emmett, Editor), Reinhold, New York, (1954).

14. Constable, F. H., Z. Elecktrochem., 35, 165 (1929).

15. Cremer, E., in "Advances in Catalysis" Vol. VII, Academic Press, New York (1955).

16. Eley, D. D., in "Advances in Catalysis", Vol. 1, Academic Press, New York, (1948).

17. Eley, D. D., Quart. Rev., 3, 209 (1949).

18. Eley, D. D., Disc. Farad. Soc., 8, 34 (1950).

19. Eley, D. D., in "Catalysis", Vol. 111, (P. H. Emett, Editor), Reinhold, New York(1955).

20. Eischens, R. P., and Pliskin, W. A., in "Advances in Catalysis", Vol. X, Academic Press, New York (1958).

21. Emmett, P.H., and Gray, J.B., J.Amer.Chem.Soc., 66, 1338 (1944).

22. Eyring, H., Colburn, C.B., and Zwolinski, B.J., Disc.Farad.Soc., 8, 39 (1950).

23. Fair, J.R., Ph.D.Thesis, University of Texas, Austin (1955).

24. Farkas, A., and Farkas, L., J.Amer.Chem.Soc., 60, 22 (1938).

25. Farkas, A., Farkas, L., and Rideal, E.K., Proc.Roy.Soc.(London), A146, 630 (1934).

26. Hoelscher, H.E., Poynter, W.G., and Weger, E., Chem.Rev. 54, 575 (1954).

27. Jenkins, F.I., and Rideal, E.K., J.Chem.Soc., 2490, 2496 (1955).

28. Kayser, R.F., and Hoelscher, H.E., Chem.Eng.Prog.Symposium Series, 50, No. 10 (1954).

29. Laidler, K.J., in "Catalysis", Vol.I, (P.H.Emmett, Editor), Reinhold, New York (1954).

30. Laidler, K.J., Disc.Farad.Soc., 8, 47 (1950).

31. Little, L.H., Sheppard, N., and Yates, D.J.C., Proc.Roy.Soc. A259, 242 (1960).

32. Mellor, J.W. (Editor), in "A Comprehensive Treatise on Inorganic and Theoretical Chemistry", Vol.XV, Lowe and Brydone, London (1957).

33. Pauling, L., J.Amer.Chem.Soc., 69, 542 (1957); Proc.Roy.Soc. A196, 343 (1949).

34. Paul, A.C., Comings, E.W., and Smith, J.M., A.II, Ch.E.Journal, 5, 453 (1959).

35. Pease, R.N., J.Amer.Chem.Soc., 45, 1196 (1923).

36. Pease, R.N., and Harris, C.A., J.Amer.Chem.Soc., 49, 2503 (1927).

37. Perkins, T.K., Ph.D. Thesis, Univ.of Texas, Austin (1957).

38. Postovskays, A.F., Zhur, Fiz.Khim., 24, 1083 (1950)

39. Rideal, E.K., J.Chem.Soc., 121, 309 (1922).

40. Rogers, G.B., Ph.D. Thesis, Univ.of Wisconsin, Wisconsin (1961).

41. Schuit, G.C.A., and van Reijen, L.L., in "Advances in Catalysis", Vol.X, Academic Press, New York (1958).

42. Schuster, C., Trans.Farad Soc., 28, 406 (1932).

43. Selwood, P. W., J. Am. Chem. Soc., 79, 3346.

44. Sidgwick, N. V., "The Chemical Elements and their Compounds", Vol. 11, Oxford Univ. Press (1950).

45. Sussman, M., and Potter, C., Ind. Eng. Chem., 46, 457 (1954).

46. Taylor, T. I., and Dibeler, V. H., J. Phys. and Coll. Chem., 55, 1036 (1951).

47. Taylor, T. I., in "Catalysis" Vol. V. (P. H. Emmett, Editor), Reinhold, New York (1957).

48. Toyame, O., Rev. Phys. Chem., Japan, 11, 153 (1937).

49. Toyama, O., Rev. Phys. Chem., Japan, 12, 115 (1938).

50. Toyama, O., Rev. Phys. Chem., Japan, 14, 86-100 (1940)

51. Tucholski, T., and Rideal, E. K., J. Chem. Soc., 1701 (1935).

52. Twigg, G. H., and Rideal, E. K., Proc. Roy. Soc. (London), A 171, 55 (1939).

53. Twigg, G. H., Disc. Farad. Soc., 8, 152 (1950).

54. Washburn, E. W. (Editor), "International Critical Tables", Vol. 1, McGraw-Hill, 1926.

55. Wynkoop, R., and Wilhelm, R. H., Chem. Eng. Prog., 46, 300 (1950).

56. Zur Strassen, H., Z. Physik. Chem. A 169, 81 (1934).

APPENDIX A

Table 5. Catalysts Used in the Present Study

Catalyst	% of metal by weight	chemical used	weight of catalyst used, gm.	net weight of metal used, gm.
Ni-pumice	10	$Ni(NO_3)_2 6H_2O$	0.460	4.48×10^{-2}
Fe-pumice	20	$Fe(NO_3)_2 \cdot 9H_2O$	0.785	14.5×10^{-2}
Co-pumice	10	$Co(NO_3)_2 \cdot 6H_2O$	0.900	8.76×10^{-2}
Pt-pumice	0.5	$PtCl_4 \cdot 2HCl \cdot 6H_2O$	0.400	0.20×10^{-2}
Pd-pumice	0.5	$PdCl_2$	0.500	0.25×10^{-2}
Rh-pumice	0.5	$RhCl_3 \cdot 3H_2O$	0.400	0.20×10^{-2}
Ir-pumice	0.5	$(NH_4)_2 IrCl_6$	0.500	0.25×10^{-2}
Ru-pumice	0.5	$RuCl_3 \cdot 3H_2O$	0.400	0.20×10^{-2}
Os-pumice	0.5	$(NH_4)_2OsCl_6$	2.00	1.00×10^{-2}

APPENDIX B

Table 6

Results for Nickel-Pumice Catalyst

Weight of nickel-pumice catalyst used = 0.460 gm.
Net weight of nickel used = 4.48×10^{-2} gm.

1. Dependence of initial rate r_0' on initial hydrogen pressure P_{H_2}
   $P_{C_3H_6} = 30 \pm 1$ mm. Hg

Run No.	Temp. °C.	P_{H_2} mm. Hg	r_0' mm. Hg/min.	Run No.	Temp. °C.	P_{H_2} mm. Hg	r_0' mm. Hg/min.
1	60	61.0	1.1	29	90	59.5	4.5
2		90.0	1.4	30		29.5	2.5
3		96.0	1.5	31		60.5	4.2
4		150.0	2.2	32		45.0	3.4
5		120.0	1.8	33		74.0	5.1
6		30.0	0.5	34		20.0	1.6
7		60.0	1.0	35		90.0	6.5
				36		110.0	7.6
8	80	60.5	2.0	37		92.0	6.5
9		90.5	3.0				
10		30.0	1.2	38	100	91.0	10.0
11		170.0	6.0	39		60.5	7.0
12		115.5	4.2	40		75.0	8.5
13		151.0	5.5	41		30.5	4.0
14		130.5	4.5	42		20.0	2.5
				43		50.0	6.5
15	69	60.5	1.5	44		76.0	8.3
16		99.5	2.0	45		39.0	5.3
17		29.5	0.7				
18		151.0	3.4				
19		170.5	3.6				
20		118.5	2.5				
21	93	61.0	5.0				
22		29.0	2.8				
23		40.0	3.6				
24		60.0	5.0				
25		121.0	10.0				
26		75.5	6.7				
27		19.5	1.8				
28		100.0	7.5				

Table 6 (Continued)

2. Dependence of initial rate r_0' on initial propylene pressure $P_{C_3H_6}$ — P_{H_2} = 60± 1 mm. Hg

Run No.	Temp. °C.	$P_{C_3H_6}$ mm. Hg	r_0' mm. Hg/min.	Run No.	Temp. °C.	$P_{C_3H_6}$ mm. Hg	r_0' mm. Hg/min.
46	69	50.5	1.6	53	80	41.0	3.4
47		71.0	1.7	54		80.5	3.5
48		91.0	1.7				
49		14.5	1.3				
50		120.0	1.7				
51		30.0	1.6				
52		71.0	1.6				

3. Summary of the results

Temp. °C.	$10^3/T$ $°K^{-1}$	m	n	Log r_{os}'	Log r_{os}	E kcal/mole	A mm. Hg/min. -gm. metal
60	3.003	1.0	-	0.255	1.604	13	1.0×10^{10}
69	2.924	1.0	0.0	0.398	1.747		
80	2.833	1.0	0.0	0.634	1.982		
90	2.755	1.0	-	0.935	2.283		
93	2.732	1.0	-	1.000	2.349		
100	2.681	1.0	-	1.114	2.463		

Table 7

Results for Iron-Pumice Catalyst

Weight of iron-pumice catalyst used = 0.785 gm.
Net weight of nickel used = 14.52×10^{-2} gm.

1. Dependence of initial rate r_0' on initial hydrogen pressure P_{H_2}
$P_{C_3H_6} = 30 \pm 1$ mm. Hg.

Run No.	Temp. °C.	P_{H_2} mm. Hg	r_0' mm. Hg/min.
55	50	120.0	2.1
56		121.0	2.1
57		178.0	2.7
58		61.0	1.3
59		150.0	2.5
60		89.5	1.7
61		221.0	3.2
62		39.0	1.0
63		120.0	2.1
64	61	121.0	3.1
65		120.0	3.0
66	69	120.0	4.0
67		181.0	5.3
68		60.5	2.6
69		151.0	4.8
70		33.5	1.8
71		91.5	3.4
72		121.5	4.2
73	85	120.0	9.5
74		119.5	9.6
75		60.0	5.5
76		80.0	8.0
77		29.5	4.0
78		100.0	8.5
79		60.0	6.5
80		149.5	11.0
81		121.0	9.5
82	77	121.0	6.0
83		59.0	4.0
84		187.5	7.8
85		29.0	2.6
86		101.5	5.1
87		43.0	3.0
88		150.5	6.6
89		121.0	5.8
90	92	61.0	8.8
91		120.0	13.0
92		40.0	6.5
93		75.0	10.0
94		23.0	4.5
95		31.0	5.5
96		59.0	8.5

Table 7 (Continued)

2. Dependence of initial rate r_0' on initial propylene pressure $P_{C_3H_6}$ – P_{H_2} = 60 ± 1mm. Hg

Run No.	Temp. °C.	$P_{C_3H_6}$ mm. Hg	r_0' mm. Hg/min.
97	50	30.5	1.4
98		117.5	1.6
99		62.0	1.5
100		12.0	0.9
101		29.0	1.4
102	69	32.0	3.1
103		61.0	3.4
104		118.5	3.5
105		13.0	2.0
106		173.0	3.4
107		30.5	2.8
108	92	59.5	10.0
109		119.0	10.0
110		15.0	5.0
111		84.5	10.0
112		46.0	8.8
113		30.0	8.8
114		29.0	8.5

P_{H_2} = 120 ± 1 mm. Hg

Run No.	Temp. °C.	$P_{C_3H_6}$ mm. Hg	r_0' mm. Hg/min.
115	69	31.0	4.0
116		117.0	5.0
117		45.5	4.5
118		83.5	5.0
119		15.0	2.5
120		62.0	5.0
121		21.0	3.3
122		30.5	3.9
123	77	121.5	8.0
124		51.5	6.5
125		20.5	4.3
126		82.0	7.3
127		205.0	8.0
128		30.5	4.8

3. Effect of the order of reactant's addition to the reaction vessel on initial rates r_0'
Reaction temperature = 50°C, P_{H_2} = 120 mm. Hg, $P_{C_3H_6}$ = 30 mm. Hg

Run No.	r_0' mm. Hg/min.	Remark
129	2.0	H_2 was added first
130	2.0	"
131	1.8	C_3H_6 was added first
132	1.8	"
133	2.0	H_2 was added first

Table 7 (Continued)

4. Summary of the results

Temp. °C.	$10^3/T$ $°K^{-1}$	m	n	Log r_{os}'	Log r_{os}	E kcal/mole	A mm. Hg/min. -gm. metal
50	3.096	0.67	0.0	0.312	1.150	10.	8.0×10^7
61	2.994	-	-	0.485	1.323		
69	2.924	0.65	0.0	0.612	1.450		
77	2.857	0.62	0.0	0.770	1.608		
85	2.793	0.67	0.0	0.980	1.818		
92	2.740	0.66	0.0	1.114	1.952		

Table 8

Results for Cobalt-Pumice Catalyst

Weight of cobalt-pumice catalyst used = 0.900 gm.
Net weight of cobalt used = 8.76 gm.

1. Dependence of initial rate r_0' on initial hydrogen pressure P_{H_2} — $P_{C_3H_6} = 30 \pm 1$ mm. Hg

Run No.	Temp. °C.	P_{H_2} mm. Hg	r_0' mm. Hg/min.	Run No.	Temp. °C.	P_{H_2} mm. Hg	r_0' mm. Hg/min.
134	52	118.5	1.3	162	87	120.0	4.3
135		121.5	1.2	163		60.5	2.2
136		240.5	2.0	164		60.5	2.1
137		60.0	0.7	165		180.5	5.8
138		182.5	1.7	166		89.0	3.2
139		80.0	0.8	167		30.0	1.1
140		160.0	1.5	168		150.5	5.3
141		120.0	1.3	169		100.0	4.0
142		200.5	1.9	170		219.5	6.8
				171		121.5	4.3
143	67.5	119.0	2.3				
144		120.5	2.3	172	96.5	120.0	5.2
145		181.5	3.1	173		60.0	2.7
146		60.5	1.2	174		91.5	4.0
147		238.5	3.9	175		181.5	7.3
148		81.5	1.6	176		30.0	1.3
149		149.5	2.7	177		124.5	5.3
150		35.5	0.7				
141		121.5	2.3	178	109	121.5	6.0
				179		93.5	4.3
152	77.5	120.0	2.9	180		31.0	1.5
153		119.5	3.0	181		60.0	2.9
154		59.5	1.6	182		119.5	6.0
155		180.0	4.5				
156		90.5	2.4	183	125	121	6.0
157		219.0	5.2	184		121	6.0
158		150.0	4.0				
159		33.0	1.0				
160		239.5	5.6				
161		119.5	3.2				

Table 8 (Continued)

2. Dependence of initial rate r_0' on initial propylene pressure $P_{C_3H_6}$ - P_{H_2} = 120± 1 mm. Hg

Run No.	Temp. °C.	$P_{C_3H_6}$ mm. Hg	r_0' mm. Hg/min.	Run No.	Temp. °C.	$P_{C_3H_6}$ mm. Hg	r_0' mm. Hg/min.
185	52	30.0	1.2	192	77.5	31.0	2.6
186		31.0	1.2	193		120.0	3.5
187		116.0	1.2	194		60.0	3.4
188		49.5	1.2	195		180.5	3.5
189		164.0	1.0	196		30.5	2.8
190		20.5	1.1				
191		80.0	1.1				

3. Summary of the results

Temp. °C.	$10^3/T$ $°K^{-1}$	m	n	Log r_{os}'	Log r_{os}'	E kcal/mole	A mm. Hg/min. -gm. metal
52	3.078	0.91	0.0	0.085	1.143	8.1	4.0×10^6
67.5	2.937	0.90	-	0.355	1.413		
77.5	2.853	0.91	00	0.490	1.548		
87	2.778	0.97	-	0.631	1.689		
96.5	2.705	-	-	0.721	1.779		
109	2.617	-	-	0.775	1.833		
125	2.510	-	-	0.775	1.833		

Table 9

Results for Platinum-Pumice Catalyst

Weight of platinum-pumice catalyst used = 0.400 gm.
Net weight of platinum used = 0.20×10^{-2} gm.

1. Aging of the catalyst
Temperature = 30° C., P_{H_2} = 120 ± 1 mm. Hg, $P_{C_3H_6}$ = 30 ± 1 mm. Hg

Run number	initial rate, r_0' mm. Hg/min.	Run number	initial rate, r_0' mm. Hg/min.
197	23	204	5.5
198	21	205	3.8
199	18	206	1.2
200	13	207	0.9
201	9.5	208	0.75
202	8.5	209	0.65
203	7.5	210	0.50

2. Dependence of initial rate r_0' on initial hydrogen pressure P_{H_2}
$P_{C_3H_6}$ = 30 ± 1 mm. Hg

Run No.	Temp. °C.	P_{H_2} mm. Hg	r_0' mm. Hg/min.	Run No.	Temp. °C.	P_{H_2} mm. Hg	r_0' mm. Hg/min.
211	89	119.0	2.0	230	117	29.5	2.6
212		209.5	2.8	231		196.5	12.2
213		30.0	0.6	232		91.0	7.2
214		149.5	2.2	233		122.5	9.0
215		63.0	1.1	234		60.5	5.0
216		119.0	1.8	235		162.0	11.5
217		90.5	1.5				
				236	129	91.0	13.0
218	100	121.5	3.0	237		28.5	4.6
219		196.5	4.8	238		163.0	18.0
220		40.0	1.3	239		122.0	15.5
221		81.5	2.3	240		46.0	7.5
222		161.5	4.0	241		61.0	10.0
				242		120.0	16.0
223	107.5	119.5	5.0				
224		199.5	6.7				
225		32.5	1.7				
226		90.5	3.9				
227		59.5	2.9				
228		159.0	6.3				
229		121.0	5.2				

Table 9 (Continued)

3. Dependence of initial rate r_0' on initial propylene pressure $P_{C_3H_6}$.

P_{H_2} = 6.0 ± 1 mm. Hg.

Run No.	Temp. °C.	$P_{C_3H_6}$ mm. Hg	r_0' mm. Hg/min.	Run No.	Temp. °C.	$P_{C_3H_6}$ mm. Hg	r_0' mm. Hg/min.
243	129	60.0	11.0	252	89	99.0	1.3
244		15.0	10.5	253		13.0	1.3
245		87.0	10.5	254		124.5	1.1
246		118.0	10.5	255		30.0	1.1
247	117	28.5	5.1				
248		62.5	5.3				
249		131.0	5.1				
250		14.5	5.2				
251		99.0	5.2				

4. Check of the activity of catalyst.
(The catalyst was pretreated with propylene)

Run number	Temp. °C.	P_{H_2} mm. Hg	$P_{C_3H_6}$ mm. Hg	r_0' mm. Hg/min.
256	129	62	31.5	10.5
257		118	31.5	16.0
258		120	29	15.5
* 259		119	31	15.5

* The run was taken after the reactor had been evacuated for 4 hours.

5. Summary of the results (see Appendix C)

Table 10

Results for Palladium-Pumice Catalyst

Weight of palladium-catalyst used = 0.500 gm.
Net weight of palladium used = 0.25×10^{-2} gm.

1. Dependence of initial rate r_0' on initial hydrogen pressure P_{H_2}.
   $P_{C_3H_6} = 30 \pm 1$ mm. Hg.

Run No.	Temp. °C.	P_{H_2} mm. Hg	r_0' mm. Hg/min.	Run No.	Temp. °C.	P_{H_2} mm. Hg	r_0' mm. Hg/min.
260	148	119.5	5.0	276	130	121.0	2.4
261		180.0	6.3	277		61.0	1.4
262		61.5	2.8	278		181.0	3.0
263		240.0	7.3	279		120.5	2.2
264		31.0	1.6				
265		83.0	3.7	280	161	120.5	6.5
266		121.0	4.5	281		181.0	8.6
				282		60.5	4.0
267	120	120.0	1.7	283		121.5	6.0
268		60.5	1.1				
269		179.0	2.6	284	138	119.0	3.2
270		30.5	0.6	285		181.5	4.0
271		240.5	3.1	286		60.0	1.6
272		89.5	1.5	287		90.0	2.2
273		119.0	1.8	288		119.0	3.0
274		46.5	0.8				
275		119.5	1.7				

2. Dependence of initial rate r_0' on initial propylene pressure $P_{C_3H_6}$. $P_{H_2} = 60 \pm$ mm. Hg

Run No.	Temp. °C.	$P_{C_3H_6}$ mm. Hg	r_0' mm. Hg/min.	Run No.	Temp. °C.	$P_{C_3H_6}$ mm. Hg	r_0' mm. Hg/min.
289	161	30.0	4.0	295	148	31.0	2.0
290		119.5	4.8	296		118.5	3.1
291		185.0	4.6	297		64.5	2.9
292		62.0	4.6	298		206.0	3.0
293		11.0	2.1				
294		23.5	3.2				

Table 10 (Continued)

3. Summary of the results

Temp. $^{o}C.$	$10^3/T$ $^{o}K^{-1}$	m	n	Log r_{os}'	Log r_{os}	E kcal/mole	A mm. Hg/min. -gm. metal
120	2.545	0.79	-	0.243	2.845	11	8.0×10^8
130	2.481	0.79	-	0.357	2.959		
138	2.433	0.81	-	0.491	3.093		
148	2.375	0.80	0.0	0.672	3.274		
161	2.304	0.80	0.0	0.794	3.396		

Table 11

Results for Rhodium-Pumice Catalyst

Weight of rhodium-pumice catalyst used = 0.400 gm.
Net weight of rhodium used = 0.20×10^{-2} gm.

1. Dependence of initial rate r_0 on initial hydrogen pressure P_{H_2}

$P_{C_3H_6} = 30 \pm 1$ mm. Hg.

Run No.	Temp. °C.	P_{H_2} mm. Hg	r_0' mm. Hg/min.	Run No.	Temp. °C.	P_{H_2} mm. Hg	r_0' mm. Hg/min.
299	40	120.0	1.0	316	78	199.0	15.5
300		200.0	1.7	317		81.0	7.0
301		160.0	1.1	318		159.5	13.5
302		120.0	1.0	319		40.0	3.5
303		61.0	0.6	320		59.5	5.3
				321		119.0	10.5
304	56	120.0	3.0				
305		181.5	4.3	322	84	58.0	7.1
306		38.0	1.1	323		100.0	12.5
307		159.0	3.7	324		140.0	17.5
308		80.0	2.2	325		30.0	3.7
309		119.5	3.0	326		82.0	10.5
310	67	120.0	5.0	327	91	39.5	5.5
311		61.0	3.0	328		59.5	11.3
312		158.5	7.2	329		19.0	3.6
313		101.0	4.7	330		80.0	15.0
314		198.5	9.0				
315		33.0	1.6				

Table 11 (Continued)

2. Dependence of initial rate r_0' on initial propylene pressure $P_{C_3H_6}$

P_{H_2} = 80 ± 1 mm. Hg.

Run No.	Temp. °C.	$P_{C_3H_6}$ mm. Hg	r_0' mm. Hg/min.	Run No.	Temp. °C.	$P_{C_3H_6}$ mm. Hg	r_0' mm. Hg/min.
331	91	91.0	15.0	341	56	93.5	2.8
332		121.5	15.0	342		121.5	2.6
				343		30.0	3.0
333	67	30.0	4.4	344		59.5	3.0
334		89.5	4.2				
335		121.5	4.0	345	78	30.0	6.5
336		58.0	4.4	346		90.0	6.2
337		161.0	3.8				
338		15.5	4.0	347	84	30.0	9.0
339		29.0	4.2	348		122.0	8.5
340		62.0	4.0	349		87.5	8.7
				350		131.5	8.5
				351		27.5	9.0

3. Summary of the results

Temp. °C.	$10^3/T$ °K-1	m	n	Log r_{os}'	Log r_{os}	E kcal/mole	A mm. Hg/min.-gm. metal
40	3.195	1.0	-	0.000	2.700	13.	1.0×10^{12}
56	3.040	1.0	-0.10	0.470	3.160		
67	2.940	1.0	-0.05	0.740	3.440		
78	2.850	1.0	-0.03	1.921	3.720		
84	2.800	1.0	-0.07	1.176	3.873		
91	2.747	1.0	0.00	1.352	4.002		

Table 12

Results for Iridium-Pumice Catalyst

Weight of iridium-pumice catalyst = 0.500 gm.
Net weight of iridium used = 0.25×10^{-2} gm.

1. Dependence of initial rate r_0' on initial hydrogen pressure P_{H_2}.
$P_{C_3H_6} = 30 \pm 1$ mm. Hg

Run No.	Temp. °C.	P_{H_2} mm. Hg.	r_0' mm. Hg/min.
352	70	120.0	1.6
353		61.0	0.8
354		150.0	1.8
355		201.0	2.3
356		119.0	1.4
357	81	121.0	3.1
358		160.5	4.4
359		39.5	1.1
360		196.0	5.0
361		80.5	2.2
362		141.5	3.6
363		180.0	4.8
364	90	121.0	5.3
365		59.5	2.7
366		160.0	6.8
367		30.0	1.3
368		90.0	3.9
369		200.0	7.8
370		119.5	5.3
371	100	120.5	8.5
372		159.0	11.0
373		81.0	5.6
374		40.0	2.8
375		100.0	6.0
376		61.0	4.0
377		120.5	8.0
378	107	120.0	9.5
379		61.0	4.8

2. Dependence of initial rate r_0' on initial propylene pressure $P_{C_3H_6}$.
$P_{H_2} = 60 \pm 1$ mm. Hg

Run No.	Temp. °C.	$P_{C_3H_6}$ mm. Hg	r_0' mm. Hg/min.
380	80	29.5	1.9
381		119.0	1.4
382		80.0	1.5
383		142.0	1.5
384	100	30.0	4.5
385		139.0	4.0
386		202.5	4.0
387		85.5	4.3
388		139.0	4.0

Table 12 (Continued)

3. Summary of the results

Temp. °C.	$10^3/T$ $°K^{-1}$	m	n	Log r_{os}'	Log r_{os}	E kcal/mole	A mm. Hg/min. -gm. metal
70	2.915	1.0	-	0.146	2.747	15	2.5×10^{12}
81	2.825	1.0	-0.07	0.491	3.093		
90	2.755	1.0	-	0.724	3.326		
100	2.681	1.0	-0.06	0.929	3.531		
107	2.631	1.0	-	0.970	3.571		

Table 13

Results for Ruthenium-Pumice Catalyst

1. Dependence of initial rate r_0' on initial hydrogen pressure P_{H_2}

$P_{C_3H_6} = 30 \pm 1$ mm. Hg

Run No.	Temp. °C.	P_{H_2} mm. Hg	r_0' mm. Hg/min.
389	60.5	121.0	1.3
390		179.0	1.7
391		90.0	1.0
392		219.0	2.0
393		59.5	0.9
394		119.0	1.2
395	78	119.0	2.0
396		217.0	3.3
397		81.0	1.6
398		172.5	2.9
399		40.5	1.0
400		122.0	2.2
401	102.5	119.5	4.0
402		161.0	5.0
403		80.0	2.6
404		219.0	6.3
405		40.0	1.5
406	124	120.0	6.2
407		38.0	2.0
408		157.5	7.4
409		60.0	2.5
410		119.5	5.5

2. Dependence of initial rate r_0' on initial propylene pressure $P_{C_3H_6}$

$P_{H_2} = 120 \pm 1$ mm. Hg

Run No.	Temp. °C.	$P_{C_3H_6}$ mm. Hg	r_0' mm. Hg/min.
411	124	120.0	5.1
412		58.0	5.0
413		161.0	5.8
414		90.0	6.0
415		31.0	5.3
416	60.5	30.0	1.2
417		61.5	1.2
418		148.5	1.0
419		50.5	1.1
420		91.5	1.1
421	102.5	30.0	2.9
422		60.0	3.0
423		141.0	2.9

Table 13 (Continued)

3. Summary of the results

Temp. $^{o}C.$	$10^3/T$ $^{o}K^{-1}$	m	n	Log r_{os}'	Log r_{os}	E kcal/mole	A mm. Hg/min. -gm. metal
60.5	2.998	0.75	-0.1	0.079	2.775	6.5	1.3×10^7
78	2.849	0.70	-	0.301	2.997		
102.5	2.663	0.80	0.0	0.602	3.298		
124	2.515	0.80	0.0	0.766	3.462		

Table 14

Results for Osmium-Pumice Catalyst

Weight of osmium-pumice catalyst = 2,000 gm.
Net weight of osmium used = 1.00×10^{-2} gm.

1. Dependence of initial rate r_0' on initial hydrogen pressure P_{H_2}.
$P_{C_3H_6} = 30 \pm 1$ mm. Hg

Run No.	Temp. °C.	P_{H_2} mm. Hg	r_0' mm. Hg/min.
424	143	119.0	1.8
425		59.0	0.7
426		182.0	4.0
427		58.0	0.7
428		171.0	3.6
429		89.5	1.1
430		240.0	6.2
431		120.0	2.0
432	160	119.0	2.7
433		41.0	0.1
434		198.0	6.8
435		62.0	1.1
436		240.0	10.0
437		178.5	7.0
438		120.0	2.8
439		141.0	4.2
440	170	120.0	3.7
441		59.5	1.0
442		177.0	7.0
443		160.0	6.0
444		101.5	2.7
445		138.0	4.5
446		119.0	3.6
447	188	122.0	5.0
448		188.0	10.5
449		64.5	1.5

2. Dependence of initial rate r_0' on initial propylene pressure $P_{C_3H_6}$.
$P_{H_2} = 120 \pm 1$ mm. Hg

Run No.	Temp. °C.	$P_{C_3H_6}$ mm. Hg	r_0' mm. Hg/min.
450	143	30	2.0
451		91	2.0
452		62	2.0
453		132	1.8
454		30	1.8

Table 14 (Continued)

3. Summary of the results

Temp. °C.	$10^3/T$ $^oK^{-1}$	m	n	Log r_{os}'	Log r_{os}	E kcal/mole	A mm. Hg/min. -gm. metal
143	2.404	1.8	0	0.275	2.277	7.4	2.5×10^6
160	2.309	1.6	-	0.478	2.479		
170	2.257	1.4	-	0.556	2.557		
188	2.169	1.6	-	0.661	2.662		

APPENDIX C

Sample Calculations

The following are the sample calculations of the kinetic parameters of the hydrogenation of propylene over the platinum-pumice catalyst.

1. The net weight of platinum used

The reaction was studied over 0.400 gm. of 0.5% platinum-pumice catalyst (Table 5). The chemical used in the preparation of the catalyst is $PtCl_4 \cdot 2HCl \cdot 6H_2O$. After being calcined in a muffle furnace at 400° C. for 6 hours, the chemical decomposed into platinum chloride whose exact formula is not clear. Since percentage of platinum by weight is as low as 0.5, the net weight of platinum used can be taken as $0.4 \times 0.005 = 0.20 \times 10^{-2}$ gm. with a negligible error.

2. The kinetics of the reaction

The experimental data for the catalyst are given in Table 9. According to the equations (IV-4) and (IV-5), the pressure exponents m and n were estimated from the slopes of the plots, Log r_0' against Log P_{H_2} and Log $P_{C_3H_6}$, respectively (Figure 17). The results are shown in section 5. Therefore, the orders of the reaction over the catalyst are 0.80 and zero with respect to hydrogen and propylene, respectively.

3. Activation energy E and frequency factor A

The most probable value of r_{os}', i.e., the initial rate obtained at $P_{H_2} = 120$ mm. Hg, $P_{C_3H_6} = 30$ mm. Hg, was chosen from the plot of Log r_0' vs. Log P_{H_2} at a certain temperature. According to equation (IV-3), r_{os} was estimated. Log r_{os} was then plotted against $10^3/T$ as shown in Figure 18. The data of Log r_{os}', Log r_{os}, $1/T$ are given in section 5. If Arrhenius' law holds over the temperature range studied, the following relationship exists:

$$\text{Log } r_{os} = a + b\left(\frac{10^3}{T}\right) \tag{1}$$

For simplification, it is rewritten as

$$y = a + bx \tag{2}$$

where y is Log r_{os}, and x is $(10^3/T)$. According to the method of least squares, the values of a and b are evaluated from the following two equations:

$$na + b\sum(x) - \sum(y) = 0 \tag{3}$$

and

$$a\sum(x) + b\sum(x^2) - \sum(xy) = 0 \tag{4}$$

where n is the number of experimental points.

Solving the above simultaneous equations,

$$a = \frac{\sum(x)\sum(xy) - \sum(y)\sum(x^2)}{(\sum x)^2 - n\sum(x^2)} \tag{5}$$

and

$$b = \frac{\sum(x)\sum(y) - n\sum(xy)}{(\sum x)^2 - n\sum(x^2)} \tag{6}$$

From the data in section 5

$$n = 5,\ \sum(x) = 13.122,\ \sum(y) = 17.125,\ \sum(x^2) = 34.482,\ \sum(xy) = 44.790$$

Substituting into (5) and (6),

$$a = 12.4 \tag{7}$$

and

$$b = -3.43 \tag{8}$$

Therefore, the best fitting line for the Arrhenius plot (Figure 18) is

$$y = 12.4 - 3.43x \tag{9}$$

or

$$\text{Log } r_{os} = 12.4 - 3.43\,(10^3/T) \tag{10}$$

Comparing the equation (10) to the equation (IV-2),

$$\text{Log } A = 12.4 \tag{11}$$

and

$$\frac{E}{2.303\,R} = 3.43 \times 10^3 \qquad (12)$$

Hence, the frequency factor

$$A = 2.5 \times 10^{12} \qquad (13)$$

and the activation energy

$$E = 2.303 \times 1.987 \times 3.43 \times 10^3 = 16 \times 10^3 \text{ cal/mole}$$

$$= 16 \text{ kcal/mole} \qquad (14)$$

4. Errors of the activation energy and the frequency factor

The probable errors* in a and b are

$$P_a = r_e \sqrt{\frac{\sum (x^2)}{D}} \qquad (15)$$

and

$$P_b = r_e \sqrt{\frac{n}{D}} \qquad (16)$$

where

$$r_e = 0.6745 \sqrt{\frac{\sum d^2}{(n-2)}} \quad , \quad D = n\sum (x^2) - (\sum x)^2$$

and

$$d = y - y_{calc.}$$

y is an observed value and $y_{calc.}$ is the corresponding calculated one using the constants a and bcfinally adopted.

For the present calculation,

$$\sum d^2 = 0.010 \qquad (17)$$

Therefore,

$$r_e = 0.6745 \sqrt{\frac{0.010}{(5-2)}} = 0.030 \qquad (18)$$

$$D = 5 \times 34.482 - (13.122)^2 = 0.223 \qquad (19)$$

Substituting into (15) and (16),

* Margenau, H., The Mathematics of Physics and Chemistry (D. Van Nostrand Co. Inc., 2nd edition, 1957), page 519.

$$P_b = 0.030 \times \sqrt{\frac{5}{0.223}} = 0.14 \qquad (20)$$

$$P_{\bar{x}} = 0.03 \times \sqrt{\frac{34.482}{0.223}} = 0.37 \qquad (21)$$

Hence, the probable error of the activation energy is

$$\frac{0.37}{3.43} \times 100 = 11\%$$

and the probable error of log A is

$$\frac{0.14}{12.4} \times 100 = 1.1\%$$

5. Summary of the results

Temp. °C.	$10^3/T$ °K^{-1}	m	n	Log r_{os}'	Log r_{os}	E kcal/mole	A mm. Hg/min. -gm. metal
89	2.762	0.79	0.0	0.279	2.978	16	2.5×10^{12}
100	2.681	0.80	-	0.691	3.190		
107.5	2.628	0.80	-	0.716	3.415		
117	2.564	0.82	0.0	1.190	3.889		

NOMENCLATURE

a_0, c_0	Edge length of unit cell along the a and c-crystallographic axes
A	Frequency factor, mm. Hg/(min. -gm. metal)
E, E_{app}	Apparent activation energy, kcal/mole
E_s	Activation energy of the surface reaction, kcal/mole
k	Rate constant
m	Reaction order with respect to initial hydrogen pressure
n	Reaction order with respect to initial propylene pressure
P	Total pressure of the reactants, mm. Hg
P_H, P_U	Partial pressures of hydrogen and olefins, mm. Hg
P_{H_2}	Initial partial pressure of hydrogen, mm. Hg
$P_{C_3H_6}$	Initial partial pressure of propylene, mm. Hg
$P_{C_3H_8}$	Pressure of propane formed, mm. Hg
Q_{ads}	Heats of adsorption of the reactants, kcal/mole
r	Reaction rate, mm. Hg/min.
r_0	Initial reaction rate over a unit weight of metal catalyst, mm. Hg/(min. -gm. metal)
r_0'	Initial reaction rate over a particular weight of metal catalyst, mm. Hg/min.
r_{os}	Initial reaction rate of the standard run over a unit weight of metal catalyst at P_{H_2} = 120 mm. Hg, $P_{C_3H_6}$ = 30 mm. Hg, mm. Hg/(min. -gm. metal)
r_{os}'	Initial reaction rate of the standard run over a particular weight of metal catalyst at P_{H_2} = 120 mm. Hg, $P_{C_3H_6}$ = 30 mm. Hg, mm. Hg/min.
R	Gas constant
$\bar{R}$	Ratio of reactants' pressures, $P_{H_2} / P_{C_3H_6}$
t	Reaction time, min.
T	Reaction Temperature, ^{o}K.